UNIVERSIDADE DE LISBOA
FACULDADE DE CIÊNCIAS
DEPARTAMENTO DE FÍSICA

Heart Beat Variability Analysis in Perinatal Brain Injury and Infection

Mariana Santos Silva

Mestrado Integrado em Engenharia Biomédica e Biofísica
Perfil em Engenharia Clínica e Instrumentação Médica

Dissertação orientada por:
Professor Alexandre Andrade
Professor Danilo Mandic

2018

Para os meus Pais

Acknowledgements

First, I would like to thank my supervisor, Professor Alexandre Andrade for his guidance, support and encouragement not only in this dissertation, but trough all my academic journey.

I would also like to thank Dr. Sudhin Tayyil, Professor Danilo Mandic and Vânia Oliveira, who gave me the opportunity to work under their supervision, in one of the most challenging projects I took part. Thank you for the support, for the time spent guiding me and for all the useful critiques to this project.

A special and a big thank you to all the fantastic people I met at Imperial College London: Tiffany, Pepe, Ilia, Chris and Ahmad, who made my stay in London the best experience of my life. You still make me miss London and the office every minute. Finishing this work would have been a lot more difficult without all of you. Thank you!

Also, a big thank you to all my friends. To Adriana, who always remembered me that it is possible to reach the impossible, to Joana who join this adventure with me, being my biggest support throughout last year, to Inês for all the friendship, support and love during these 5 years and to all of my friends that walked with me in this journey.

To my sister Maria, a big thank you, for being my source of inspiration, strength and determination. That for more kilometers or oceans that separate us, we were always together.

I would like to express my deep gratitude to my family, specially to my parents, Sérgio and Alice, for always supporting and believing in me, but also for always encouragement me to get out of my comfort zone and follow my dreams. Words cannot express how proud I am to be your daughter.

Lastly, I would like to thank the Erasmus+ program for enabling this experience.

Resumo

Todos os anos, mais de 95 mil recém-nascidos são admitidos nas Unidades de Cuidados Intensivos Neonatais (UCIN) do Reino Unido, devido principalmente a partos prematuros ou outras complicações que pudessem ter ocorrido, como é o caso da encefalopatia hipóxico-isquémica (EHI), que assume 3% de todas as admissões nas unidades referidas. EHI é o termo que define uma complicação inesperada durante o parto, que resulta em lesões neurológicas a longo prazo e até em morte neonatal, devido à privação de oxigénio e fluxo sanguíneo ao recém-nascido durante o nascimento. Estima-se que tenha uma incidência de um a seis casos por 1000 nascimentos.

Nos países desenvolvidos, a hipotermia é utilizada como método preventivo-terapêutico para esta condição. No entanto, existem dois grandes obstáculos para a obtenção da neuroprotecção pretendida e totalmente benéfica, na prática clínica. Em primeiro lugar, esta técnica é eficaz se for iniciada dentro de seis horas após o parto. Visto que o estado clínico da encefalopatia neonatal evolui nos dias posteriores ao nascimento, a sua deteção precoce é um grande desafio. Tal situação pode levar a diversos erros nas UCIN, tal como indivíduos sujeitos à terapia de hipotermia desnecessariamente, ou ainda mais grave, casos em que recém-nascidos foram inicialmente considerados como saudáveis, não tendo sido submetidos à terapia referida, apresentarem sinais de EHI após seis horas de vida.

A segunda questão prende-se com o facto de a neuroprotecção poder ser perdida se o bebé estiver stressado durante o tratamento. Para além disso, não existe nenhuma ferramenta válida para a avaliação da dor dos recém-nascidos submetidos a esta terapia. Os obstáculos frisados anteriormente demonstram duas necessidades ainda não correspondidas: a carência de um método não invasivo e largamente adaptável a diferentes cenários para uma correta identificação de recém-nascidos com maior probabilidade de HIE, dentro de uma margem de seis horas após o parto, mas também um método preciso de stress em tempo real, não invasivo, que possa orientar tanto pessoal médico, como pais, de modo a oferecer um tratamento mais responsável, célere e individualizado.

Deste modo, a análise do ritmo cardíaco demostra um enorme potencial para ser um biomarcador de encefalopatia neonatal, bem como um medidor de stress, através da eletrocardiografia (ECG), visto que é um importante indicador de homeostase, mas também de possíveis condições que podem afetar o sistema nervoso autónomo e, consequentemente, o equilíbrio do corpo humano.

É extremamente difícil a obtenção de um parâmetro fisiológico, sem a presença de artefactos, especialmente no caso de recém-nascidos admitidos nas UCIN. Tanto no caso da aquisição de ECGs, como de outros parâmetros, existe uma maior probabilidade de o sinal ser corrompido por artefactos, visto que são longas aquisições, normalmente dias, onde o bebé é submetido a diversas examinações médicas, está rodeado de equipamentos eletrónicos, entre outros. Artefactos são definidos como uma distorção do sinal, podendo ser causados por diversas fontes, fisiológicas ou não. A sua presença nos dados adquiridos influencia e dissimula as informações corretas e reais, podendo mesmo levar a diagnósticos e opções terapêuticas erradas e perigosas para o paciente.

Apesar de existirem diversos algoritmos de identificação de artefactos adequados para o sinal cardíaco adulto, são poucos os que funcionam corretamente para o de recém-nascido. Para além disso, é necessário bastante tempo tanto para o staff clínico, como para os investigadores, para o processo de visualização e identificação de artefactos no eletrocardiograma manualmente.

Deste modo, o projeto desenvolvido na presente dissertação propõe um novo algoritmo de identificação e marcação de artefactos no sinal cardíaco de recém-nascidos. Para tal, foi criado um modelo híbrido de um método que tem em consideração todas as relações matemáticas de batimento para batimento cardíaco, com outro que tem como objetivo a remoção de *spikes* no mesmo sinal. O algoritmo final para além de cumprir com o objetivo descrito acima, é também adaptável a diferentes tipos de artefactos presentes no sinal, permitindo ao utilizador, de uma forma bastante intuitiva, escolher

o tipo de parâmetros e passos a aplicar, podendo ser facilmente utilizado por profissionais de diferentes áreas. Deste modo, este algoritmo é uma mais-valia quando aplicado no processamento de sinal pretendido, evitando assim uma avaliação visual demorada de todo o sinal.

Para obter a melhor performance possível, durante o desenvolvimento do algoritmo foram sempre considerados os resultados de validação, tais como exatidão, sensibilidade, entre outros. Para tal, foram analisados e comparados eletrocardiogramas de 4 recém-nascidos saudáveis e 4 recém-nascidos com encefalopatia. Todos possuíam aproximadamente 5 horas de sinal cardíaco adquirido após o nascimento, com diferentes níveis de presença de artefactos.

O algoritmo final, obteve uma taxa de sensibilidade de 96.2% (±2.4%) e uma taxa de exatidão de 92.6% (±3.2%). Como se pode verificar pelos valores obtidos, o algoritmo obteve percentagens altas nos vários parâmetros de classificação, o que significa uma deteção correta. A taxa de exatidão apresenta um valor mais baixo, comparativamente ao parâmetro da sensibilidade, pois em diversas situações, normalmente perto de artefactos, os batimentos normais são considerados como artefactos, pelo algoritmo. Contudo, essa taxa não é alarmante, tendo sido considerada uma taxa reduzida, pelo pessoal médico.

Após o processamento do sinal cardíaco dos grupos mencionados acima, um estudo comparativo, utilizando parâmetros da variabilidade do ritmo cardíaco, foi realizado. Diferenças significativas foram encontradas entre os dois grupos, onde o saudável assumiu sempre valores maiores. SDNN e baixa frequência foram os parâmetros que traduziram uma diferença maior entre os dois grupos, com um p-value <0.01.

De modo a corresponder ao segundo obstáculo referido nesta dissertação, outro objetivo desta tese foi a criação de um algoritmo que pudesse identificar e diferenciar uma situação de stress nesta faixa etária, com recurso ao ritmo cardíaco. Um estudo multidimensional foi aplicado aos diferentes métodos de entropia utilizados nesta tese (*approximate entropy, sample entropy, multiscales entopy* e *fuzzy entropy*) de modo a estudar como os diferentes métodos de entropia interagem entre si e quais são os resultados dessa relação, especialmente na distinção de estados normais e stressantes. Para tal, a utilização de *clusters* foi essencial. Dado que para todos os ECGs de bebés saudáveis analisados neste projeto foram registados todas as possíveis situações de stress, como é o caso de choro, examinações médicas, mudança de posição, entre outros, foram escolhidos 10 minutos do sinal do ritmo cardíaco adquirido, antes da situação, para análise. Infelizmente, associado a um evento stressante, na maioria dos casos encontra-se uma percentagem bastante alta do sinal corrompida por artefactos. No entanto, em alguns casos foi possível observar uma clara distinção de grupos de *clusters*, indicando que naquele período de tempo, houve uma mudança de estado.

Foi também realizado um estudo intensivo de diversos métodos de entropia aplicados ao grupo de sujeitos apresentados nesta dissertação, onde foi provado que o método mais adequado a nível de diferenciação é a Fuzzy Entropy ($p=0.0078$).

Ainda é possível sugerir alguns aspetos e apontar algumas limitações, no âmbito de poderem ser ultrapassadas no futuro. Em primeiro lugar, é necessária a aquisição de mais eletrocardiogramas, quer de recém-nascidos saudáveis, quer com encefalopatia hipóxico-isquémica, de modo a aumentar o tamanho da amostra e, deste modo diminuir os valores do desvio-padrão em todos os parâmetros calculados. Relativamente ao estudo do stress, seria interessante, com uma amostra maior, a definição de clusters, de modo a ter uma identificação precisa de situações stressantes. Para além disso, a transformação do software atualmente escrito em MATLAB para *GUI* (interface gráfica do utilizador), a fim de tornar mais acessível a sua utilização por profissionais de diversas áreas.

Palavras-chave: Variabilidade Cardíaca, Deteção de Artefactos, ECG Neonatal, Complexity Science, Stress;

Abstract

In Neonatal Intensive Care Unit (NICU), the heart rate (HR) offers significant insight into the autonomic function of sick newborns, especially with hypoxic ischemic encephalopathy condition (HIE). However, the intensity of clinical care and monitoring contributes to the electrocardiogram (ECG) to be often noisy and contaminated with artefacts from various sources. These artefacts, defined as any distortion of the signal caused by diverse sources, being physiological or non-physiological features, interfere with the characterization and subsequent evaluation of the heart rate, leading to grave consequences, both in diagnostic and therapeutic decisions. Besides, its manual inspection in the ECG trace is highly time-consuming, which is not feasible in clinical monitoring, especially in NICU.

In this dissertation, it is proposed an algorithm capable of automatically detect and mark artefacts in neonatal ECG data, mainly dealing with mathematical aspects of the heart rate, starting from the raw signal. Also, it is proposed an adjacent algorithm, using complexity science applied to HR data, with the objective of identifying stress scenarios. Periods of 10-minute ECG were considered from 8 newborns (4 healthy and 4 HIE) to the identification of stress situations, whereas for the artefacts removal algorithm small portions varying in time length according to the amount of noise present in the originally 5 hours long samples were utilised. In this report it is also present several comparisons utilising heart rate parameters between healthy and HIE groups.

Fuzzy Entropy was considered the best method to differentiate both groups ($p=0.00078$). In this report, substantial differences in heart rate variability were found between healthy and HIE groups, especially in SDNN and low frequency ($p<0.01$), confirming results of previous literature.

For the final artefact removal algorithm, it is illustrated significant differences between raw and post-processed ECG signals. This method had a Recall rate of 96.2% (±2.4%) and a Precision Rate of 92.6% (±3.2%), demonstrating high efficiency in ECG noise removal. Regarding stress measures, associated with a stressful event, in most cases there is a high percentage of the signal corrupted by artefacts. However, in some cases it was possible to see a clear distinction between groups of clusters, indicating that in that period, there was a change of state. Not all the time segments from subjects demonstrated differences in stress stages, indicating that there is still room for improvement in the method developed.

Keywords: Heart Rate Variability, Artefact Detection, Neonatal ECG, Complexity Science, Stress;

Table of Contents

List of Figures

List of Tables

List of Abbreviations

aEEG | amplitude-integrated EEG

ANS | Autonomic nervous system

ApEn | Approximate Entropy

DBSCAN | Density-Based Spatial Clustering of Applications with Noise

DWI | Diffusion Weighted Imaging

ECG | Electrocardiography

EEG | electroencephalography

FN | False Negative

FP | False Positive

FuzzyEn | Fuzzy Entropy

HF | High Frequency

HIE | hypoxic ischemic encephalopathy

HR | Heart Rate

HRV | Heart Rate Variability

IBI | Interbeat Interval

LF | Low Frequency

MRI | Magnetic Resonance Imaging

ms | Milliseconds

MSE | Multiscale Sample entropy

NICU | Neonatal Intensive Care Unit

PNS | Parasympathetic nervous system

RRi | Cardiac beat-to-beat interval

SA | Sinoatrial node

SampEn | Sample Entropy

SDNN | standard deviation of RR intervals

SNS | Sympathetic nervous system

TN | True Negative

TP | True Positive

1. Introduction

Heart rate is one of the most studied areas in medicine and science, being an important indicator of homeostasis, but also of adjacent conditions that may affect the autonomic nervous system, and consequently, the equilibrium of the human body. However, there is so much still under research, and with the goal to understand the human heart and its influence in the human body, one must consider all the processes that lead to the development of such important mechanisms. Therefore, it is very important to comprehend not only the adult heart and its influences in the human body, but also the newborn one. This aim is more difficult to achieve due to the constant developmental processes occurring.

The study and understating of heart rate variability is even more significant in infants admitted to the Neonatal Intensive Care Unit (NICU) with hypoxic ischemic encephalopathy condition, where, besides brain activity, heart rate variability is monitored in periods of several days, with the purpose of a better understanding of all the underlying physical processes.

In the case of HIE newborns, cooling therapy (also referred as hypothermia) is used as a preventive-therapeutic method: reduces death and improves survival without disability after moderate or severe neonatal encephalopathy. Nevertheless, there are two major issues in ensuing optimal hypothermia neuroprotection in clinical practice. The first point is that cooling is effective only if initiated within six hours of birth. Early detection of moderate encephalopathy is a challenge, as the clinical status of the neonatal encephalopathy evolves over the first few days after birth. This can lead to several mistakes in the NICU, where subjects were submitted to treatment unnecessarily, whereas many newborns were initially considered to have no or mild HIE, and hence not offered cooling, develop signs of moderate encephalopathy after six hours of age, leading to adverse outcomes. The second issue is that hypothermic neuroprotection may be lost if the baby is stressed during cooling. Preclinical work has shown that cooling therapy in un-sedated and stressed piglets is not neuroprotective [1, 2]. In the absence of trustful methods for real-time stress monitoring, clinical staff frequently rely on shivering and increase in heart rate to access stress, which is not ideal, since that shivering is not that common in this group of babies, due to brown fat metabolism and cooling therapy, which reduces heart rate. Besides, there are no valid pain assessment tools for newborns undergoing hypothermia therapy.

The two issues evolving the one therapy that currently is capable of reduce death and improve survival without severe consequences, demonstrate two unmet needs: a widely usable cotside non-invasive tool for accurate identification of “at-risk” HIE newborns, within six hours of birth and an accurate real-time stress monitor for the same group, which can guide clinical staff and parents into offering more responsive and individualised care. Thus, heart rate variability analysis presents an untapped potential to be a bedside biomarker of neonatal encephalopathy, brain injury and stress monitor in hypoxic ischemic encephalopathic newborns, through electrocardiography (ECG).

Like any other physiological parameter’s acquisition, it is extremely difficult to obtain only the desired information without artefacts, especially in the case of HIE newborns, where the presence of those in ECGs records is increased by several factors such as medical examinations or electronic equipment nearby. Artefacts are defined as any distortion of the signal caused by diverse sources, being physiological or non-physiological features. They disrupt the data, influence and camouflage the real and correct information of the patient’s health, and, therefore, respective HRV parameters, which leads to a wrong prognosis and/or treatment options.

Thus, there is an urgent need to develop a method that automatically detects artefacts in neonatal electrocardiograms, being employed by users with different backgrounds, preventing the extensive and time-consuming manually checking of all the data, by researchers and clinical staff. Also, a method

using complexity science applied to heart rate, can identify situations of stress without being invasive or prolongated, is beneficial in the cases present above.

Although there are many algorithms regarding artefacts in adult ECGs, few perform well in newborns ones, due to all the differences and peculiarities in the signal. This is the principal motivation of this dissertation project: the creation of an algorithm capable of identifying and marking artefacts in newborn ECG data, mainly dealing with mathematical aspects of beat to beat time. With this in mind, the algorithm proposed will be focused and personalised according to the type of ECG and consequently artefacts presented. The development of a method that automatically detects noise in neonatal ECG would avoid time-consuming visual assessment of all the data, like mentioned before, but also, be an addition to the signal processing tools that already exist.

The second aim of this dissertation is the creation of a method, using heart rate variability, to identify and predict stress in newborns. Using several clusters applied to the pos-processed data with complexity science, it may be possible to distinguish different states of stress during a period of time. Being complexity science very sensitive to the presence of artefacts in the data, the utility of the algorithm proposed in the last paragraph is also increased.

Both algorithms were created and developed in a basis of trial-and-error, since this is the first approach on the project. To do it, several methods of analysis and artefacts detections were created, comparing those results with manual annotations and calculations of several classification parameters, such as Recall or Accuracy. In the section Methods, all the algorithms are described with a higher level of detail. The next steps were analysing all the results and understand which aspects of the methods could be improved.

As is understandable, not all attempts for each algorithm could be detailed in this dissertation, so only the successful attempts are detailed, and the respective results are included in the Results chapter. Furthermore, a discussion of the algorithm's results is also present, followed by a conclusion for this report, with some topics to reflect upon future work on this research area.

2. Theoretical Background

2.1. Biosignals

Recording a signal to understand the cause of a problem is a common practice in medicine and healthcare.

Biosignal, also called as bioelectric signal, is the definition of all types of signals originated due to the physiological processes in the living beings [3], which can be measured and monitored continuously, typically recorded as univariate or multivariate time series. These vital signals permit the probe the state of the underlying biological and physiologic structures and dynamics [4].

There are numerous types of biosignals, ranging from electrical to mechanical. They can be classified as: biochemical, biomechanical, biomagnetic, biooptical, bioimpedance and bioelectric signals. The bioelectric signal is unique to biomedical systems [4]. These signals are generated by muscle cells and nerves: in this situation, an action potential is measured with surface or intramuscular electrodes, where the electrocardiogram, electromyogram and electroencephalogram are examples of such signals.

Bioelectric signals are considered to be the most important biosignals [4], due to the fact that the majority of biosystems use excitable cells that can be used as biosignals to study and monitor the main functions of the system.

In biomedical applications, as in many other applications, the acquisition of the signal is not enough. It is necessary to process it to get the relevant information, since the detected signals are frequently corrupted with noise. Also, frequently the information cannot be readily extracted from the raw signal. For this reason, the signal must be processed to reach useful results [4]. The developments in medicine and computer science improved the tools and the knowledge to correctly analyse and understand the significance of a particular feature extracted from a biosignals. Several techniques: time- or frequency-domain methods including filtering, averaging, spectral estimation are used for such purpose. The recent progress of digital technology makes digital rather than analog processing more efficient and flexible, in terms of both hardware and software. As referred above, regarding signal processing, digital techniques bring more advantages: the facility of implement complex algorithms, the performance is generally more powerful, and the accuracy only depends on the round-off error and truncation, whose errors can be controlled by the designer [4].

2.2. Electrocardiography

The electrocardiography (ECG) constitutes a recording of the heart's electrical activity that occurs successively over time [5], and is one of the parameters acquired in several healthcare settings.

Figure 2.1. contains features that correspond to different event in the cardiac cycle. The P wave corresponds to current flows during atrial depolarization and PR interval represents the onset between atrial and ventricular depolarization [5]. The most predominant feature of the ECG is the QRS complex, result of ventricular depolarization. Furthermore, the T wave is the representation of ventricular repolarization. The atrial repolarization does not usually show on an ECG record because it occurs simultaneously to the QRS complex [6].

An action potential is generated when a muscle contract. After that, there is an absolute refractory period, which for cardiac muscle, lasts approximately 250 ms. During the period mentioned, the cardiac muscle cannot be re-exited, which results in an inability for heart contraction [7]. For this reason, a theoretical heart rate limit is about 4 beats per second or 240 beats per minute.

The newborn's ECG characteristics are different from the adult ones. The most significant difference is the heart rate (HR): the neonate's heart rate is normally faster than in adults, where the newborn normal resting HR is between 90-190 beats per minute (bpm). Furthermore, the QRS duration and the PR interval (distance between P wave and R peak) tend to be shorter, due to the smaller heart size [8].

Another significative difference, and the main purpose of this dissertation is the existence of more artefacts and noise in newborn's ECG, when compared to adult ones. The acquisition of these exams is done under a stressful medical environment, where is normal that the newborn is submitted to several medical exams, which can cause many movement or missing leads. The presence of innumerous electronic devices, such as ventilators, monitoring devices, among others near the newborn can also influence the present of electromagnetic interference.

Regulation of the heart in neonatal period has its own peculiarities, based on biochemical, morphological and other differences not only in cardiovascular system, but also in the autonomic nervous system (ANS) [9]. Since the referred system has two components (sympathetic and parasympathetic) that control the rhythm of the heart, the study of its electrical activity and variability, with resource to ECG records, gives a non-invasive assessment of the autonomic control of heart rate, via both the sympathetic and parasympathetic nervous system [10].

In cases of illness after delivery, the normal practice is to measure and monitor the heart rate and not acquire the ECG. This represents a disadvantage in the sense that several methods, such as time and frequency domain, but also complexity science, can be applied to study different features obtained with resource to the electrocardiogram. These types of analysis can be more beneficial in terms of quantification if the sympathetic and parasympathetic components of the ANS, being useful in terms of medical diagnosis and decision.

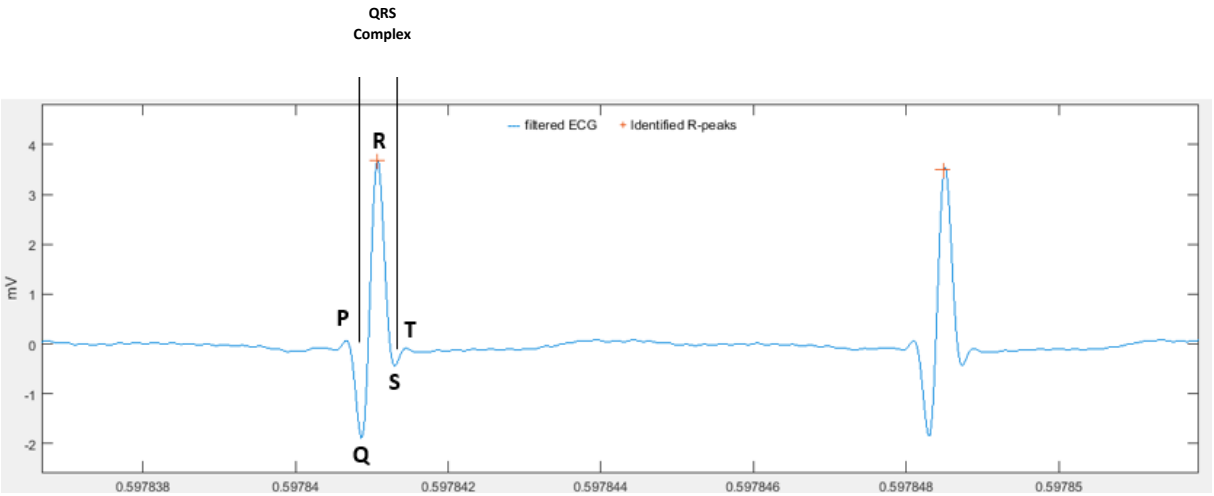

Figure 2.1 - Example of a newborn ECG in normal sinus rhythm.

2.3. Heart Rate Variability

Every system can be described with a mathematical model. Having its basis in mathematics, chaos theory is focused on the behaviour of dynamical systems that are extremely sensitive to initial conditions [11]. While healthy biological systems demonstrate spatial and temporal complexity, disease can involve either a loss or increase of complexity [12]. The heart experiences accelerations and decelerations on its rhythm, mathematically non-linear and complex. These fluctuations in the time intervals between adjacent heartbeats are called heart rate variability (HRV); Thus, heart rate is the number of heartbeats per minute [13].

HRV is the result of autonomic nervous system (ANS) regulation of the sinoatrial (SA) node, where ANS has two components: sympathetic and parasympathetic nervous system [14]. Sympathetic activation generates an increase in heart rate with a norepinephrine release at SA node pacemaker cells, while parasympathetic activation triggers a decrease in heart rate via acetylcholine [14].

In newborns, the evaluation of heart rate variability gives a significant information regarding the maturation and current dynamical balance of the ANS as well as the capacity of the heart to react to the regulatory commands [9]. The HRV values in newborns are also influenced by several factors, among which genetics determinants, mode of delivery, gestational and postnatal age [9].

2.4. HRV Analysis Parameters

The analysis of heart rate variability has been increasingly used and improved, in order to upgrade the estimation of the state of human body and mind [15]. While the clinical use with the purpose of diagnosis of the ECG is well understood, less is known regarding how to utilise it for the study of the balance between the sympathetic (SNS) and parasympathetic (PNS) nervous system, and hence mental physical stress levels [16].

With resource to an electrocardiogram, by identifying the QRS, it is possible to get time series of the heart rate variation over time. One of the most important indices, the cardiac beat-to-beat interval (RRi), is obtained by calculating the intervals between two consecutive occurrences of QRS complexes. When compared to the raw ECG, this parameter contains more informative basis for further analysis [15]. It is important to refer that in some literature, the term to define the successive heart beats, RRi, is also defined as the normal-to-normal interval (NNI).

In terms of recording time, the recommended length is 24h for a long-term and 5 minutes for short-time monitoring [17]. While the short-time recording offers several advantages, for example, easy application and post-processing, the long-term recording can keep track of physiological regulations related in overall HR changes, including day-night difference [18].

For stress assessment RRi time series are used, normally with time and frequency domains, but also non-linear metrics analysis, that reflects the structural complexity of the signal.

2.4.1. Time domain analysis

Using measurements of the RRi it is possible to obtain time domain indices of HRV, which quantify the amount of variability from one heart beat to another. Normally, the processing algorithms are applied to sliding time windows of the RRi time series, with the length of the window depending on the purpose of the analysis. These time windows can range length from less than a minute up to 24 hours, depending on the influence of time variance on the parameter desired.

One of the most important parameters regarding the analysis of the variation of the heart is the standard deviation of RR intervals (SDNN), measured in milliseconds (ms). Several articles indicate

that the conventional recording standard is 5 minutes [19], but there are also researchers' proposals of ultra-short-term recording periods from 60 s [20] to 240 s [18]. SDNN is a very important parameter regarding medical precision in terms of cardiac risk. The values of this parameters differ significantly when comparing healthy adults to newborns. For adults the mean of SDNN is around 100 ms [21], whereas in newborns, with 72 hours of life, the mean is 47 ms [22].

$$SDNN = \sqrt{\frac{\sum_{i=1}^{N}\left[Ri - \left(\frac{1}{N-1}\sum_{i=1}^{N} Ri\right)\right]}{N-1}} \quad \textbf{(2.1)}$$

R_i is the inter-beat interval and N is the total number of RR intervals.

RMSSD is the abbreviation for square root of the mean of the sum of the squares of difference between successive RR intervals. RMSSD expresses the cardiac beat-to-beat interval variance in heart rate. Below is the equation that defines RMSSD:

$$RMSSD = \sqrt{\frac{\sum_{i-1}^{N-1}(R_i - R_{i+1})^2}{N-1}} \quad \textbf{(2.2.)}$$

Where N is the total number of RR intervals in the evaluated signal and R_i is the inter-beat interval.

This index is one of the time-domain measures utilised to predict the vagally mediated changes reflected in HRV [19]. Similar to the parameter above, recording time is recommended to be 5 minutes and researchers have proposed ultra-short-term periods of 10 s, 30 s and 60 s [19].

pNN50 defines the proportion of number of pairs of successive RR intervals that differ by more than 50 ms, divided by total number of RR intervals. This parameter is closely correlated with PNS activity [23], but also with High Frequency Power and RMSSD. On the other hand, pNN25 is ruled by the same purpose as the above parameter, but with a difference of 25 ms. This index is often applied to newborn and children HRV analysis.

2.4.2. Frequency domain analysis

Although the time-domain measures described above give important information regarding the heart rate changes, they do not necessarily indicate if it was caused by the SNS or the PNS. Due to a clear dominance of a deterministic component in either system, the structural complexity of the RRI time series can decrease [15]. Frequency domain analysis can be indeed useful, since they manifest in two non-overlapping frequency bands: low and high.

Importantly, the PNS is responsible for the homeostasis of the body and the SNS controls the body's responses to a perceived threat, being also in charge for the "fight or flight" response [24]. It has been previously accepted that the high frequency (HF) power in HRV reflects PNS activity influenced by vagal control, while low frequency (LF) power is multifaceted and was before believed to represent SNS [25]. Vagus nerve is a motor and a sensory nerve. It is a functionally diverse nerve, offering many different modalities of innervation. The efferent fibers are distributed to the involuntary muscles of diverse organs, among which the heart.

Sympathovagal balance reflects the autonomic state resulting from the sympathetic and parasympathetic influences [26]. In order to indicate sympathovagal balance, the ratio of the power in

the LF and HF frequency, the LF/HF ratio is indicated [27]. Nevertheless, due to the nonlinear behaviour of the vagus nerve, the LF/HF is not a trusty indicator of stress, as the LF band reflects both SNS and PNS activity [28]. Previous work [29] demonstrated that to the average heart rate of the subject, LF was directly related, while HF was indirectly related. As a result, researchers affirmed that LF/HF varied depending on the heart rate: lower at slower and higher at faster heart rates. The conclusion was that the heart rate can influence LF/HF independent of changes in cardiac autonomic nerve activity.

The values for different frequencies vary significantly between different group ages. For adults, the activity of the SNS influences the LF band of the HRV, from 0.04 to 0.15 Hz, while the PNS is represented by the HF band, from 0.15 to 0.4 Hz [17, 30]. In newborns, the low-frequency band varies between 0.04 to 0.02 Hz and the high-frequency 0.02 to 2 Hz [30].

2.5. ECG Artefacts

Noise is inherent in most measurements systems and often the limiting factor in the performance of a medical instrument. By definition, noise is considered to be a part of the real signal that confuses analysis and artefact is defined to be any distortion of the signal caused by diverse sources, such as patient movement, respiration, intermittent or detached electrodes and also electromagnetic impedance [31].

In practice, it is possible to observe different kinds of perturbations in heart rate data: baseline wander or amplitude changes which can cause missed detection, external noise or electrode motion which results in bad detection, power noise and physiological perturbations such as ectopic beats [32].

Given the long periods of time of acquisitions of various physiological parameters, it is normal that some disturbance may occur in those exams, coming from physical sources. Thus, artefacts, corrupt the integrity of data, and may even lead to wrong diagnosis and therapeutic decisions.

Analysing **Figure 2.2**., is clear the presence of a periodic artefact, with a consistent frequency, representing the interference of an electronic device.

With visual inspection, in **Figure 2.3.** it is clear that, although the complex QRS is clear, the baseline is changed, due to a movement occurred at the acquisition.

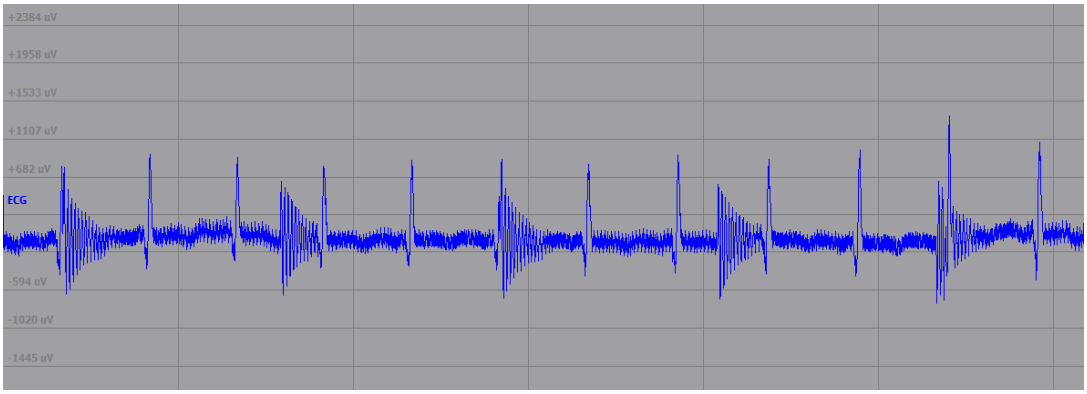

Figure 2.2 - Example of electromagnetic interference artefact.

Figure 2.3 - Example of movement artefact.

2.6. Complexity Science

Biological control systems do not often behave in a linear manner. Quantifying the complexity of these signals in health and disease has been the focus of substantial attention [33-35]. Structural complexity can be interpreted as the manifestation of intricate inter-connectivity of elements within a system and between a system and its surroundings. Nonlinear analysis in the form of structural complexity has recently been used to quantify the degree of randomness in signals [25], especially in the identification and quantification of stress.

Entropy is defined as the loss of information in a time series or signal [36]. Traditional entropy-based algorithms quantify the regularity or orderliness through the amount of structure in a considered time series.

Currently, the most commonly used methods for biological data are approximate entropy (ApEn) and sample entropy (SampEn), but also multiscale sample entropy (MSE) and recently, fuzzy entropy (FuzzyEn). There are common input parameters for all the methods: *m*, the length of data that will be compared; *r*, the similarity criterion and *N*, the length of the data. Typically, for clinical data in adults, *m* is to be set at 2, *r* to be set between 0.1 and 0.25 times the standard deviation of the data and *N* as 1000 [33]. Like expected, the confidence and accuracy of the entropy estimate improves as the number of matches of length *m* and *m*+1 increase. Although *m* and *r* are critical in determining the outcome of either method for entropy estimation, no guidelines exist for optimising their values [33].

Pincus and co-workers developed ApEn as a measure of regularity to quantify levels of complexity within a time series [37]. ApEn is approximately the negative natural logarithm of the conditional probability that a dataset of length *N*, having repeated itself within a tolerance *r* for *m* points, will also repeated itself for *m*+1 points. $C_i^m(r)$ is the number of $j \leq N-m+1$ such that $d[x(i), x(j) \leq r)/(N-m+1)]$. The parameter *r* is commonly expressed as a fraction of the standard deviation of the data and, in this way, makes ApEn a scale-invariant measure. We can define:

$$\Phi^m(r) = (N-m+1)^{-1} \sum_{i=1}^{N-m+1} \log(C_i^m(r)) \qquad \textbf{(2.3.)}$$

Approximate Entropy is defined as:

$$ApEn = \Phi^m(r) - \Phi^{m+1}(r) \qquad \textbf{(2.4.)}$$

Years later, Lake et al [38] developed Sample Entropy. This measure uses the conditional probability of the dataset chosen (with length *N*), having repeated itself for for *m* +1 points. Then it calculates the negative natural logarithm of the product described above. This method doesn't allow self-matches, contrary to Approximate Entropy.

The principal reason for the creation of this method was the reduction of ApEn bias, but also having a closer agreement with theory for datasets with known probabilistic content. It is important to refer that bias is a feature of a specific technique or if its results whereby the expected value of the results differs from the true underlying quantitative parameter being estimated. ApEn have two poor properties in practice: is heavily dependent on the record length and is uniformly lower than expected for short records; also, it lacks relative consistency. In other words, if ApEn of one data set is higher than that of another, it should, but does not, remain higher for all conditions tested. In several studies, SampEn has demonstrated more consistent results than ApEn [38, 39].

The entropy measures above described are maximized for completely random processes and are used to quantify the regularity of univariate time series on a single scale.

In 2002, multiscale entropy was proposed by Costa et al [35]. This method evaluates sample entropy of coarse grained (averaged over increasing segment lengths) univariate time series. The underlying idea is that course graining defines temporal scales. Hence, a system without structure would exhibit a rapid decrease in entropy with an increase in time scale.

The MSE procedure is more complex than the above ones. Given a one-dimensional discrete time series $\{x_1, \dots, x_i, \dots, x_N\}$, it is construct coarse-grained time series, $\{y^{(\tau)}\}$, determined by the scale factor, τ, according to the equation:

$$y_j^{(\tau)} = \frac{1}{\tau} \sum_{i=(j-1)\tau+1}^{j\tau} x_i \qquad \textbf{(2.5.)}$$

With $1 \leq j \leq \frac{N}{\tau}$. For scale one, the time series $\{y^{(1)}\}$ is the simply the original time series [35]. The length of each coarse-grained time series is equal to the length of the original time series divided by the scale factor, τ. Then, an entropy measure (SampEn) is calculated for each coarse-grained time series and plotted as a function of the scale factor τ.

To sum up, MSE is based on the simple analysis that complex biological and physical systems normally demonstrate dynamics that are far from complete regularity and randomness. Instead, complex dynamics typically reveal structure on multiple spatial and temporal scales. These multiscales features, ignored by conventional entropy calculations, are obviously addressed in the MSE algorithm [35].

The phenomenon of statistical stability is the definition for a weak dependence of statistics on the sample size, if the size is large. To overcome the poor statistical stability in the methods before, it was created Fuzzy Entropy [40]. To understand this method, it is important to define Heaviside function:

$$\theta(z) = f(x) = \begin{cases} 1, & if\ z \geq 0 \\ 0, & if\ z < 0 \end{cases} \qquad \textbf{(2.6.)}$$

The belongingness to a given class by whether it satisfies certain precise properties required of membership is judged, when considering an input pattern to Heaviside function.

Chen et al [40] proposed Fuzzy Entropy, where the Heaviside function is replaced by Zadeh fuzzy sets. Zadeh induced the "fuzzy sets" concept. By introducing the "membership degree" with a fuzzy function $\mu_c(x)$ which links each point x with a real number in the range $[0,1]$. This way it is provided a mechanism for measuring the degree to which a pattern belongs to a given class: the near the value of $\mu_c(x)$ to unity, the higher the membership grade of x in the set C. In FuzzyEn, the method described above was introduced and utilised the family of exponential functions:

(2.7.)

$$\exp(-\frac{\left(d_{ij}^{m}\right)^{n}}{r})$$

as the fuzzy function to get a fuzzy measurement of two vectors' similarity based on their shape [40].

As mentioned above, this method achieves a better statistical stability than the ApEn and SampEn. It also adopts the modifications in which SampEn differs from ApEn. Regarding its limitations is the focus only on the local characteristics of the sequence [41] and the application is only to relatively short physiological signals, by using a small embedding dimension *m*.

3. State of the Art

3.1. Hypoxic Ischemic Encephalopathy

Hypoxic-ischemic encephalopathy (HIE) is an evolving pattern of neurological dysfunction following perinatal hypoxic-ischemic injury. This term defines an unexpected complication during birth, which leads to brain injury, due to oxygen and blood flow deprivation to the newborn [42].

According to Volpe [43], perinatal hypoxic-ischaemic injury remains a major cause of neurodevelopmental disability: it is thought to affect between 1 and 6 per 1000 live births and accounts for 23% of all neonates' deaths worldwide [44]. Moreover, 25-30% of survivors develop permanent neurodevelopmental abnormalities [45]. Like expected, in more severe HIE, there is an increased risk of death or neurodisability. The sequels in survivors include sensory and cognitive problems, cerebral palsy and epilepsy [46]. Factors that have been found to be associated with neonatal encephalopathy include maternal thyroid disease, socioeconomic status, antepartum hemorrhage and preeclampsia [47]. Based on the criteria of Sarnat and Sarnat [48], hypoxic ischemic encephalopathy can be classified in mild, moderate and severe. The grading is based on the responses of the infants to handling, level of consciousness, changes in tone or reflexes, presence of seizures and the duration of the symptoms within seven days after birth.

Gressens et al [49] affirmed that hypoxic-ischemic injury leads to periventricular white matter damage in premature infants, whereas term infants develop cortical/subcortical lesions. Recently, whole body controlled hypothermia is used as a preventive-therapeutic method aimed at reducing the consequences above [50, 51].

Hypothermia is kept on the body temperature level around 33.5 °C and after the determined time, the process of the rewarming last about 12 to 15 hours. It starts almost immediately-to 6 hours postpartum and lasts approximately 72 hours. For rewarming, the temperature is increased at a rate of $0.5°C$ every two hours. Several studies [52-54] indicate that hypothermia reduces the release of excitatory neurotransmitters, mitigates abnormal ion fluxes, reduces the formation of edema and lactate, lowers the rate of blood coagulation and reduces the concentration of leukotrienes. The effect of hypothermia or any combination of these factors that complicate cerebral ischemia account for neuronal preservation. Apart from hypothermia, no established therapies exist.

Nevertheless, there are two main issues in guaranteeing optimal hypothermic neuroprotection in the NICUs. The first problem is that hypothermic neuroprotection may be lost if the newborn is stressed during cooling. Previous work [1, 2] has shown that hypothermia in un-sedated and stressed piglets is not neuroprotective. Different cooling trials addressed sedation during cooling, although stress counterproductive effects were recognized in all. This is the reason why the control of HRV is extremely important in these cases. Heart rate variability stands out as one of the most important stress markers [17]. Using time and frequency domains, but also nonlinear metrics, it is possible to monitor any alterations in the autonomic nervous system.

Furthermore, cooling is effective only if initiated within six hours of birth [55]. As the clinical picture of neonatal encephalopathy evolves over the first few days after birth, early detection of moderate encephalopathy is a challenge.

A good ECG data without noisy segments will reduce the probability of camouflage of real information that could lead to wrong prognosis and treatments in these cases. Like mentioned, this is one of the main reasons why the study of newborn's heart rate and the consequent existence of an algorithm that can accurately identify and eliminate noisy artefacts is so important.

3.2. Status of HRV analysis in newborns

In fetal and neonatal period, the regulation of heart has its own peculiarities based on morphological, biochemical and several differences, not only in cardiovascular system, but also in the central nervous system. These peculiarities during early postnatal life are based mainly on the maturity/immaturity of the autonomic nervous system. Besides, several variables such as genetic determinants, gestational and postnatal age, medical conditions and environment can influence heart rate and heart rate variability [56].

As referred before, the short-term HRV reflects a dynamical cardiac regulation, which is conditioned by the activity of the autonomic nervous system and the ability of the heart to react to the regulatory commands. Therefore, an evaluation of the short-term HRV provides and important information about maturation and current dynamical balance of the ANS in newborns.

Important intraindividual stability of HR and HRV was found both in the prenatal period up to the age of two years, which indicates clear "inertia" of cardiovascular characteristics (tracking phenomenon) that is transmitted from prenatal to postnatal life. As expected, the lower the gestational age, the higher the mean HR, lower HRV and blood pressure, being very likely these findings to be related to the degree of maturity of the autonomic nervous system [22, 57, 58].

In their study, Makarov et al [59] found that heart rate declines with increasing postnatal age, whereas in preterm babies the mean HR remains in higher values for a long time.

Regarding to the mode of delivery, there are studies with contrary results. Gonzales and Salirossas [60] demonstrated in their paper that spontaneously delivered newborns had significantly higher HR when compared with neonates born by sectiocesarea or with maternal epidural analgesia administration. With different results shown, Toth et al [61] demonstrated that HR was higher in spontaneously born neonates with epidural analgesia, when compared to neonates with administration of maternal analgesia. Later, Kozar et al [62] demonstrated that there were no significant differences in HR according to mode of delivery, but also in time domain parameters of HRV. Therefore, the use of effective and only a short time acting anaesthetic guarantee equivalent postpartum neonatal adaption, at least in terms of chronotropic regulation of the heart.

The data acquisition of ECG analog signals can vary from research to research. Thoracic ECG lead of portable devices for continuous heart rate recording with a sampling frequency of $1000\ Hz$ and a telemetric transmission of data to pc were used by Javorka et al [9]. In their research, Metzler et al [63] used a bedside cardiorespiratory monitor with a sampling rate of $1000\ Hz$. Kozar et al [62], with the purpose of studying the relationship between gestational term and delivery mode, used three neonatal ECG electrodes placed on the newborn's chest to record the RR intervals, using a telemetric system, with a sampling frequency of $1000\ Hz$. In terms of pos-processing the ECGs Metzler et al [63] filtered using a bandpass between $0.5 - 60\ Hz$ using Butterworth filter with zero-phase distortion. The Hilbert transform and an adaptive threshold detection approach created by Ulusar et al [64] were used to identify the R wave and beat-to-beat interval, all using MATLAB.

In their paper, "Heart rate variability in encephalopathic newborns during and after therapeutic hypothermia", Massaro et al [65] processed the acquired data at $256\ Hz$, using MATLAB. After, ECG data was isolated and bandpass filtered between $0.5 - 70\ Hz$ using Butterworth filter with zero-phase distortion. Like almost every research involving the study of heart rate, the R wave was identified using adaptive Hilbert transform approach [66]. The RR interval was converted into evenly sampled data using cubic-spline interpolation at a sample rate of$4\ Hz$. Goulding et al [30] used the Pan-Tompkins method [67] in order to get the R peaks of the ECG waveforms, in each one hour recording. The time of each R peak was adjusted using quadratic interpolation. Therefore, each ECG file was divided into 5 minutes epochs and all the HRV features ere estimated from those intervals. The interpolation was performed using Hermite splines [68] and the sampling frequency was $256\ Hz$. The frequency-domain

representation of the interpolated RR interval was estimated using a Periodogram [17]. In their research, Lasky et al [69] used Custom Lab View (National Instruments Inc., Austin, Tex., USA) instrumentation to record the ECG from the leads used for clinical monitoring of vital signs. The latencies of the start of the P wave, the start of the Q wave, the Q, R and S peaks, the end of the S wave, the T peak, the end of the T wave, and the peak of the U wave (if present) were measured for 10 consecutive heart beats from segments of stable and artefact-free ECG. Furthermore, the R waves of QRS complexes were identified and a vector of interbeat intervals was generated to analyse HRV. In almost all the literature regarding HRV processing the methods are similar to what is described above.

Temko et al [44] segmented into 60 s the 1-hour HR signal. Normally, a window length of 2 to 5 minutes is recommended to calculate short-term HRV in adults [17]. However, the resting HR of a newborn infant is on average twice for a typical adult. Thus, the window length can be set to 60 s in newborn analysis and a set of 60 features is then extracted from each 60 s epoch of ECG. These features have been used in apnoea studies [48], automated ECG-based neonatal seizure detection [48], sleep monitoring [70], sepsis monitoring [71], central nervous system innervations in adults, and detection of food allergy from paediatric ECG.

3.3. Artefact detection and removal

Electrocardiograms are often corrupted by different types of artefacts and many efforts have been taken to develop their quality by reducing the noise or artefacts. Artefacts in the ECG can lead to the spurious quantification of RRIs, which might result in substantial misinterpretation of the data [72]. Results of Berntson and Stowell [73] revealed that even a single artefact, occurring within a 128-s interbeat interval series, can impart substantial spurious variance into all commonly analysed frequency bands, including that associated with respiratory sinus arrhythmia. They emphasize the importance of artefact awareness for studies of heart period variability [12].

In the study of electrocardiograms, there is a high percentage of ectopic beats. Ectopic heartbeats are small changes in a heartbeat that is otherwise normal, which leads to extra or skipped heartbeats. The most two common types of ectopic heartbeats are premature ventricular contractions and premature atrial contractions, caused by changes in the blood (low potassium level, for example), decrease in blood supply to the heart or enlarged heart. Furthermore, spikes are also present in electrocardiograms. Although most them represent the heart emission of a series of electrical discharges, some assume a bigger and physiologically impossible value, leading to a wrong interpretation of the data. They can be caused by movement or by an electronic equipment near by the acquisition. Thus, the removal of ectopic beats and spikes remains an important point to considered when dealing with artefact removal techniques, due to their influence on the studied data.

Analogue or digital filters are commonly employed to reduce the influence of interference superimposed on the ECG [31]. However, digital filters and adaptive methods can be applied to signal whose statistical characteristics are stationary in many cases. Traditionally, many algorithms for noise reduction in ECG's use either spatial or temporal averaging techniques. Assuming noise to be random and stationary, the noise reduction by the temporal averaging requires a larger number of time frames for effective noise reduction that is proportional to the square root of the number of frames or beats averaged [74, 75]. On the other hand, the main drawback of spatial averaging is the physical limitation of placing a large number of electrodes in the same region [31, 76]. Besides liner noise filtering, numerous adaptive filtering methods have been proposed for separation and detection of the component waves from noisy ECG's. One of those was proposed by Talmon et al [77], describing an adaptive Gaussian filter for detection of the QRS component from noisy ECG's: the adaptive tuning was performed on the frequency response of the Gaussian filter, in order to minimize the distortion of the

undisturbed signal by the filter. In the same field, Thakor et al [78] described a second method for adaptive noise cancellation of ECG recordings and worked on the principle that electromyography noise recorded using two different orthonormal limb leads are uncorrelated.

The quasi periodic pattern of the cardiac signal has also been employed, by synchronizing the parameters of the filter with heart period signal [79, 80]. Another proposed methods include subspace rotations [81], neural networks [82], and bi-spectral analysis [83]. A few years later, some authors applied independent component analysis techniques to enhance the quality of the cardiac signal [31, 82, 84].

Nevertheless, almost all the methods presented above are only partially successful. The first reason is that some of the noise and artefacts are random in nature and have a wide range of frequency content. Because of that, filters fail to remove the interference when it is within the same frequency range as the cardiac signal. The second reason is that the filters often lead to a reduction in the amplitudes of the component waves, the Q-, R- and S-waves or the QRS complex.

Lippman et al [85] analysed several approaches for correcting artefacts in interbeat intervals (IBI), including linear and cubic spline interpolation, nonlinear predictive interpolation and exclusion of ectopy-containing data segments. In linear interpolation, when ectopic beats are identified, the RR intervals immediately preceding and after the ectopic beat are marked for replacement. The total time encompassed by these RR intervals is determined, and the number of new beats that is to be inserted is computed by diving the total time by the average and after the beats to be replaced. In the general case, where a sequence of N RR intervals represents sequential ectopic beats, the number of RR intervals to be insert (B) is:

$$B = \frac{\sum_{j=i}^{i+N} RR_i}{[(RR_{i-1} + RR_{i+N+1})/2]} \qquad \textbf{(3.1.)}$$

After determination of the number of RR intervals to insert, they are computed using linear interpolation, with the sinus-to-sinus RR interval preceding and after those which were being replaced used as the endpoints of the line.

For the cubic spline interpolation, the initial process is the same as described above. To perform the interpolation, four RR intervals (two RR intervals preceding and two after those to be replaced) were used as anchor points already on the "curve", and the RR intervals to be inserted were computed by the method of cubic splines. Regarding nonlinear predictive interpolation, ectopic beats were identified and marked for replacement, and the number of beats to insert was computed as described above for linear interpolation [85]. A sequence of the M RR intervals before and the N RR intervals after the sequence of ectopic beats to be replaced is defined. This step result in a sequence of $M + B + N$ RR intervals, in which the initial M and final N RR intervals are obtained using the values in the RR interval sequence. The factors from the sequence of $M + B + N$ RR intervals are compared with the M and N intervals from all other RR interval sequences that could be obtained from the entire 5-minute listing of RR intervals, which were $M + B + N$ beats long and contain no ectopic beats. With resource of Cartesian distance metric, the closest matching such sequence of RR intervals is found and the middle B RR intervals from the sequence extracted. After these RR intervals are adjusted (in order to their mean would be the same as the mean of the $M + N$ RR intervals surrounding the ectopy-containing segment), they are inserted into the RR interval list in place of the ectopic beats.

In view of these considerations, and the increasing applications of heart period variability measures in psychophysiological studies, an important question arises as to the quantitative impact of unsolved artefacts in the heart period data [73]. This is even more important when working with newborn data, where this group age has significantly more presence of noise and artefacts in ECG records. In

many situations, the "human eye" plays an important role, being considered the gold standard to discern heart rate characteristics. Yet, the visual inspection process used in the conventional filter method is very slow and cumbersome because it requires the presence of a specialist and the handling of a huge amount of data.

One approach to the issue of presence of artefacts in the HR signal has been to exclude those beats that occur outside of a physiologically plausible range [86]. In their work, Wessel et al [87] used a filter based on the adaptive values of the mean and the standard deviation which change and adapt both themselves in a way that follows the variability of the series under analysis. In the same context, Govindan et al [88] proposed a two-step process to correct noisy segments in heart rate data. This process has the aim of replacing spikes with upward deflection and downward deflecting, with the median value of 10 beats starting 15 beats back in time from the current position; if 15 points were not available, it was used the available number of points to calculate the median. In order to do it, it was used the ratio of the local maximum in relation to average of immediate local minima on both sides of the maximum.

Assuming that in the short term time, a normal healthy human RR time series is characterised by a few dominant frequency components which tend to change quite slowly, Clifford et al [89] created a timing threshold system that distinguishes artefacts, ectopy and sinus beats. The classification system is based on the frequency of artefacts occurrences in relation to state changes. In their paper, a state change is considered to have occurred if the mean of the 100 segments before is significantly different from the mean of 100 segments after the considered RR interval, or if their variances are expressively different. Also, they defined the percentage change as ΔRR_n:

$$\Delta RR_n = 100 \times \frac{RR_n - RR_{n-1}}{RR_{n-1}} \qquad \textbf{(3.2.)}$$

Where if $|\Delta RR_n|$ is greater than some threshold λ, the two beats that constitute the current RR interval are defined to be a non-sinus beat pair, and, consequently be ignored. The choice of the threshold depended on the prevalence of artefact, the application and the associated tolerances. However, the use of a strict threshold may lead to problems at stage changes. For example, when the heart rate increase, the ΔRR_n is often greater than 20%. Also, the use of threshold gives rise to either Type I, or more likely, Type II errors, especially when unaccounted interindividual differences in baseline heart rate are present.

ARTiiFACT, a software tool for processing electrocardiograms and interbeat intervals, was proposed by Kaufmann et al [90]. For removing artefacts, this method derives the artefact detection criterion from the distribution of IBI differences of the individual subject and applies percentile-based distribution indices. The next step in this process is to remove artefacts in the first and fourth quartile and estimate the overall standard deviation based on the interquartile range. This way, this method calculates an individual threshold criterion for beat-to-beat differences to identify artefacts.

In their paper, "Heart Rate Variability as a Biomarker for Sedation Depth Estimation in ICU Patients", Nagaraj et el [91], in order to remove artefacts created due to the effect of mechanical ventilation, calculated the differences between adjacent RRI and the inter-quartile range of the absolute value of RRI difference was measured. The outliers above a set threshold of 98% quartile were identified as artefacts which were discarded. The missing samples were later adjusted using a linear interpolation.

Logier et al [32] in their work of algorithm detection, considered a 20's samples moving window, mean m_{20} and standard deviation σ_{20} values, to establish the two thresholds: $m_{20} - 2\sigma_{20}$ and $m_{20} + 2\sigma_{20}$. Therefore, any sample outside the range described is submitted to three conditions: $RR_i < m_{20} - 2\sigma_{20}$ and $RR_{i+1} < m_{20} + 2\sigma_{20}$; $RR_i < 0.75RR_{i-1}$ and $RR_{i+1} < 0.75RR_{i-1}$; $RR_i > 1.75RR_{i-1}$. If the sample agrees with one of these conditions, it is marked as a wrong sample. Otherwise,

it is placed as an indeterminate sample. In such case, all new sample will be stored until the detection of a correct sample, inside of the first threshold or in one of the conditions described.

It is important to refer that artefacts can be treated in two ways: deletion or estimation. In one hand, deleting artefacts prevents incorrect estimation of artefacts IBIs, but unavoidably crops the data set, which reduces data reliability and may bias it, especially when noisy parts are correlated systematically with experimental conditions. On the other hand, interpolation maintains both, the length and structural characteristics of the IBI series, but contains the risk of misestimating the inserted IBIs. In conclusion, the performance of the techniques will depend on the particular application [90].

3.4. Complexity Science and Stress Study

Stress changes the physiological balance of autonomic nervous system. As mentioned before, both components of this system operate simultaneously and balance each other dynamically in normal situations [92]. When stress is given acutely, sympathetic system gets activated to increase the heartbeat and breathing rates, but also the perspiring activity of adrenal glands. When stress is stopped, parasympathetic system takes over to decrease the heartbeat, sweating, and breathing rates [17].

Heart rate variability stands out as one of the most important stress markers [17]; several studies investigated cardiovascular reaction induced by stress using HRV focussing on acute, laboratory stressors: cognitive [93-95], psychomotor challenges [96] and physical stressors [97-99]. Also, real life stressors are often applied [100, 101].

Besides the time domain parameters to analyse the variations in homeostasis [19, 23], frequency domains are also used to describe important information regarding heart rate changes [24, 26]. However, the LF/HF has received some criticism as a measure of cognitive and physical aspects of stress [15]. Accumulating published literature clearly demonstrate the assumption of LF/HF reflect precisely sympatho-vagal balance oversimplifies the complex non-linear interactions between the sympathetic and the parasympathetic divisions of the autonomic nervous system [102-105]. In other words, changes in heart rate do not result from the dimple algebraic summation of the sympathetic and parasympathetic nerve activity.

To overcome it, non-linear metrics are applied within the framework of a complex systems approach to human physiology and serve as a toolset for investigation of complex inter-organ interaction in the body. Several studies in which entropy has been used to assess the effects of stress on signal complexity have concluded that stress reduces the complexity within cardiac signals, supporting the complexity loss theory.

Pincus et al [106] discovered that for different groups of fetuses (acidotic and nonacidotic fetuses) ApEn values were significantly different, affirming that “ApEn appears to be able to detect subtle and possibly important differences in heart rate that are not visually apparent”. In their work, they conclude that larger ApEn values correspond to greater randomness and unpredictability and smaller values to more instances of recognizable patterns or features in data. Caldirola et al [107] showed that patients with panic disorder showed greater entropy in baseline respiratory patterns, indicating higher levels of irregularity and complexity in their respiratory function.

Regarding SampEn, Lake et al [38] found that entropy falls before clinical signs of neonatal sepsis. One important finding is that entropy estimates inevitably fall in any record with spikes.

Years later, Costa et al [35] claimed that MSE consistently indicates a loss of complexity with aging, atrial fibrillation and congestive heart failure.

According to Chanwimalueang et al [25] in their musician’s stress study, before and during performances in both low- and high-stress conditions (with no audience and in front of an audition panel,

respectively), like expected, the cardiovascular reactivity of the participants was pronounced in the high-stress condition. In the nonlinear domain, both multiscale entropy and fuzzy entropy indicated an increase in entropy values from the pre-performance to performance period, this is, from the low-to high stress condition. In the same field, Williamon et al [108] investigate psychosocial stress in public performance, with a single expert pianist. They provided evidence of a reduction in HRV complexity in response to increased stress levels and concluded that the complexity of HRV was expressively lower during the high-stress performance and the SampEn method exhibited better discrimination between the stress conditions, compared with standard spectral analysis.

Vuksanovic and Gal [109] results showed that non-linear measures could detect the influence of arithmetic stress aloud on automatic modulation of the heart rate.

Regarding stress in newborns, less is known, and no study has yet used complexity science applied to HRV as a useful tool to predict and study precisely newborns stress. Lucchini et al [110], in their research related to premature babies exposed to sudden infant death syndrome, proved that entropy measures can be extremely helpful in detecting critical medical conditions.

It is known that the mode of delivery influences the stress response. An article written by Taylor et al [111] shown that baby's stress (salivary cortisol) and crying response to inoculation at 8 weeks was related to mode of delivery, with the greatest response shown in those born by assisted delivery and the least response in those born by elective caesarean section.

More studies regarding oxidative stress exist in the literature [112, 113], although, as referred before, no one uses heart rate variability to predict stress in newborns.

4. Methods

The current chapter focuses on the description of the algorithms developed through this research project. All the algorithms were developed on MATLAB R2017a (The MathWorks, Inc., Natick, Massachusetts, USA).

This chapter contains all the information regarding the ECG acquisition and processing of the data used in this research project.

Furthermore, the first part of this section will consist on an explanation of each noise reduction algorithm's method and their assembly. On a second part, regarding the use of complexity science applied to stress study, the processes are also described.

4.1. ECG Acquisition

The ECG signals that were used as training and testing set were not acquired as part of this project, and therefore the author took no part in the process. However, it is relevant to explain how the data were acquired, for the sake of clarifying.

All the ECGs signals from healthy newborns (aged < 6 hours) were acquired in the NICU from two hospitals in central London: Queen Charlotte's and Chelsea Hospital and Hammersmith Hospital, whereas the ECG signals from encephalopathic babies were acquired in the NICU from five NHS hospitals: Medway, Coventry, Norwich, Newcastle and Imperial NHS Trust. A total of 8 subjects were considered for this project (4 healthy and 4 HIE). Subjects' age and gender were not discriminated.

Electrocardiograms are obtained using 3 electrodes on chest: right upper chest, left upper chest and midline of axillary line, 5th rib, using the device Faros 180 (**Figure 4.1.**), with a frequency sample of 500 Hz.

Figure 4.1 – Example of a Faros 180 device.

4.2. HR Processing Algorithms

The R peaks of the ECG waveforms in each recording were automatically identified using an algorithm developed by Chanwimalueang et al [114]. In their work, they proposed a new method which combines matched filtering and Hilbert transform (MT-HT) to precisely detect R peaks.

The idea of matching filtering is to start from a defined waveform or function and to search for a similar pattern in a time series. By taking the convolution between the conjugate of the defined mother pattern $h(k)$ and the original signal $x(n)$ with length N, the matching filtering is performed:

$$y(k) = \sum_{k=0}^{N-k} h(k)x(n-k) \quad \textbf{(4.1.)}$$

The result of the equation presented above is a high amplitude at times when the time series resembles the mother pattern and a low amplitude elsewhere. This technique is advantageous for locating the QRS complex in the ECG.

Regarding the Hilbert transform is frequently used to extend a real function into the complex domain. The equation is shown below, where $x(t)$ is a real function and the complex output of the transform is $x^h(t)$.

$$x^h(t) = H[x(t)] = \frac{1}{\pi}\int_{-\infty}^{\infty} x(\tau)\frac{1}{t-\tau}d\tau \quad \textbf{(4.2.)}$$

By taking the Fourier transform, it results in a $\pi/2$ phase-lead for a negative frequency and a $\pi/2$ phase-lag for a positive frequency. In an analytic from it can be written as $s(t) = x(t) + jx^h(t)$ in which the Euclidean norm of the complex from is calculated from:

$$|s(t)| = \sqrt{x^2(t) + x^{(h)2}(t)} \quad \textbf{(4.3.)}$$

The amplitude of the norm represents the local maxima or the envelope of signal $x(t)$. Applying the HT to $x(t)$ and computing it magnitude $|s(t)|$ result in a positive envelope of the ECG data which is convenient to locate the R peak within a specific time window.

The MF-HT algorithm is performed by shifting time windows for the length of the ECG time series. All the process is explained in a graphic diagram in **Appendix I**. The former is applied to find several potential QRS that are similar to a template QRS patterns. It utilises a single QRS pattern manually selected once, to avoid artefacts when estimating this complex computationally. In case of multiple ambiguous R peaks, the possible occurrences in time are limited by a dynamical time window which depends on the standard deviation of previously detected RR intervals. Therefore, the selection of the R peaks is computed using the cross correlation between potential QRS and the template. The main feature of this algorithm is the automated R peak search using the MF-HT method and the simultaneous computation of the RR intervals. The R peak detection run automatically until an uncertain peak is found. Also, the program pauses, and the user can select the R peak from various choices: one of the suggested peaks as identified by MF-HF, manually selecting a peak or ignoring the detected peak. The extraction and editing of the HRV from ECG data is facilitated by an interactive graphic user interface (**Figure 4.2.**).

During the preprocessing, a notch filter at the power line frequency and a filter with a passband of $8 - 30\ Hz$ (the frequency range composing the QRS), are applied to the original data. It is important to refer that both filters are 6th order IIR Butterworth filters.

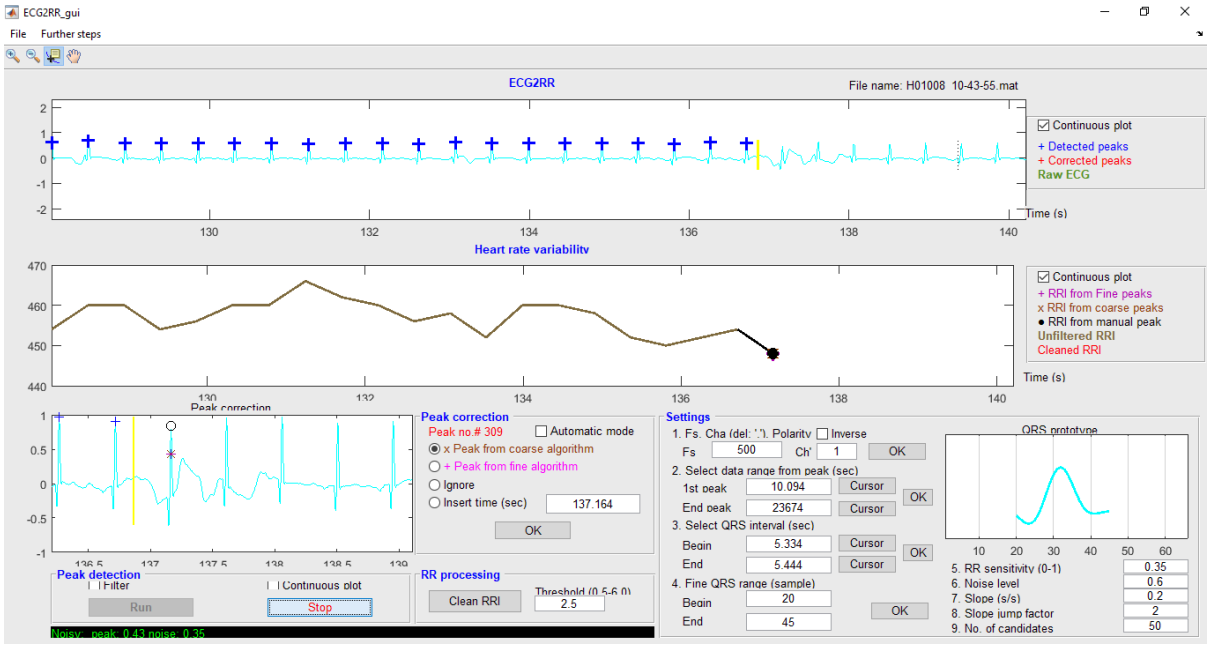

Figure 4.2 – Software for R peak extraction using the MF-HT algorithm.

For the next steps, HRV Analysis Toolbox, created by the group that hosted this dissertation , was used. Although there are no papers published with the method, there are several articles that describe its functionalities [15, 16]. This toolbox has the purpose of processing all kinds of RR intervals and posteriorly obtain the HRV parameters required.

Like the algorithm described before, this toolbox is ruled by the principle of reusable functions and the flexibility of the steps, that can be performed in a user-selected order, added or removed from the main algorithm.

By default, the main steps of this toolbox are: removing unwanted beats; excluding missing segments; detrending; calculation of stress parameters (time domain, frequency domain and complexity); plotting stress parameters over time; plotting stress parameters in 2D and classifying according to scenarios.

In the first step of this algorithm, the purpose is to remove long RRI due to missing heart beats, but also to remove sharp features on these intervals. This method also identifies time windows where too many RR intervals are missing, with a threshold of 30% missing in 20s time windows. Regarding detrending, it removes low-frequency trend that affect parameters such as SDNN and sample entropy. The cut-off is lower than $0.04\ Hz$, which is the lower cut-off of LF.

Although the toolbox was performing relatively well, the resulting parameters of this analysis were wrong and completely different from what was expected. The main reason for this situation was the large number of artefacts and noise present in the analysed ECGs. Due to this, there was an urgent need to implement an algorithm in this toolbox that could precisely identify and reject noisy segments. The development of it is the first aim of this dissertation and is described in the following chapters.

4.3. Artefacts Removal Algorithm

As mentioned in the previous chapter, there was an urgent need to create an algorithm that could precisely identify and reject noisy segments and artefacts in neonatal electrocardiograms, but also to be utilised by users with different backgrounds, where it would be possible to add and remove steps and change the order of them.

Therefore, the first aim of this dissertation was the creation and development of an algorithm that could accomplish the requirements above. For its creation, mathematical aspects of beat to beat time were considered.

It is important to refer that all intervals considered as noise were ignored by the algorithm, by changing their value to NaN (Not a Number). All the steps were run four times for each analysis.

Below are the detailed steps of the proposed algorithm:

Step 1 – Normally, in healthy stages the normal heart rate in newborns can vary between 90-190 bpm [115]. In sick conditions, it can come down until 60 bpm. In terms of RR intervals values, it corresponds to values above 1000 ms, due to the conversion present below:

$$ms = \frac{60000}{BPM} \qquad \textbf{(4.4.)}$$

Therefore, the first step of the proposed algorithm is to exclude all the RRI values above 1000 ms, i.e., below 60 bpm.

Step 2 – In the same context as the step before, Step 2 also works with physiologically impossible values. In stressful events, newborns HR can increase until 200 bpm. For this reason, the present step eliminates all the RR intervals that assume values below 300 ms that correspond to intervals bigger than 200 bpm.

Step 3 – After the elimination of physiological impossible values, another aspect to consider is the abrupt changes in small data segments. This step discards all RR intervals that are outside of a range of +/- 50% of the mean of the last 10 intervals.

Step 4 – Still considering abrupt changes in minor segments of the RR data, Step 4 discard the intervals whose difference from the previous interval is not within 5 standard deviation of the mean of the previous 512 differences. This is also justified by the presence on all ECG waveforms of certain artefact presence caused by clinical interference, myoelectrical noise and other spurious inputs.

Step 5 – After the process with the steps present above, which are more focused on the relations between closer RR intervals, there are still some noisy segments that were not eliminated. In terms of data, this means that, within long segments of excluded data (represented by NaN), there are one or two RR values in the middle of the excluded segment. This situation can induce to artificial and false parameters of HRV. To correct that, all values are transformed to binary: NaN to 1 and RR intervals to 0. After that, it is calculated the sum of intervals of 5, 6, 8 and 10, using MATLAB command *movsum*, depending of which situation above described occurs. Each time a number 0 (correspondent to a RR interval) matches a certain sum of the sliding window (for two existing values, for sums of 6 is 5, for sums of 8 is 6: for one value present, for sums of 5 is 2, 3 or 4 and for sums of 10 is 5) the RR interval value considered will be eliminated (**Figure 4.3.**).

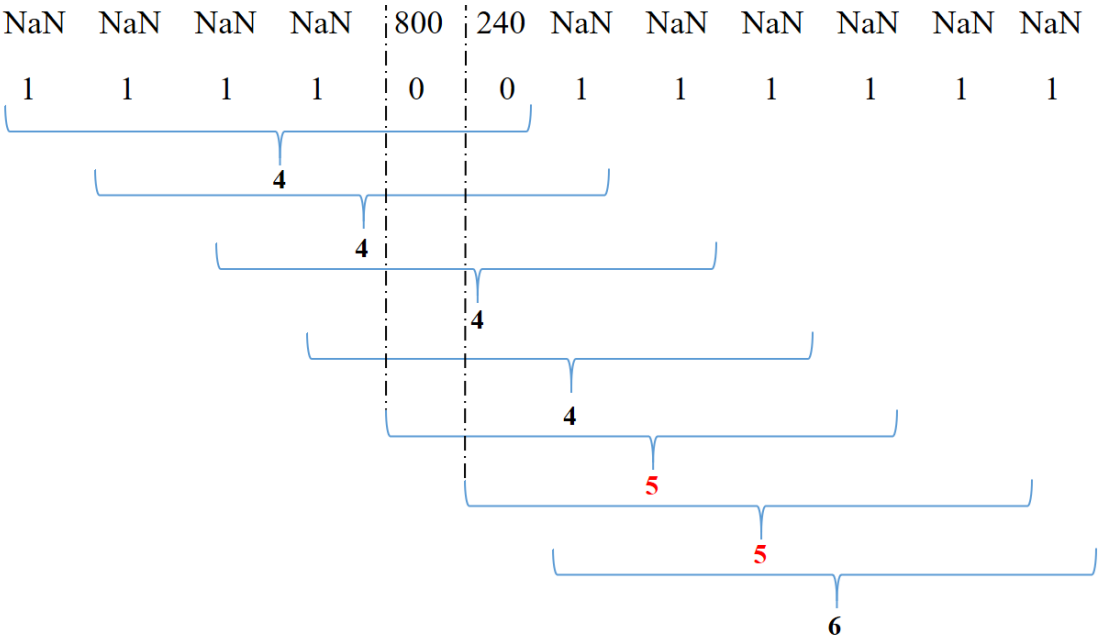

Figure 4.3 – Example of the process developed on Step 5. In this case, sums of 6 were done, to eliminate the RR intervals between the ignored parts.

Step 6 – Based on the paper written by Logier et al [32], considering a 20's sample moving window, mean (m_{20}) and standard deviation (σ_{20}) values are used to establish two thresholds as:

$$[m_{20} - 5\sigma_{20} \quad , \quad m_{20} + 5\sigma_{20}] \qquad \textbf{(4.5.)}$$

This interval includes 99% of the valid RR values. Therefore, 1% of valid values, representing the RR extremes values of the window, will be detected as perturbations. After this first selection, to differentiate between valid samples and perturbations, any sample outside the threshold mentioned before is submitted to three conditions:

$$RR_i < m_{20} - 5\sigma_{20} \; and \; RR_{i+1} > m_{20} + 5\sigma_{20} \qquad \textbf{(4.6.)}$$

$$RR_i < 0.75 RR_{i+1} \; or \; RR_{i+1} < 0.75 \, RR_{i-1} \qquad \textbf{(4.7.)}$$

$$RR_i > 2 \, RR_{i-1} \qquad \textbf{(4.8.)}$$

If the sample agrees with one of these conditions, it is marked as noise.

Step 7 – This step considers the standard deviation of all signal length, after all the steps mentioned before. The purpose is to eliminate (with a 99% confidence interval) all the intervals whose difference from the previous one is not within 5 times the total standard deviation.

Step 8 – The last step also considers physiologically impossible values. In this case, it excludes the intervals which have a difference bigger than 200 ms from the previous one.

4.4. Other Algorithms

Faced with the same problems originated by the presence of noisy segments and spikes in neonatal data, Govindan et al [88] in their paper " A spike correction approach for variability analysis of heart rate sick infants" proposed a two-step process to correct spikes in HR data. Being working with the same objectives as the group the author is insert is, it is beneficial and will improve this dissertation if a comparison between the two methods is done.

Superficially, the first step involves an iterative procedure to correct spikes based on the ratio of the local maxima to their immediate minima, on both sides exceeding a predefined tolerance. The second step involves repeating the first step for different tolerance values. The threshold that yields optimal correction is identified using the root mean square (RMS) of the difference between the corrected HR and the uncorrected HR. The threshold for which RMS was a minimum or remained unchanged for two or more tolerance values is identified as an optimal threshold.

Considering the sequence $x_i, i = 1\ to\ N$ to denote HR. The first step is to identify the local maxima and minima in x_i where a local maximum is defined if a point $x_i > x_{i-1}$ and $x_i \geq x_{i+1}$ and a local minimum is if a point is insert in $x_i < x_{i-1}$ and $x_i \leq x_{i+1}$. For each local maximum, r_i is defined as the ratio of the local maximum to the average of immediate local minima on both sides of the maximum. If there is no local minimum on one of the sides of the maximum, it is used the side for which the minimum is available and then its calculated r_i. The next step is to confirm if $r_i > \epsilon$, the point is replaced with the median value of 10 beats starting 15 beats back in time from the current position. If 15 points are not available, it is used the available number of points to calculate the median. To correct spikes with downward deflection, it is calculated $^{60}/_{x_i}$, which represents the conversion in RR intervals. The sub-steps described before are followed again to correct spikes with upward deflection. At the end of this process, the sequence is converted back to HR.

The steps above mentioned are repeated until the sequence entering a correction step remained the same at the end of the step. In other words, until the sequence requires no further corrections.

For Step 2, Step 1 (described before) is repeated for different values of ϵ. It is calculated the RMS of the difference between uncorrected HR and corrected HR. The correction is considered optimal if either RMS value remained almost the same value for two or more consecutive ϵ values. This indicates that most of the spikes were corrected without compromising the actual RR interval. Mathematically, optimal ϵ^* is identified as:

$$\epsilon^* = min\{RMS_j - RMS_{j+1}\}, j = 1\ to\ n-1 \quad \textbf{(4.9.)}$$

Where n is the number of ϵ values. The total of 21 ϵ values, starting from 1.05 to 2.05 was used, in steps of 0.05.

4.5. Assembling the algorithms

Govindan's method try to accomplish its objective via the identification and replacement of spikes in data, whereas the algorithm proposed by the author is more directed to the identification and rejection of medium to long artefacts occurring in newborns ECGs. In other words, these algorithms try to reach the same objectives with different approaches.

After a discussion with the clinical staff, the idea of a third algorithm, joining both methods proposed before, was suggested, mainly due to its potential on identifying several different types of artefacts in this type of data.

Therefore, according to the type of data that is being studied, the user has the freedom to choose which type of steps are more suitable to insert in the noise removal process.

4.6. Algorithm Validation

After the development of the algorithms proposed in the previous chapter, the validation of them is an important step to consider. The methods had to be checked with visual inspection – the current method available before – to assess if the algorithms were identifying and rejecting artefacts as it should be. This evaluation of the algorithm's performance considered four different classifications: recall, accuracy, precision and F1 score. To support the acquisition of these classifications, the confusion matrix method, frequently used in machine learning, was used. The confusion matrix is a specific table layout that allows visualization of the performance of an algorithm. Each row of the matrix represents the instances in a predicted class while each column represents the instances in an actual class **Table 4.1.** [116].

Table 4.1 – Confusion matrix applied to the algorithm.

		Actual Class	
		Condition Positive	Condition Negative
Predicted condition	Predicted condition positive	True Positive (TP)	False Positive (FP)
	Predicted condition negative	False Negative (FN)	True Negative (TN)

In the case of this research project, the actual class is if the peak is noisy or not. Consequently, the predicted condition is if the algorithm recognise the peak as noisy or not. The True Positive (TP) is defined as all the peaks of signal that represent artefacts and that are marked as that by the algorithm. False Positive (FP) explains the condition of normal peaks that are marked by the algorithm as peaks representing noise. False Negative (FN) is defined as the noisy segments that are not marked as noisy by the algorithm. Lastly, True Negative (TN) describes the condition when a peak is good, and the algorithm considered it as good peak too.

The four different types of classification evaluate algorithm's performance, allowing for its optimization upon training and testing with the data available.

Recall – when the algorithm detects an interval that is indeed a noisy segment. This parameter is calculated when dividing the number of artefacts correctly detected by the algorithm by the overall number of artefacts in the data:

$$Recall = \frac{\#\ artefacts\ detected\ corretly}{\#\ artifacts\ in\ data} = \frac{TP}{TP + FN} \quad \textbf{(4.10.)}$$

Accuracy – it is a measure of statistical bias. This parameter is calculated when diving the number of artefacts peaks marked as noise and the number of good peaks marked as good peaks, by all the number of peaks in the data:

$$Accuracy = \frac{\#peaks\ marked\ corretly}{all\ peaks} = \frac{TP + TN}{TP + FP + FN + TN} \quad \textbf{(4.11.)}$$

Precision – this parameter refers to how close estimates from different samples are to each other. In this case, the calculation is done by diving the number of artefacts detected correctly by the algorithm, by all the peaks marked correctly or incorrectly by the same method.

$$Precision = \frac{\#artefacts\ detected\ corretly}{\#peaks\ marked\ as\ noise} = \frac{TP}{TP + FP} \quad \textbf{(4.12.)}$$

F1 Score – This parameter considers both precision and the recall of the data. It is the harmonic mean of precision and recall:

$$F1\ score = \frac{2}{\frac{1}{recall} + \frac{1}{precision}} = \frac{2TP}{2TP + FP + FN} \quad \textbf{(4.13.)}$$

4.7. Entropy Study

Considering all the advantages in using complexity science to differentiate between different groups, normally healthy and sick ones, several methods were applied to the data used on this dissertation , with the main objective to discover which entropy method performs better to distinguish between groups.

For this analysis and comparison, algorithms of approximate entropy [33], sample entropy [38], multiscale entropy [35] and fuzzy entropy [41] were employed. **Appendix V** and **Appendix VI** describe the algorithms that used the entropy methods mentioned above. It is important to refer that the several entropy methods were not altered from its original process. The selected parameters were: embedding dimension, m, was defined with the value of 3, the tolerance, r was 0.20 times the standard deviation of the data, and the N, the number of points used was 1000.

For defining which scales are more suitable to distinguish the two groups, considering multiscale and fuzzy entropy, the number of points used, N, is bigger than 3×10^4 points, a major value than the previous analysis. By this, the when coarse-grain reach up to scale 20 the shortest time series has, at least, 1500 points.

For fuzzy entropy the order chosen was 2. It is important to refer that the parameters were found empirically.

4.7.1. Multidimensional Entropy Study

To a better understanding how entropy can be useful on determining whether it is a stressful or a normal event, a multidimensional analysis using different entropy methods was proposed. Two different analysis, using in each case 3 methods were employed: Approximate Entropy, Sample Entropy and Multiscale Entropy; and Sample Entropy, Multiscale Entropy and Fuzzy Entropy.

For both cases, as before, the parameters were: $m = 3$, the tolerance, r was 0.20, and $N = 1000$. To identify clusters, it was used the command from MATLAB: $knnseach(X, Y)$. This command finds the nearest neighbour in X for each query point in Y and returns the indices of the nearest neighbours in a column vector. This method first uses the Minkowski distance metric, and then the Chebyshev distance metric [117].

The Minkowski distance is a metric in a normed vector space which can be considered as a generalization of both the Euclidian distance and the Manhattan distance [118]. The Minkowski distance of order p between two points $X = (x_1, x_2, \dots, x_n)$ and $Y = (y_1, y_2, \dots, y_n)$ is defined as:

$$D(X,Y) = \left(\sum_{i=1}^{n} |x_i - y_i|^p\right)^{1/p} \quad \textbf{(4.14.)}$$

Manhattan distance [119], d_1, is a form of geometry in which the usual distance metric of Euclidian geometry is replaced by a new metric in which the distance between two points is the sum of the absolute of their Cartesian coordinates d_1, between two vectors p and q is defined as:

$$d_1(\mathrm{p},\mathrm{q}) = \|p - q\|_1 = \sum_{i=1}^{n} \|p_i - q_i\| \quad \textbf{(4.15.)}$$

Lastly, Chebyshev distance is a metric defined on a vector space where the distance between two vectors is the greatest of their differences along any coordinate dimension [120]. Given two vectors or points, p and q, with standard coordinates p_i and q_i, Chebyshev distance is:

$$D_{Chebychev}(p,q) := max_i(|p_i - q_i|) \quad \textbf{(4.16.)}$$

Density-Based Spatial Clustering of Applications with Noise (DBSCAN) was also employed on this research. It is a density-based clustering algorithm, proposed by Ester et al [121]. This method discovers neighbours of data points, within a circle of radius (in this case $\varepsilon = 5$) and joins them into the same cluster. For any point, that its ε-neighborhood contains a predefined number of points, the cluster is enlarging to contain its neighbours, as well. Nevertheless, for the unallocated points, if the number of points in the zone is less than predefined threshold, the point is considered as noise. By this, this algorithm can also distinguish the normal and noisy data.

5. Results

In this chapter, the results obtained from the previously described methods are presented. To clarify the interpretation process, the results for each step of the algorithms will be shown, as well as an example of every algorithm's result.

The results for the four classification criteria (Recall, Accuracy, Precision and F1 Score) are also presented, as a way of demonstrating the overall results of the algorithm.

Regarding the entropy study involving complexity science, all the comparisons between healthy and sick newborns are demonstrated. The multidimensional study, with different clusters methods, will be also presented in this chapter.

5.1. Silva&Rosenberg algorithm

Silva&Rosenberg was the name given to the artefact removal algorithm created by the author, in partnership with a team in Communication and Signal Processing Group, at Imperial College London.

This chapter will go through an elucidative explanation of the results for each step of this algorithm, clarifying the output of every process within the algorithm. The focus will be in small portions of signal from the 5 hours long samples of data from various subjects. It will be possible to see the raw signal along with the corrections made by the algorithm.

In this sample of signal, it is possible to observe artefacts periods, clearly different from normal signal acquires with ECG. The artefactual periods can vary, depending on the source, from few seconds to minutes. It is important to note that the utility of the steps of the algorithm can vary, depending on the amount and the type of noise present.

The blue lines on the top represent the ECG signal and the orange crosses the R peaks. Below, there are the RR intervals plotted along with the recorded time. The red line indicates the identified and reject artefact.

The following figures illustrate the first steps of the proposed algorithm. In those are represented the exclusion of RR intervals above 1000 ms and below 300 ms, corresponding, respectively, to values below 60 bpm and above 200 bpm. These values are physiological impossible for a newborn heart rate.

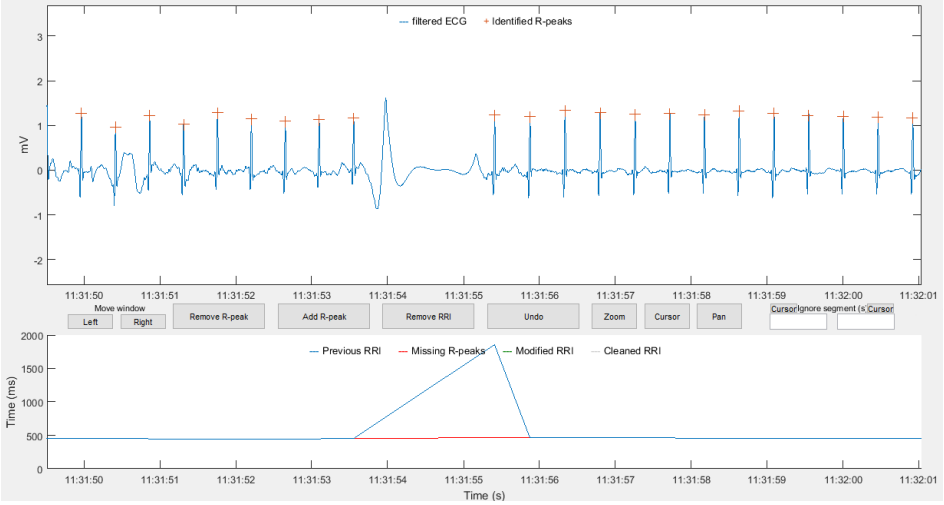

Figure 5.1 – Example of the first step of Silva&Rosenberg algorithm. In this case, a RR interval greater than 1000 ms was rejected.

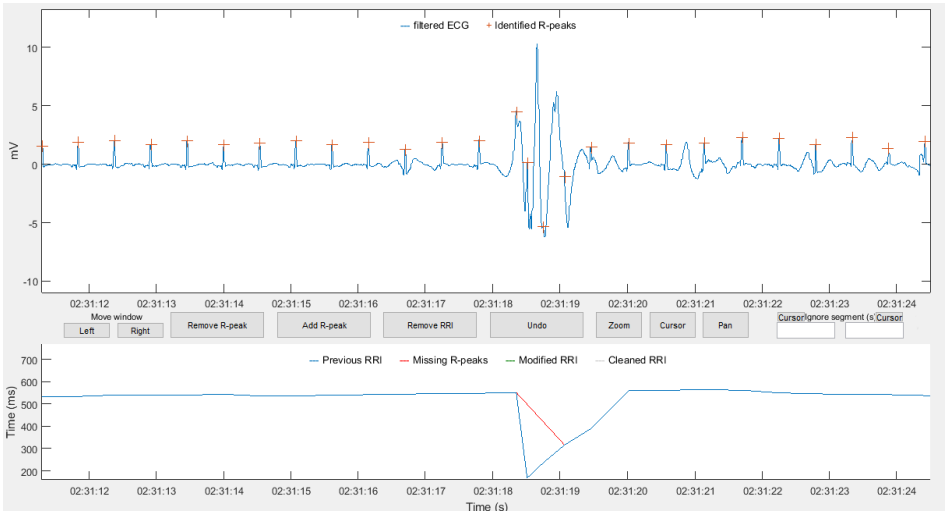

Figure 5.2 – Example of the second step of Silva&Rosenberg algorithm. In this case, a RR interval smaller than 300 ms was rejected.

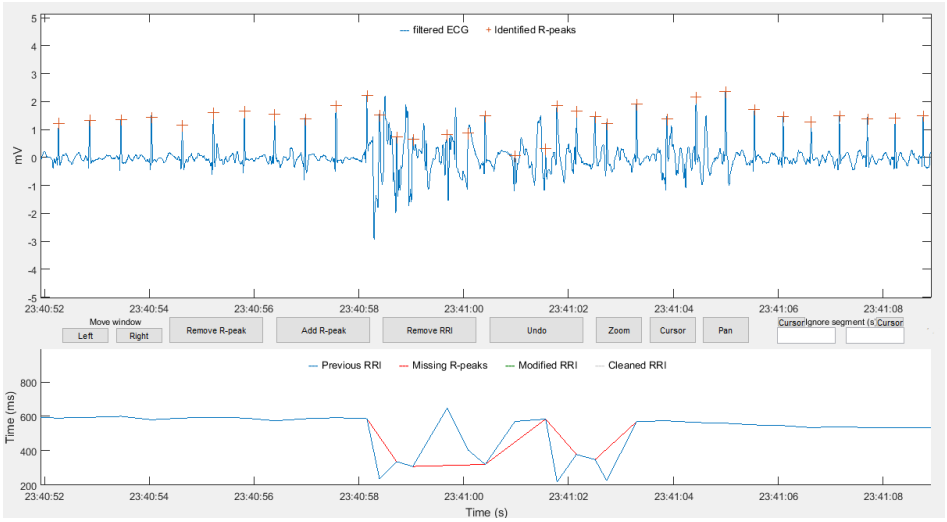

Figure 5.3 – Example of Silva&Rosenberg algorithm.

With the examples above, artefacts caused by missing beats, as shown in **Figure 5.1.** or from other origins, like in **Figure 5.2** and **Figure 5.3.**, can be correctly marked as noise by the algorithm.

On the last figure, it is possible to observe some beats that, on a first approach, may look good for further analysis. However, the peaks on that area are considered as noisy, due to the third step of this algorithm: identification of abrupt changes in small segments. This step discards all the RR intervals that are outside a range of +/- 50% of the mean of the last intervals. Still considering the identification of rapid changes in minor segments, step 4 discards the intervals whose difference from the previous interval is not within 5 standard deviation of the mean of the previous 512 differences. The next figures are examples of these conditions.

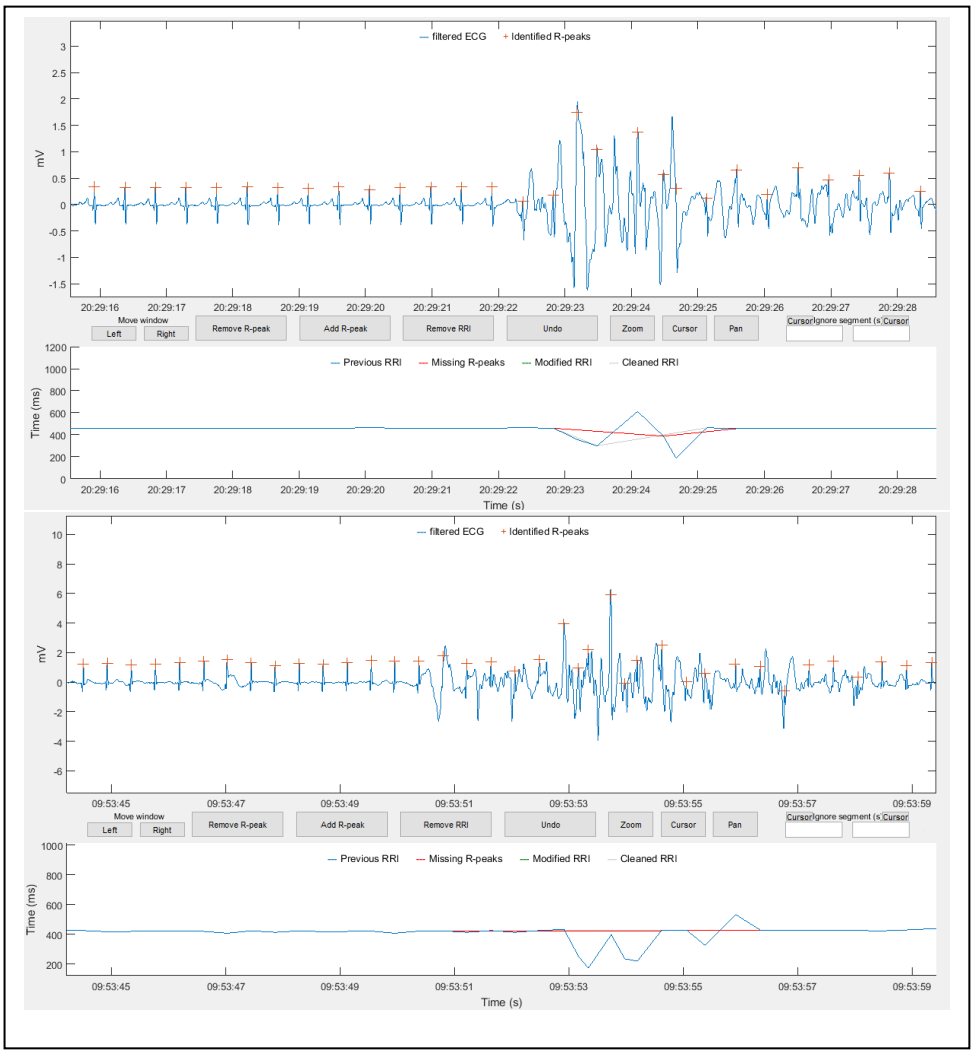

Figure 5.4 – Example of the third and fourth step of Silva&Rosenberg algorithm.

As explained in the chapter Methods, the target of the fifth step of this algorithm are long segments of noise. Succinctly, it eliminates remaining values of RR intervals in long artefacts periods.

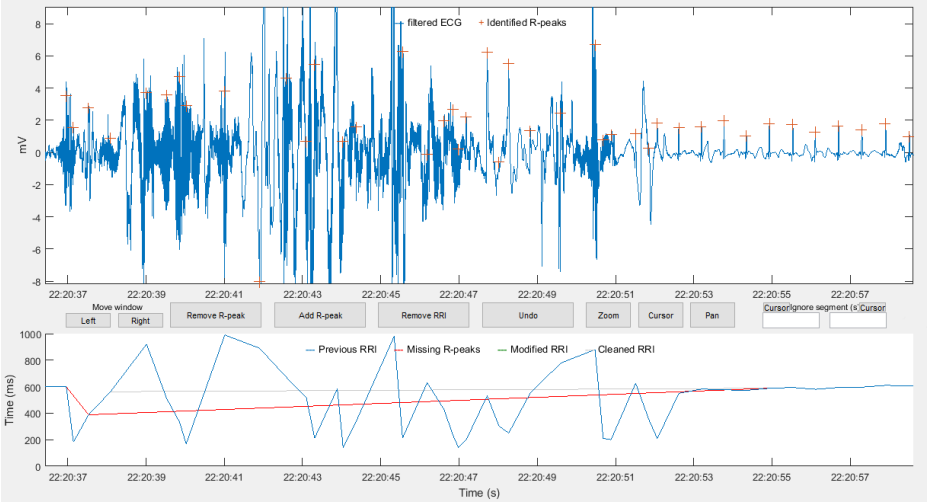

Figure 5.5 – Example of the fifth step of Silva&Rosenberg algorithm.

After all the steps exemplified before, step 6 reutilises the concept of step 3 and 4, with more conditions to the data analysed. Therefore, the next step considers all the length of the signal, and eliminates, with a 99% confidence interval all the intervals which difference from the previous one is not within 5 times the total standard deviation.

The last step excludes the remaining values for the intervals which have a difference bigger than 200 ms from the previous one. Since this algorithm works with time differences, the mentioned step will also identify and reject peaks that have a voltage physiologically impossible, like shown on the figures below.

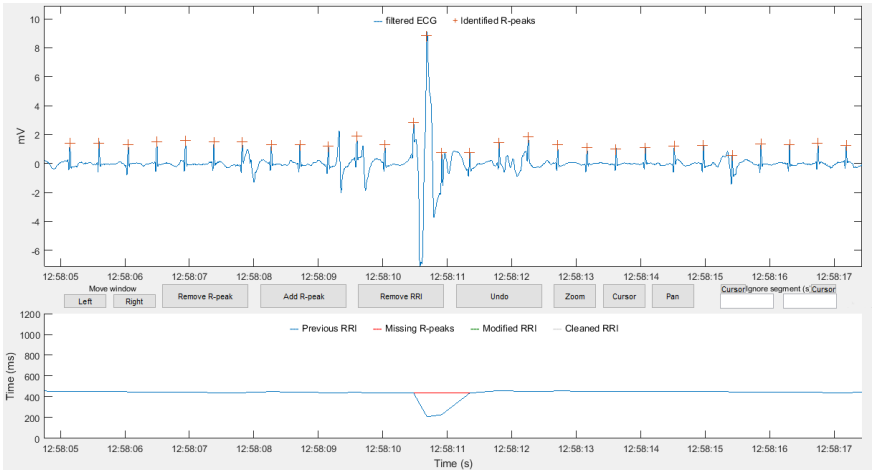

Figure 5.6 – Example of the last step of Silva&Rosenberg algorithm.

Below there are some examples of the output of the data, after the application of the present algorithm, from small to long segments of noise. It is important to refer that the majority of segments present are from HIE newborns, where the presence of ECG artefacts is higher.

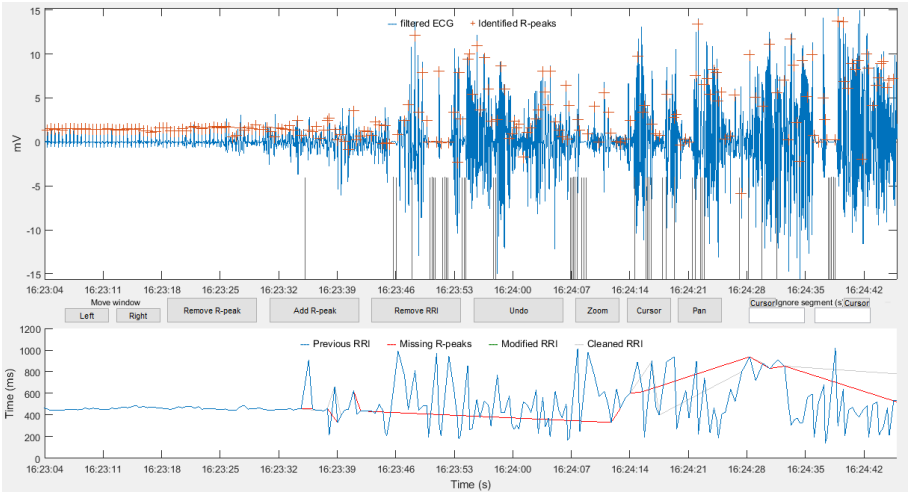

Figure 5.7 – Example of Silva&Rosenberg algorithm performance for long noisy segments.

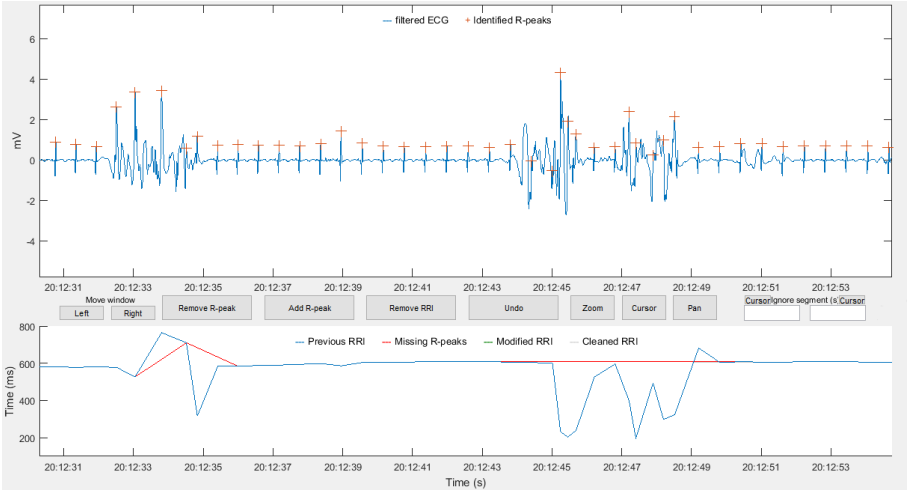

Figure 5.8 – Example of Silva&Rosenberg algorithm performance for short noisy segments.

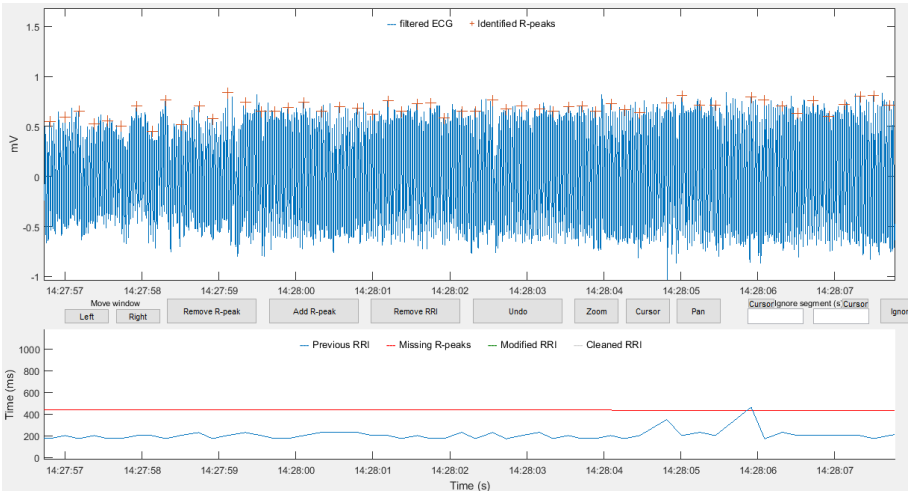

Figure 5.9 – Example of Silva&Rosenberg algorithm performance for electromagnetic artefacts.

Although the algorithm performs indeed well, there are some cases where not all the length of the artefact is identified, as exemplified in **Figure 5.10**. Like expected, these situations will influence the validations parameters for the algorithm proposed.

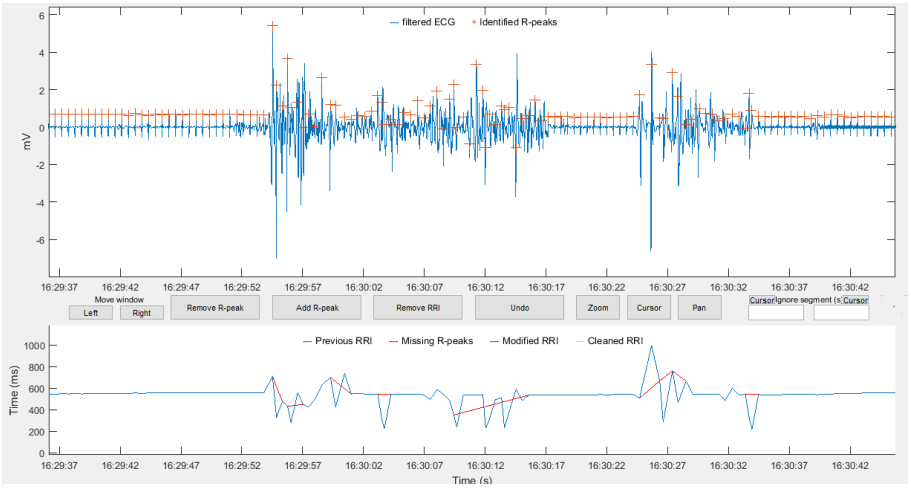

Figure 5.10 – Example of Silva&Rosenberg algorithm error.

Table 5.1. shows the validation results for Silva&Rosenberg algorithm, for all the data analysed. **Table 5.2** presents the mean and standard deviation of all the four criteria. All the process for the obtention of these values is explained in the previous section.

Table 5.1 – Results of Silva&Rosenberg algorithm, for all subjects.

Subjects	Silva&Rosenberg Algorithm			
	Recall	**Accuracy**	**Precision**	**F1 Score**
#1 Healthy	97.50	97.93	98.91	98.20
#2 Healthy	93.53	99.89	96.39	97.94
#3 Healthy	91.97	92.87	95.19	92.04
#4 Healthy	98.26	99.95	98.43	98.34
#1 HIE	94.95	93.83	94.64	94.79
#2 HIE	94.72	95.90	93.41	96.46
#3 HIE	80.75	82.91	82.96	82.35
#4 HIE	94.55	95.77	93.55	95.55

***Table 5.2** – Mean of the results from Silva&Rosenberg algorithm, for all subjects.*

Criteria	Mean ± Standard Deviation (%)	
	Healthy	**HIE**
Recall	95.3 ± 2.6	91.2 ± 6.0
Accuracy	97.6 ± 2.8	92.1 ± 5.3
Precision	97.2 ± 1.5	91.1 ± 4.7
F1 Score	96.6 ± 2.6	92.2 ± 5.7

By observing both tables presented above, it is possible to conclude that all the parameters assume higher values, around 90%, with few exceptions. The main reason for some lower values is exemplified by **Figure 5.10**: although the algorithm identified most noisy intervals, there are some of them that are still considered good. This happens principally because the present algorithm works with temporal aspects of the data.

HIE subjects have lower values for all the parameters, mainly due to the higher presence of artefacts from different sources. This factor is also confirmed by the results presented in **Table 5.2**., where all the HIE parameters have a lower value. For both groups, accuracy assumes the higher value, describing how peaks are correctly marked. Recall, an important type of classification, that translates the number of artefacts properly detected by the algorithm, by the overall number of artefacts in the data, assumes also a higher value on the data from both groups.

5.2. Other algorithms

As explained in the chapter Methods, Govindan and his team [88] proposed a two-step process to correct spikes and consequently artefacts, in HR data. This section will go through an explanation of results for this algorithm, applied to the same data as the Silva&Rosenberg method. The focus will also be in 5 hours long samples of data from the same subjects. Also, a view of the all signal, before and after the alterations will be shown.

The following figures illustrate the performance of this algorithm, with its full signal length. On the top row it is represented the raw HR, the second and the third illustrate the first iteration for HR and RR intervals; fourth and fifth row represent also the same parameters as before, but for a second iteration. The last graphic represents the final output, where in orange there is the post-processed signal.

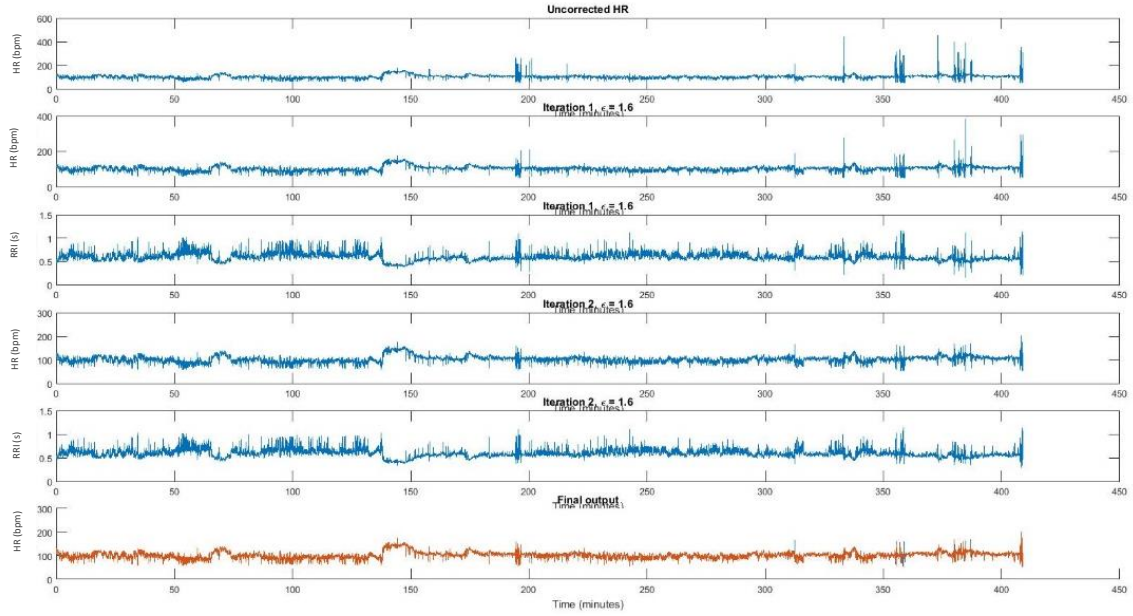

Figure 5.11 – Example of Govindan algorithm process.

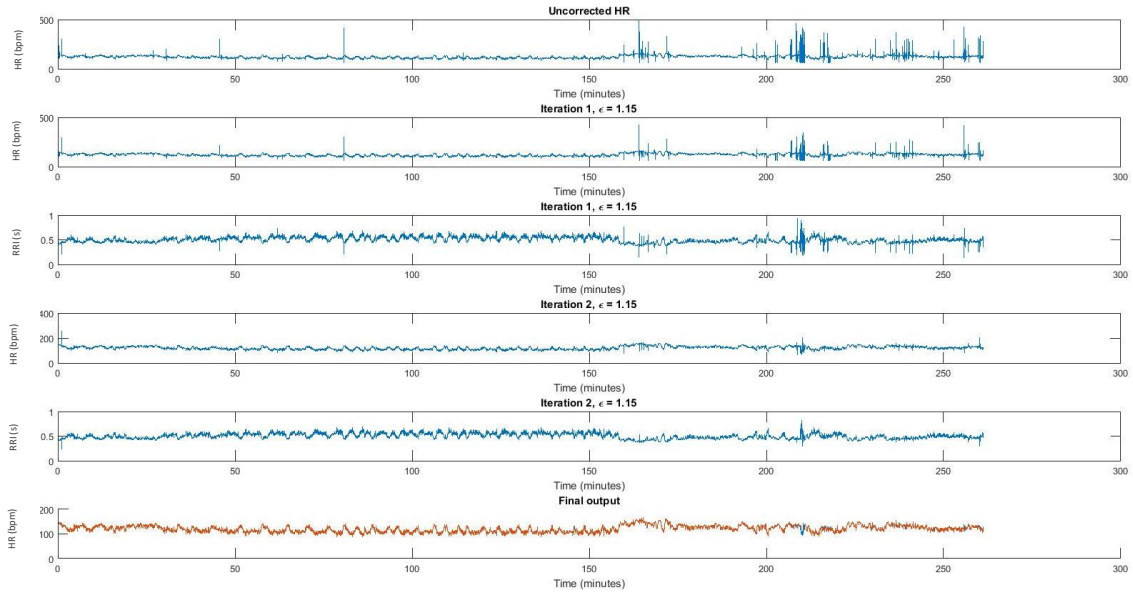

Figure 5.12 – Example of Govindan algorithm process.

It is important to refer that, originally in this method, all the peaks considered as noise would be replaced by a value calculated involving the median adjacent. In the case of this research, all the peaks were replaced with NaN values, like the previous method. Different subjects assume different optimal values, ϵ^*.

Observing the two examples above (**Figure 5.11** and **Figure 5.12**), for spikes or short segments of noise, the algorithm performs well. Regarding extended segments of artefacts, as it can be observed on **Figure 5.11**, the algorithm cannot identify all the peaks on those parts, maintaining artefacts in the final output signal.

Table 5.3 – Results of Govindan algorithm, for all subjects.

Subjects	Govindan Algorithm			
	Recall	**Accuracy**	**Precision**	**F1 Score**
#1 Healthy	46.39	99.18	95.61	62.47
#2 Healthy	79.44	99.12	87.88	83.45
#3 Healthy	64.99	98.28	53.65	58.78
#4 Healthy	37.41	99.48	81.25	51.23
#1 HIE	68.62	98.31	95.14	90.68
#2 HIE	54.94	99.03	98.62	70.57
#3 HIE	54.56	95.52	95.66	69,48
#4 HIE	64.52	96.01	91.88	75.80

Table 5.4 – Mean of the results from Govindan algorithm, for all subjects

Criteria	Mean ± Standard Deviation (%)	
	Healthy	**HIE**
Recall	57.0 ± 16.3	60.6 ± 6.0
Accuracy	99.0 ± 0.4	97.2 ± 1.5
Precision	79.5 ± 15.8	95.3 ± 2.3
F1 Score	63.9 ± 11.9	76.6 ± 8.4

Regarding the tables above, it is evident that the results are scattered, which can be confirmed by the values of standard deviation in almost all the parameters. The main reason for this situation is the different number of artefacts and spikes present, which vary from subject to subject. Like mentioned before, this method is more suitable for data with numerous spikes. Having HIE data a superior number of spikes and, therefore, artefacts, it is normal that in this case, some parameters assume a bigger value, when compared to healthy ones. Even though there are differences on the classification parameters values, precision assumes the bigger difference between groups. Precision refers to how close estimates from different samples are to each other. In other words, it exemplifies the number of peaks detected correctly by the algorithm, by all the peaks marked by the same one. In this case, the algorithm was more precise on HIE data, probably due to a bigger number of noisy segments in these data

5.3. Assembling the algorithms

Considering that both algorithms proposed, although with different approaches, try to reach the same objectives, and their results indicate a better performance for different groups, the idea of combining the two of them into a third algorithm raised, mainly due to its potential on identifying correctly different types of artefacts in ECG data.

This chapter will go through an exemplification and explanation of the algorithm results. The focus will be in small portions of signal from the 5 hours long samples of data from various subjects. It will be possible to see the raw signal along with the corrections made by the algorithm. Graphics illustrating the influence of this algorithm in HRV analysis parameters will also be present in this chapter.

The blue lines on the top represent the ECG signal and the orange crosses the R peaks. Below, there are the RR intervals plotted along with the recorded time. The red line indicates the identified and reject artefact.

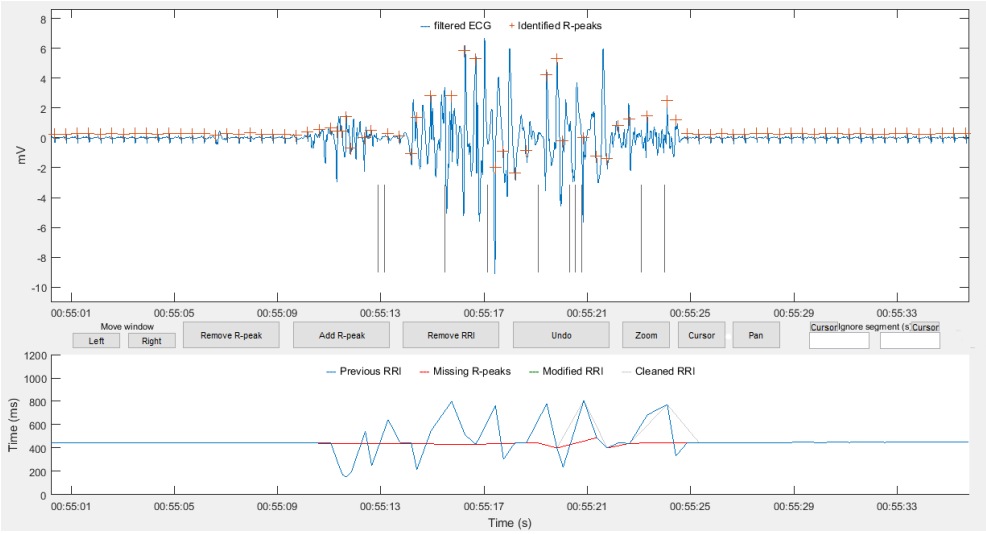

Figure 5.13 – Example of the final algorithm performance.

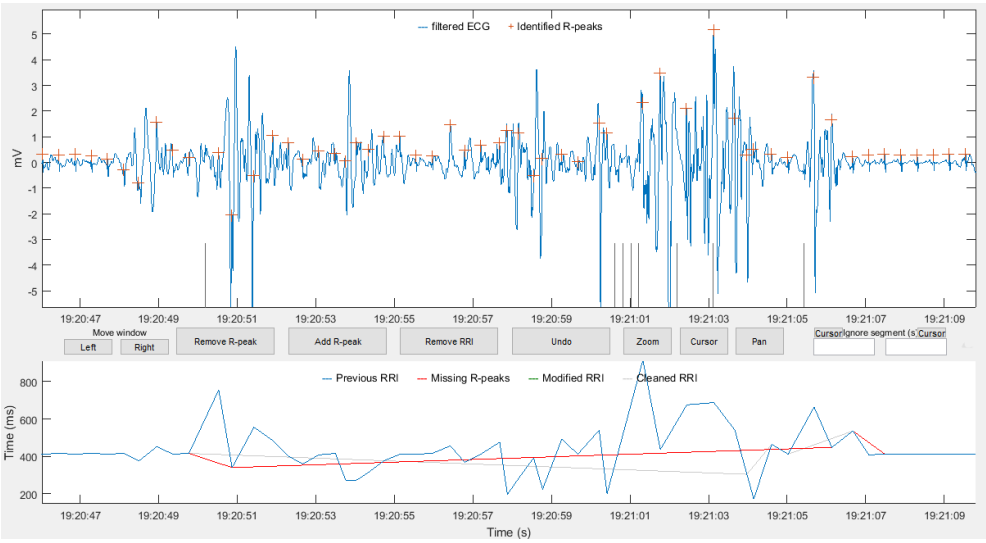

Figure 5.14 – Example of the final algorithm performance for long artefacts.

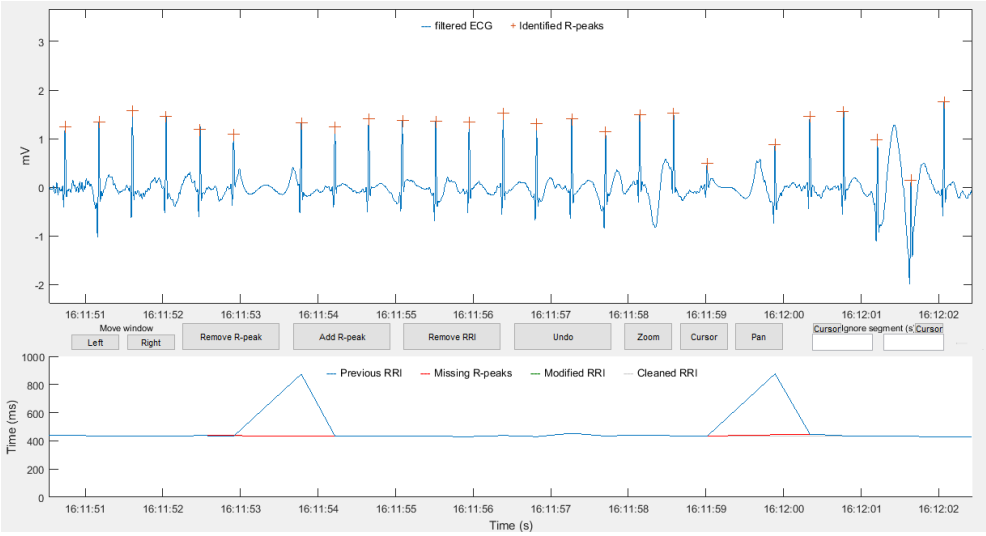

Figure 5.15 – Example of the final algorithm performance for small artefacts.

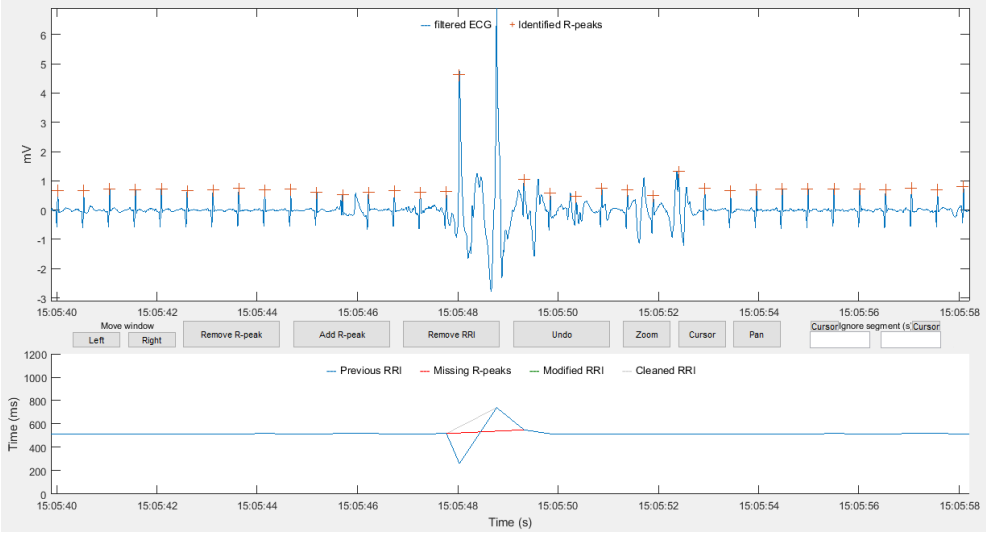

Figure 5.16 – Example of the final algorithm performance for spikes.

Observing the figures above, is possible to affirm that the final algorithm can correctly identify those segments as noise, varying from spikes to long portions. By joining two algorithms, Silva&Rosenberg, that has its higher performance on medium to long noisy segments, and Govindan's method, which is very good on identifying spikes, the creation of this final algorithm is certainly beneficial when working with data with different types of artefacts.

With the final artefact detection algorithm developed, the demonstration of the overall results from every subject in the study is crucial. **Table 5.5.** and **Table 5.6.** shows the results for its validation, for all the data analysed.

Regarding the results shown below, there is an increase in all the parameters when comparing to Govindan's and Silva&Rosenberg's, mainly due to the combination of methods to reach different types of artefacts. Recall, which is one of the most important parameters since it defines the result of the number of artefacts correctly detected by the overall number of artefacts in the data, assumes higher values in both groups, with a slightly increase in the healthy group. Accuracy always assume higher values: since this parameter is calculated when diving the number of artefacts correctly detected by the algorithm by the overall number of artefacts in the data, these parameters have higher values due to the

ability of both methods identify different types of artefacts. Precision in the last algorithms and in the final one assumes the smallest value because of the incorrectly marking of normal peaks as noise, normally in long segments, by the algorithm. F1 score, which considers both recall and precision, assumes a higher and similar value in both groups.

Table 5.5 – Results of the final algorithm, for all subjects.

Subjects	Final Algorithm			
	Recall	**Accuracy**	**Precision**	**F1 Score**
#1 Healthy	98.84	99.82	98.20	98.52
#2 Healthy	95.20	99.80	90.32	92.54
#3 Healthy	92.74	99.90	92.00	92.37
#4 Healthy	98.36	99.79	90.10	97.73
#1 HIE	95.11	99.57	94.24	98.89
#2 HIE	94.54	99.74	91.55	95.38
#3 HIE	90.30	99.76	92.86	94.55
#4 HIE	95.93	98.54	93.05	94.49

Table 5.6 – Mean of the results from the final algorithm, for all subjects.

Criteria	Mean ± Standard Deviation (%)	
	Healthy	**HIE**
Recall	96.2 ± 2.4	93.9 ± 2.1
Accuracy	99.8 ± 0.0	99.4 ± 0.5
Precision	92.6 ± 3.2	92.9 ± 0.9
F1 Score	95.2 ± 2.8	95.8 ± 1.8

The figures above demonstrate the before and after of HRV parameters, after the application of the reject noise algorithm, demonstrated before. The blue line represents the raw signal and the orange one exemplifies the post-processed signal. The long areas in orange, similar to rectangles, characterise the area of the ECG that was totally ignored by the algorithm, due to the higher number of artefacts present on the zone. The x axis is the real time when the signals were acquired.

Observing **Figure 5.17** and **Figure 5.18,** the difference between the raw signal and the post-processed one is clear. Most of the spikes and segments that are artefacts were correctly ignored by the algorithm. Regarding the parameters, it is evident that entropy in high and low frequency bands, but also HF and LF are more sensible to the presence and posterior elimination of noisy segments, being reflected in oscillations in the data. Additionally, pNN25 assumes values lower than expected due to the higher percentage of artefacts in both cases.

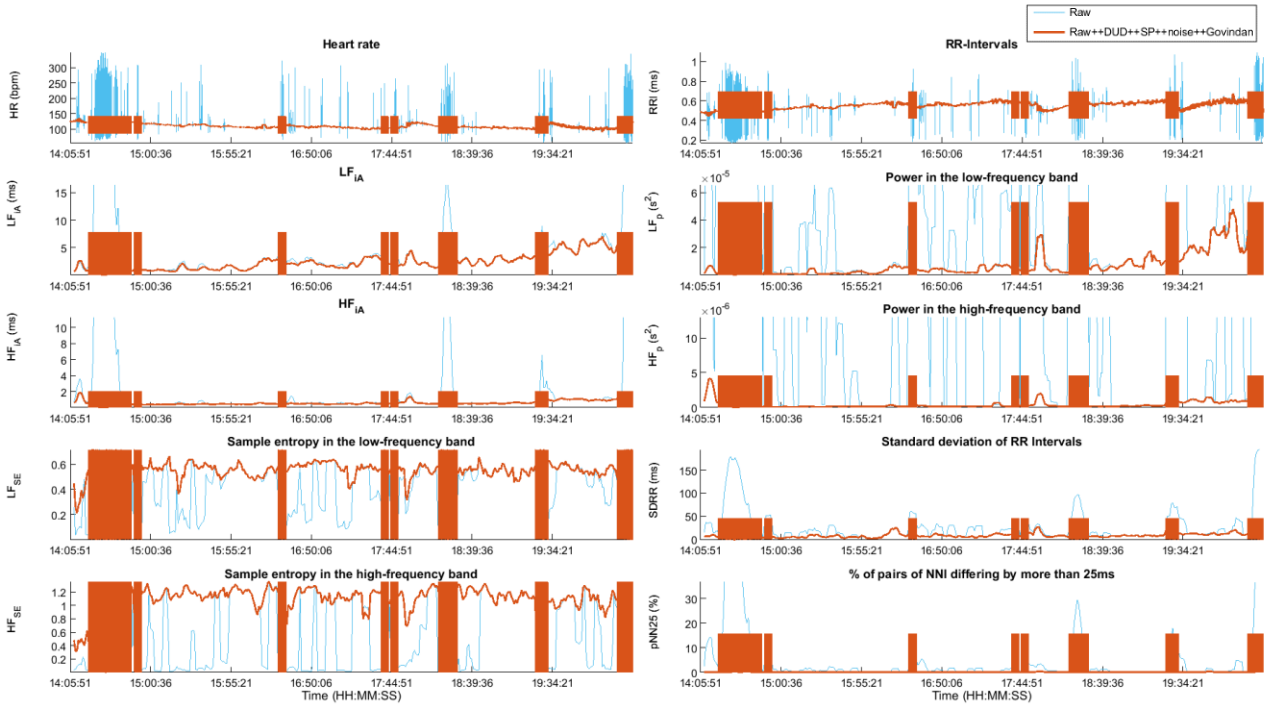

Figure 5.17 – HRV parameters before and after the application of the reject noise algorithm.

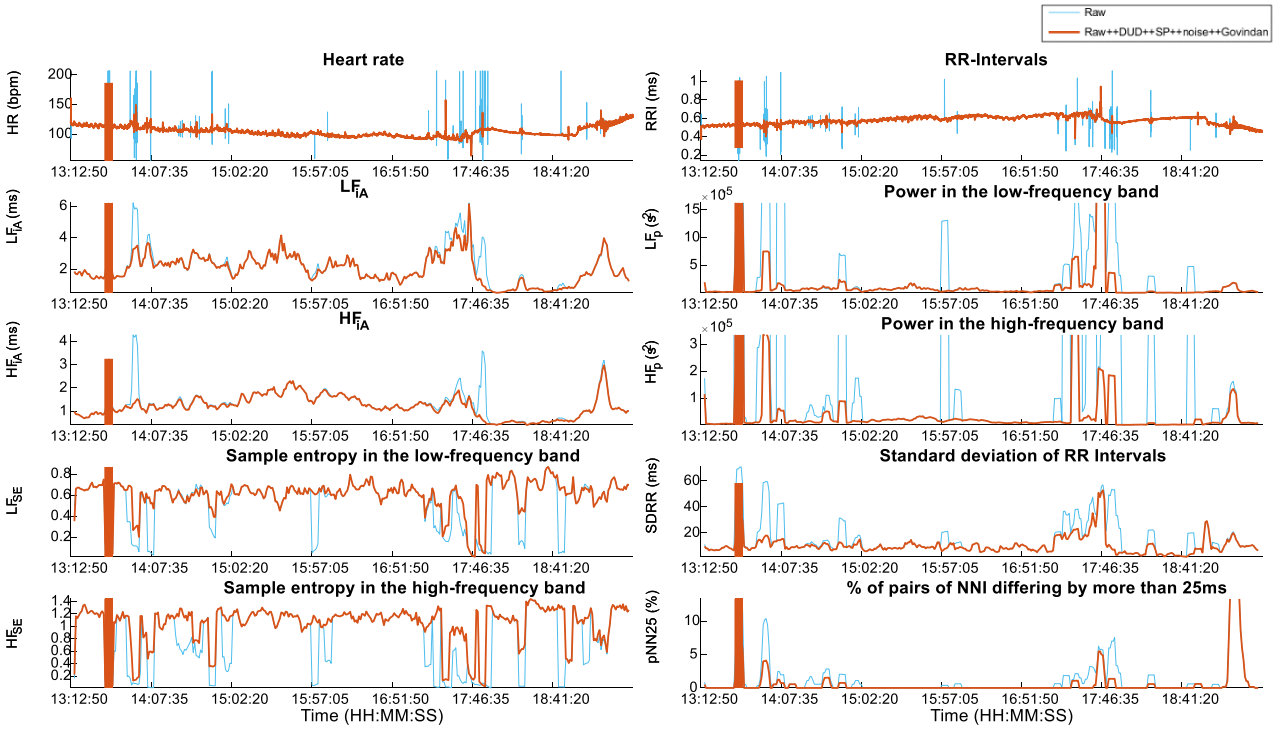

Figure 5.18 – HRV parameters before and after the application of the reject noise algorithm.

5.4. HRV Parameters

After all the post-processing involved, especially regarding the noise removal process, the time comes to analyse heart rate variability parameters and its differences among the two groups: healthy and hypoxic ischemic encephalopathic newborns. In this section will be presented the means and standard deviations of the main parameters (heart rate, SDNN, rMSSD, pNN50, pNN25, HF, LF and sample entropy) as well as the respective graphics in relation to the hours of life. Four newborns were include in each outcome group.

Table 5.7 – HRV parameters per hour of life, for the normal group.

HRV Parameters	Normal Group							
	HR	**SDNN**	**rMSSD**	**pNN50**	**pNN25**	**HF**	**LF**	**SE**
Hour 3	124.59	31.954	0.5157	0.4173	1.9715	1.665E-05	0.00016	0.7244
Hour 4	119.24	39.382	0.4940	0.3643	2.2319	1.910E-05	0.00022	0.6648
Hour 5	131.22	32.725	0.5164	0.4181	4.1950	2.519E-05	0.00019	0.6321
Hour 6	127.80	32.137	0.5447	0.4966	3.0564	2.031E-05	0.00026	0.5479
Hour 7	117.70	41.455	0.5760	2.5413	10.083	4.363E-05	0.00045	0.6551
Hour 8	110.63	43.539	0.5792	5.5506	15.878	6.789E-05	0.00047	0.6600
Hour 9	116.33	36.799	0.5614	3.7225	16.021	7.588E-05	0.00038	0.6887
Hour 10	113.12	43.511	0.5498	2.6365	8.5308	5.789E-05	0.00035	0.6027
Hour 11	110.37	47.640	0.5826	8.3465	21.592	6.314E-05	0.00053	0.6802

It is important to refer that, for the HIE group, ECG data was not acquired within two hours of birth. Since these babies are born with many complications, they are summited to several medical exams as soon as the birth. For this reason, the acquirement of data for this research project could only start around 3 hours after birth.

Table 5.8 – HRV parameters per hour of life, for the HIE group.

HRV Parameters	HIE Group							
	HR	**SDNN**	**rMSSD**	**pNN50**	**pNN25**	**HF**	**LF**	**SE**
Hour 3	120.66	17.434	0.4821	0.0859	0.1715	2.542E-05	9.26E-05	0.5046
Hour 4	116.09	20.917	0.4984	0.0637	4.7566	2.408E-05	0.000309	0.6459
Hour 5	111.36	12.785	0.4640	0.0814	5.6470	2.875E-05	6.11E-05	0.4810
Hour 6	106.49	15.033	0.4893	0.2509	2.1810	1.114E-05	0.000117	0.6039
Hour 7	105.38	16.705	0.5116	0.5041	4.2615	1.888E-05	9.98E-05	0.6211
Hour 8	108.69	15.768	0.5497	0.4855	3.9136	1.719E-05	9.38E-05	0.6636
Hour 9	108.60	23.260	0.5229	0.5301	3.6549	1.743E-05	0.000149	0.6056
Hour 10	102.03	15.689	0.5439	0.7632	5.3533	1.720E-05	9.62E-05	0.5323
Hour 11	102.37	16.014	0.5500	1.6383	3.1404	2.857E-05	9.62E-05	0.4532

Table 5.9 – Mean of the HRV parameters for both groups.

HRV Parameters	Mean ± Standard Deviation (%)		
	Healthy	HIE	p-value
HR	118.97 ± 6.67	109.91 ± 5.62	0.048
SDNN	37.084 ± 5.001	17.087 ± 5.0101	< 0.01
rMSSD	0.5396 ± 0.0292	0.5124 ± 0.0300	0.106
pNN50	2.8720 ± 2.6634	0.4893 ± 0.4955	0.017
pNN25	10.166 ± 7.298	4.5925 ± 1.698	0.018
HF	5.030E-05 ± 3.219E-05	2.703E-05 ± 2.115E-05	0.008
LF	0.00034 ± 0.00012	0.00013 ± 0.00072	<0.01
SE	0.6467 ± 0.1564	0.5680 ± 0.1588	0.015

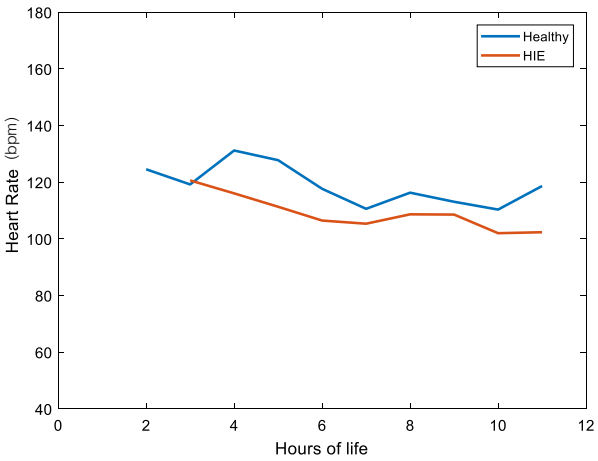

Figure 5.19 – Heart rate parameter through time after birth (h) of healthy and HIE groups.

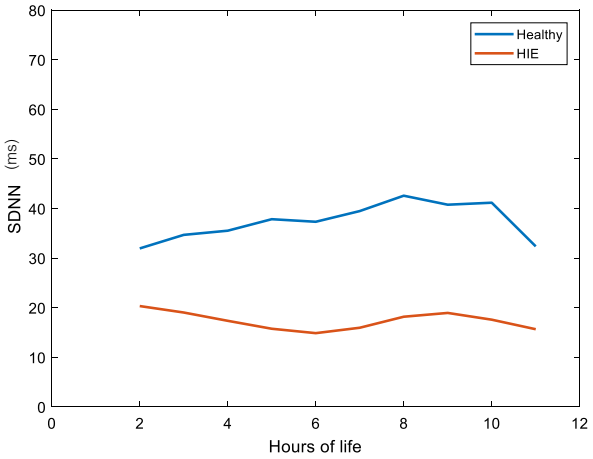

Figure 5.20 – SDNN parameter through time after birth (h) of healthy and HIE groups.

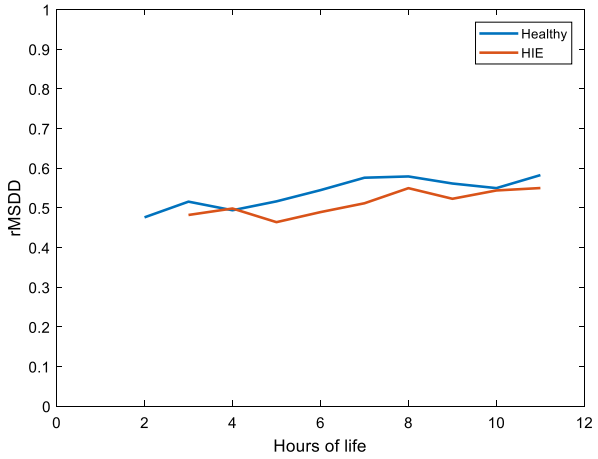

Figure 5.21 – rMSDD parameter through time after birth (h) of healthy and HIE groups.

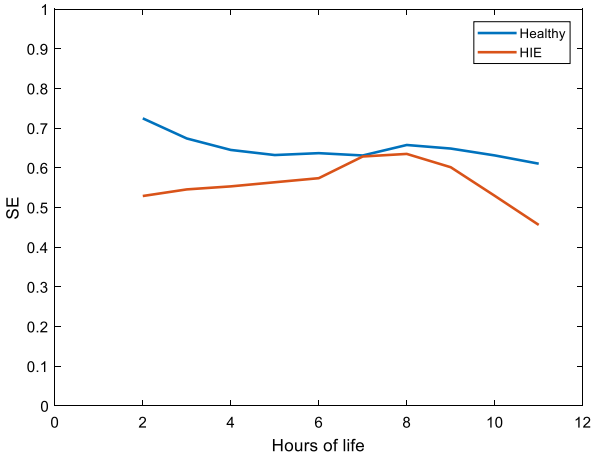

Figure 5.22 – Sample entropy parameter through time after birth (h) of healthy and HIE groups.

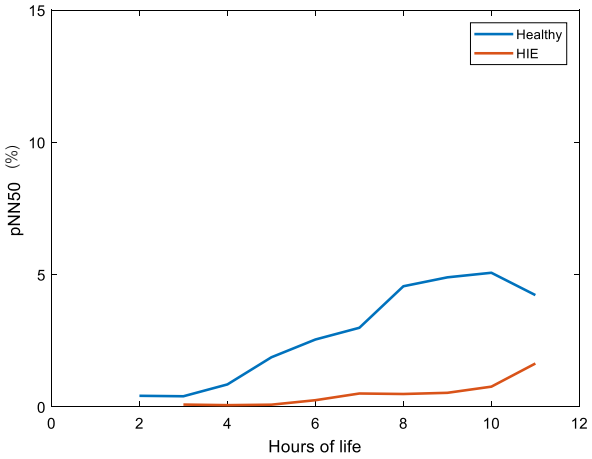

Figure 5.23 – pNN50 parameter through time after birth (h) of healthy and HIE groups.

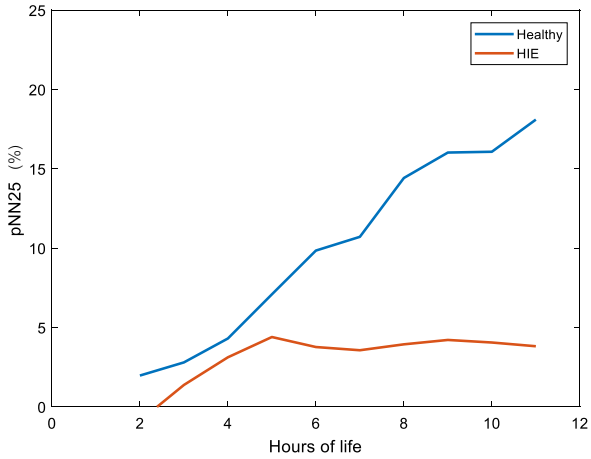

Figure 5.24 – pNN25 parameter through time after birth (h) of healthy and HIE groups.

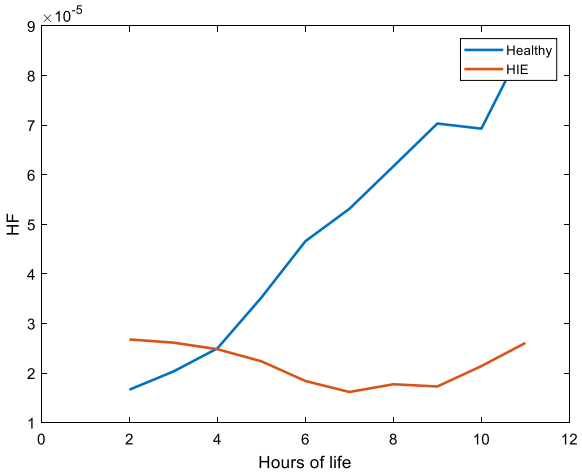

Figure 5.25 – HF parameter through time after birth (h) of healthy and HIE groups.

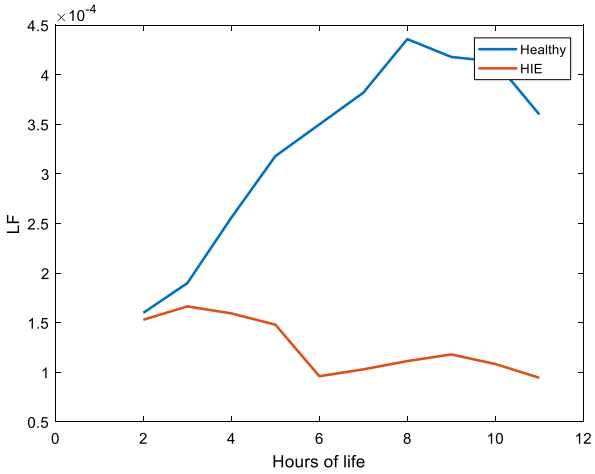

Figure 5.26 – LF parameter through time after birth (h) of healthy and HIE groups.

When comparing the healthy and HIE groups, a clear difference was found: measured HRV parameters were reduced in neonates with HIE. Analysing **Table 5.9.** it is possible to infer that all HRV measures are different from one group to another, with substantial differences for SDNN (p-value <0.01), low- and high- frequency (p-value=0.008 and p-value<0.01), pNN50 and pNN25 after a few hours of life. It is clear a considerable increase in low- and high- frequency values through hours of life, for the healthy group. This might be explainable with the maturation of the autonomic nervous system.

Regarding heart rate, the values are similar within groups, with a slight difference of 10 beats per minute. This might have influenced the results of rMSDD for not being different between healthy and encephalopathic neonates, since this parameter defines the square root of the mean of the sum of the squares of difference between successive RR intervals.

5.5. Entropy Study

In a first stage, the RR sequences of the HIE and healthy groups were applied to approximate entropy, sample entropy, multiscale entropy and fuzzy entropy to analyse the trends of the different entropy measures with r increasing from 0 to 1 (**Figure 5.27** to **Figure 5.30**).

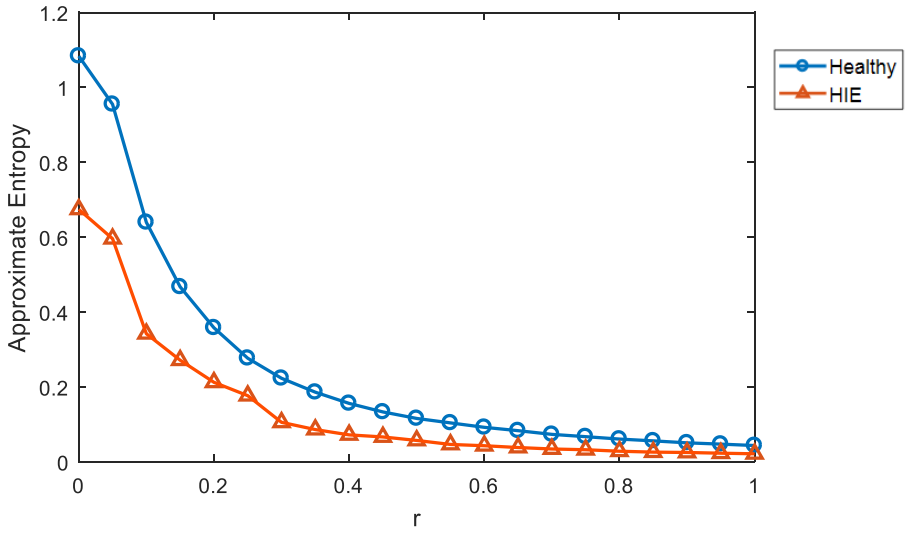

Figure 5.27 – Approximate entropy with r increase in both groups.

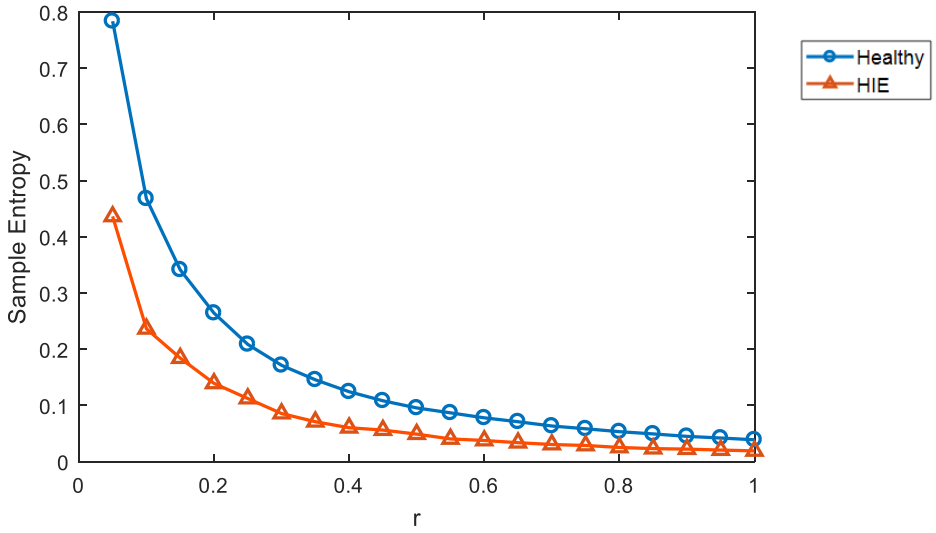

Figure 5.28 – Sample entropy with r increase in both groups.

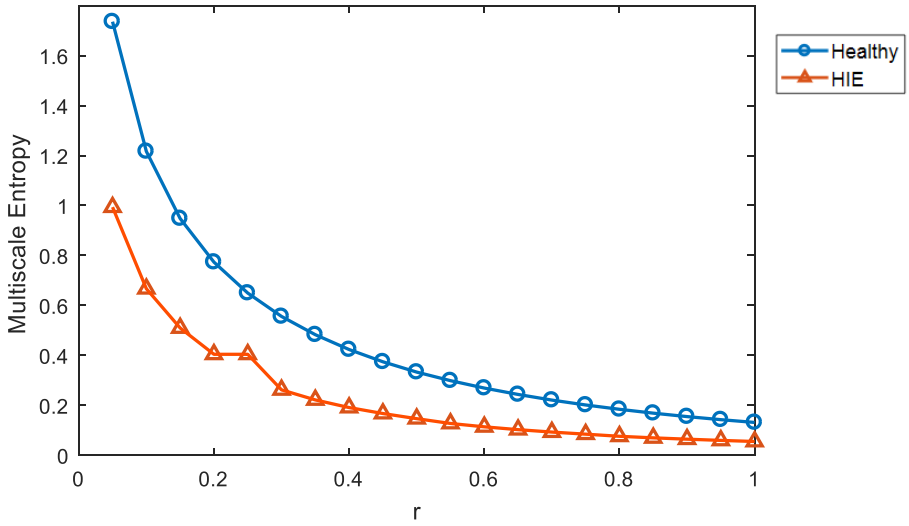

Figure 5.29 – Multiscale entropy with r increase in both groups.

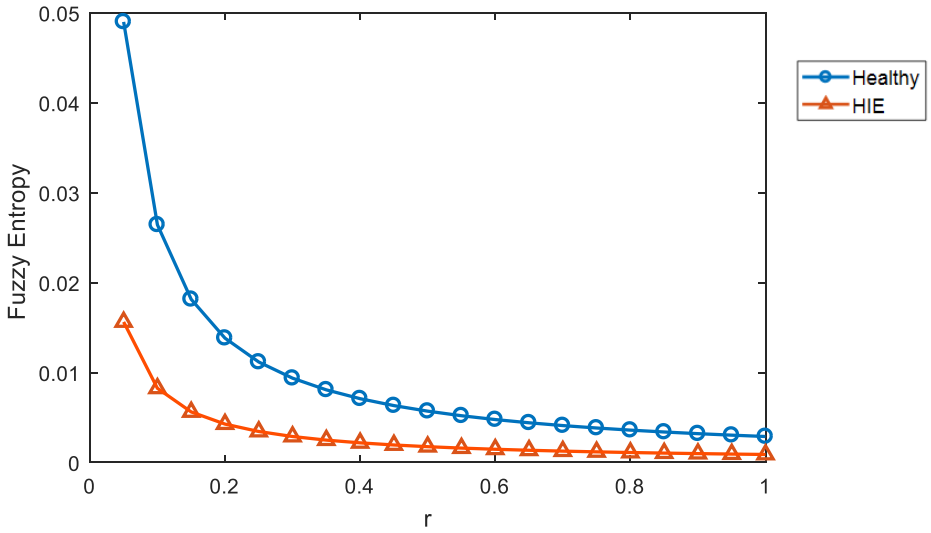

Figure 5.30 – Fuzzy entropy with r increase in both groups.

Analysing the figures above, Fuzzy entropy exhibits a better consistency, when compared to the other methods. The inherent reason for the poor statistical stability in the approximate, sample and multiscale entropy is that these methods are based on the Heaviside function of the classical sets. Fuzzy entropy (**Figure 5.30**) overcome the poor statistical stability, as we can see from the figures shown above, mainly due to the replacement on the method, of the Heaviside function by the Zadeh fuzzy set. When r is smaller, all the methods show a bigger difference between the two groups, confirming previous literature, where the suggested values for r are between 0.15 and 0.20 [36, 38].

For sample entropy (**Figure 5.28**), values for $r = 0$ are null, due to its mathematical equation. Since SampEn is the negative logarithm of the probability that if two sets of simultaneous data points of length m have distance $< r$, then two sets of simultaneous data points of length $m + 1$ also have distance $< r$. Since the value of r is 0, then the sample entropy will be also 0.

Additionally, multiscale and fuzzy entropy, for $r = 0$, their entropy results are also null, since their mathematical base is also sample entropy.

Regarding scales, below are the figures for the two groups, representing entropy measures (multiscale and fuzzy) according to different scales. In these cases, the r utilised was 0.20.

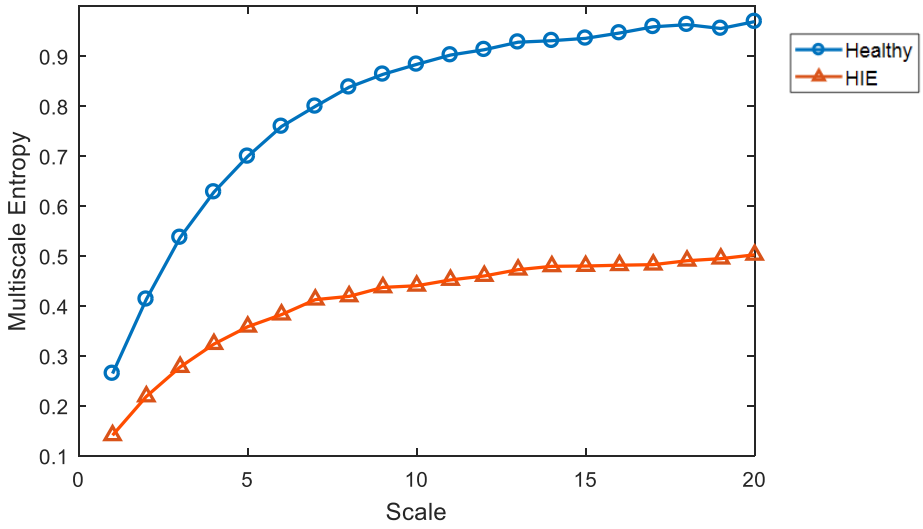

Figure 5.31 – Multiscale entropy with scale increase in both groups.

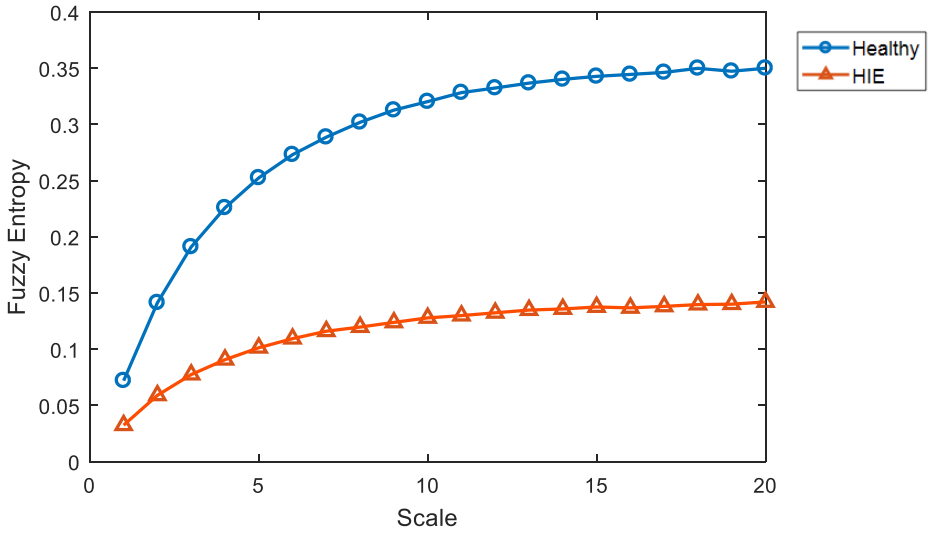

Figure 5.32 – Fuzzy entropy with scale increase in both groups.

In both cases, there is a discrepancy between the two groups. The strongest separation for multiscale entropy is obtained for time scale 8, being constant for all the further scales. In the case of fuzzy entropy, the solidest separation is around scale 12.

Using independent samples *t-test*, a study between the different scales of the two methods, for the healthy and HIE group was performed (**Table 5.10.**). For the multiscale entropy analysis, the p-value was lower for the scales 16, 17 and 20 and for the fuzzy entropy the scales were 17, 18 and 19. A smaller p-value indicates that there is a statistical difference between the two groups. Although, it is important to note that higher scales indicate less data in the analysis.

Table 5.10 – p-values for different MSE and FE scales between normal and HIE group.

Scale	p-values	
	MSE	**FE**
1	0.0444	0.0549
2	0.0382	0.0176
3	0.0313	0.0078
4	0.0254	0.0049
5	0.0214	0.0038
6	0.0164	0.0030
7	0.0171	0.0026
8	0.0106	0.0018
9	0.0108	0.0016
10	0.0075	0.0015
11	0.0079	0.0012
12	0.0072	0.0011
13	0.0072	0.0010
14	0.0079	0.0007
15	0.0068	0.0007
16	0.0061	0.000
17	0.0048	0.0005
18	0.0064	0.0005
19	0.0065	0.0005
20	0.0059	0.0007

After applying the approximate, sample, multiscale and fuzzy entropy to the RR sequences of the HIE and healthy groups, the results of entropy measures are shown in the table below (**Table 5.11.**). Considering a confidence interval of 99%, the independent sample *t-test* results demonstrated that ApEn ($p = 0.0679$), SampEn ($p = 0.0416$) and multiscale entropy ($p = 0.0313$) had no statistical value between the two groups; while fuzzy entropy ($p = 0.0078$) had a significant difference. This result showed that FuzzyEn, for this data, has a better performance in distinguishing the hypoxic ischemic encephalopathic newborns from the healthy ones. Decreasing the confidence interval for 95%, like fuzzy entropy, multiscale entropy demonstrates a noteworthy difference, whereas sample entropy has a borderline result.

As expected, almost all the values for the healthy group are superior, when compared to the HIE group. The standard deviation is bigger on the second group, mainly due to acute fluctuations in the RR sequences caused by arrythmias or exterior interferences.

Table 5.11 – The results of ApEn, SampEn, MSE and FuzzyEn between normal and HIE groups.

Entropy measures	Healthy group				HIE group				*p-values*
	Mean	Maximum	Minimum	SD	Mean	Maximum	Minimum	SD	
ApEn	0.3583	0.5492	0.2383	0.0901	0.2127	0.4554	0.0652	0.1576	0.0679
SampEn	0.2644	0.4013	0.1819	0.0633	0.1394	0.3560	0.0532	0.1255	0.0416
MSE	0.5367	0.7239	0.3972	0.1048	0.2774	0.7330	0.1078	0.2637	0.0313
FuzzyEn	0.1910	0.2464	0.1456	0.0328	0.0775	0.2337	0.0155	0.0906	0.0078

The boxplots of four entropy measures are present above, in **Figure 5.33**. In all the methods, the differences between groups are similar, being the HIE group always with lower entropy values.

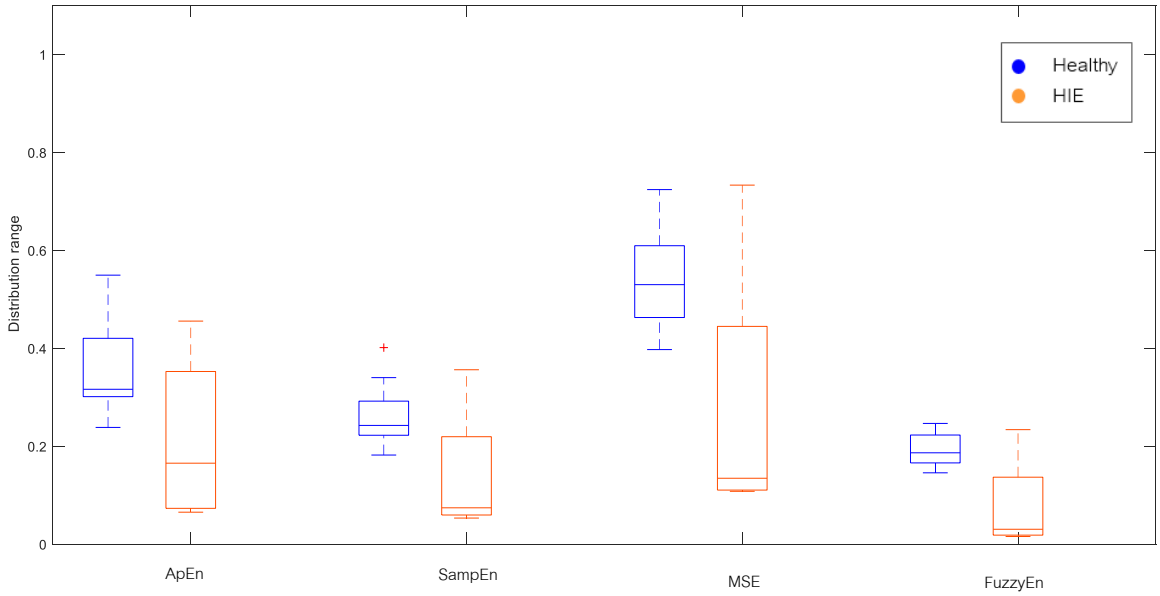

Figure 5.33 – The distribution ranges of ApEn, SampEn, MSE and FuzzyEn between HIE and healthy groups.

5.5.1. Multidimensional Entropy Study

With the aim of investigating how different methods of entropy interact with each other and which are the results of that interface, especially to distinguish and identify stressful and normal states, a multidimensional study was applied to the entropy methods used on this dissertation.

Giving that for all the healthy babies on the research project it was registered all the stress events during hospital stay, it is more intuitive to select the time frame for the type of event wanted. These events can be crying, feeding, sleeping, medical examination, vomit, position change, among others. It is important to note that, for this analysis, the time window must not be too large, since the changes are very subtle.

On a first analysis, approximate, sample and multiscale entropy were employed. After that, on a second one, approximate entropy was replaced by fuzzy entropy.

For the initial case, it was registered that the baby started crying at 11:30. For this analysis, a time window of 10 minutes before the event was employed.

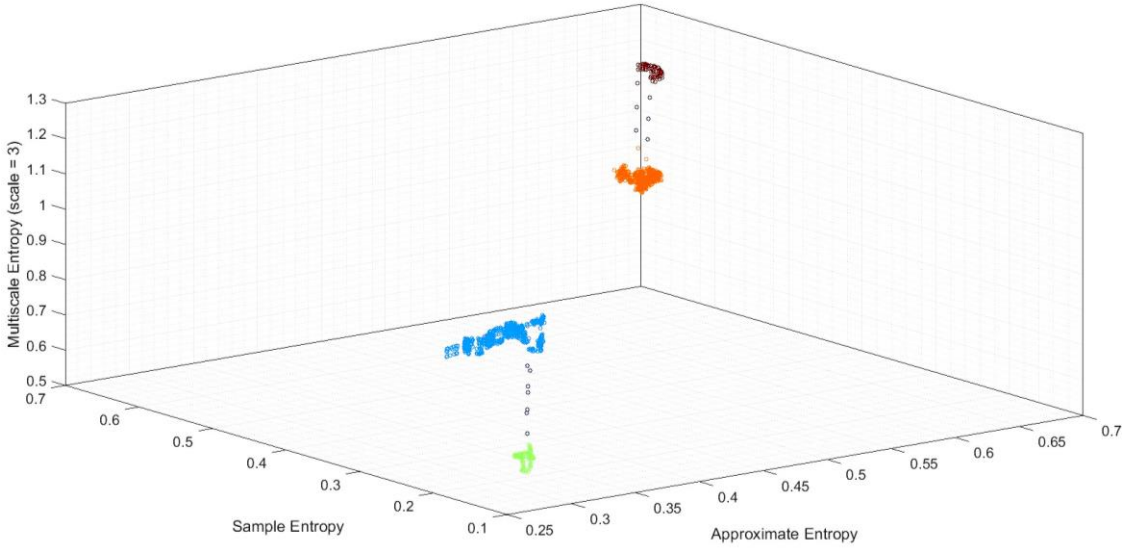

Figure 5.34 – Multidimensional study involving approximate, sample and multiscale entropy in a stressful situation.

Figure 5.35 – Stage difference, approximate, sample and multiscale entropy measures during a stressful situation.

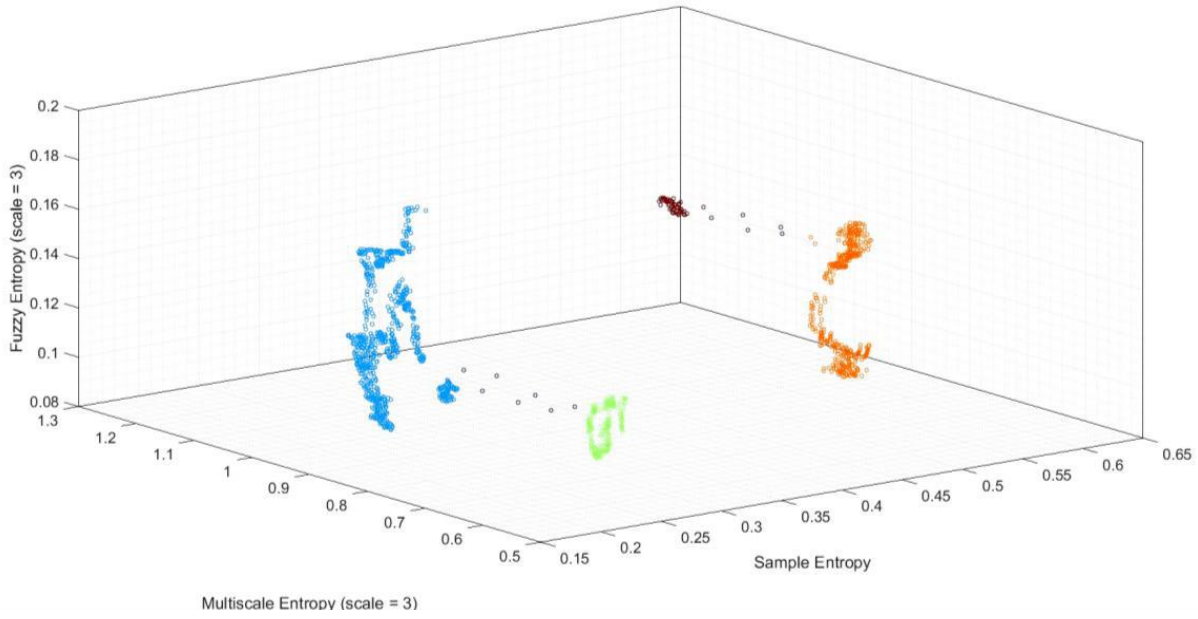

Figure 5.36 – Multidimensional study involving sample, multiscale and fuzzy entropy in a stressful situation.

Figure 5.37 – Stage difference, sample, multiscale and fuzzy entropy measures during a stressful situation.

The main reason for choosing a time window ten minutes before the event and a few minutes after was due the fact that something must have happened before the crying and alterations in the autonomic nervous system and consequently on the heart rate should be present. This could be confirmed by both 3D graphics present above (**Figure 5.34** and **Figure 5.36**).

In the same context, below are the results for a low-stress condition, where no register of stress event was written, for the same subject.

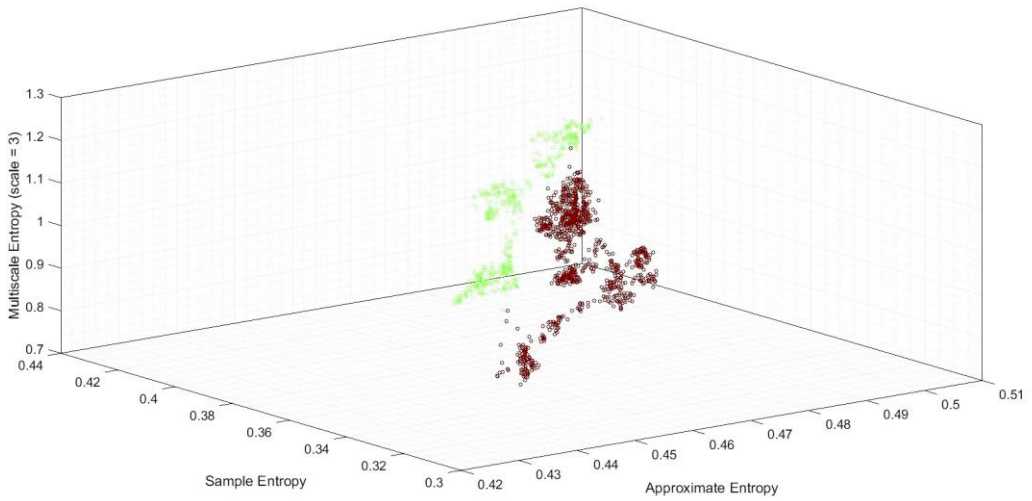

Figure 5.38 – Multidimensional study involving approximate, sample and multiscale entropy in a non-stressful situation.

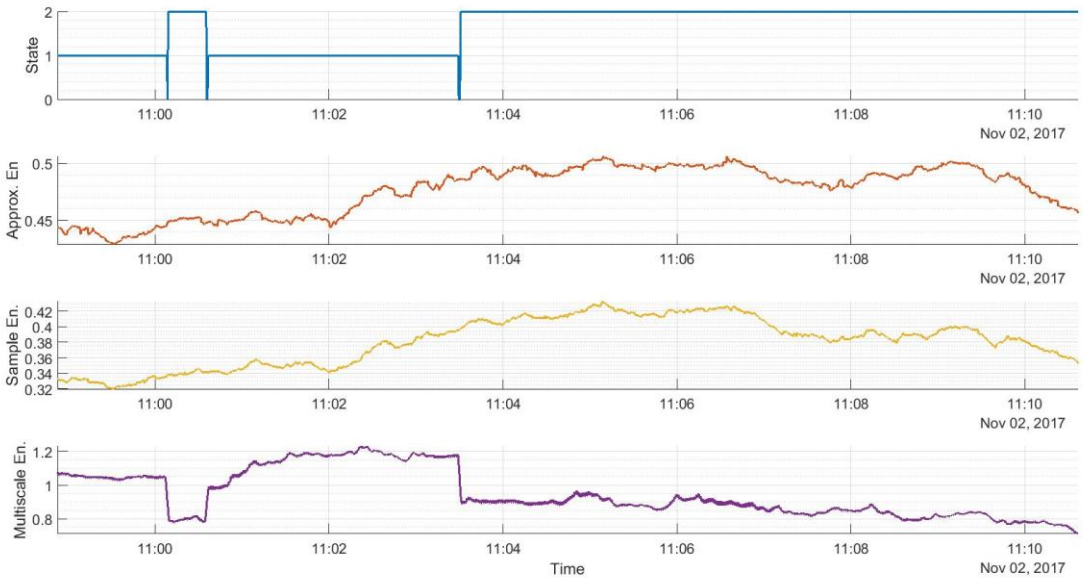

Figure 5.39 – Stage difference, approximate, sample and multiscale entropy measures during a non-stressful situation.

It is clear the difference regarding the 3D plots between a stressful and a normal status. In the last case (**Figure 5.38**), it is only possible to identify 2 states, even though they are indeed close to each other.

Regarding the analysis using fuzzy entropy instead of approximate entropy (**Figure 5.40**), the results are more non-stationary, which is reflected on the respective 3D plot. Nevertheless, it is also possible to distinguish two different clusters, corresponding to the previous results.

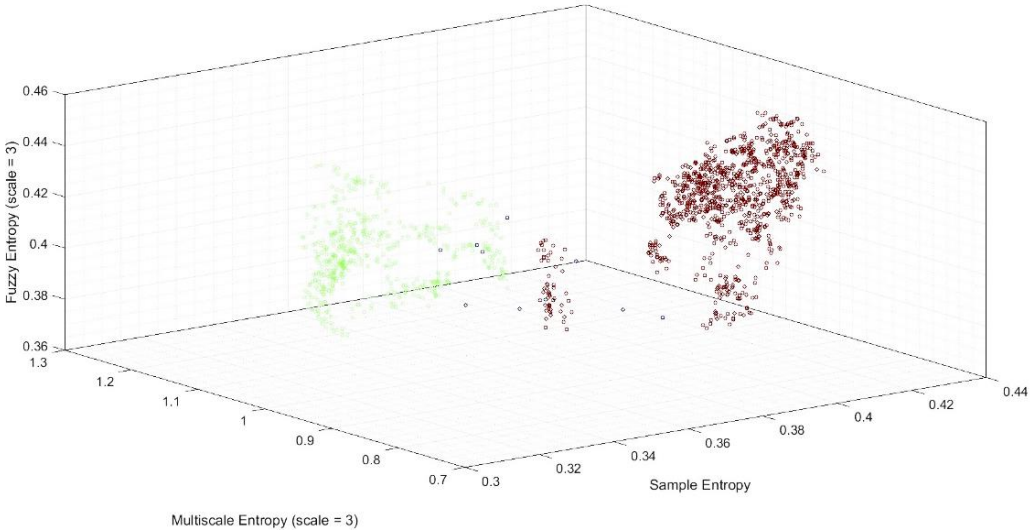

Figure 5.40 – Multidimensional study involving sample, multiscale and fuzzy entropy in a non-stressful situation.

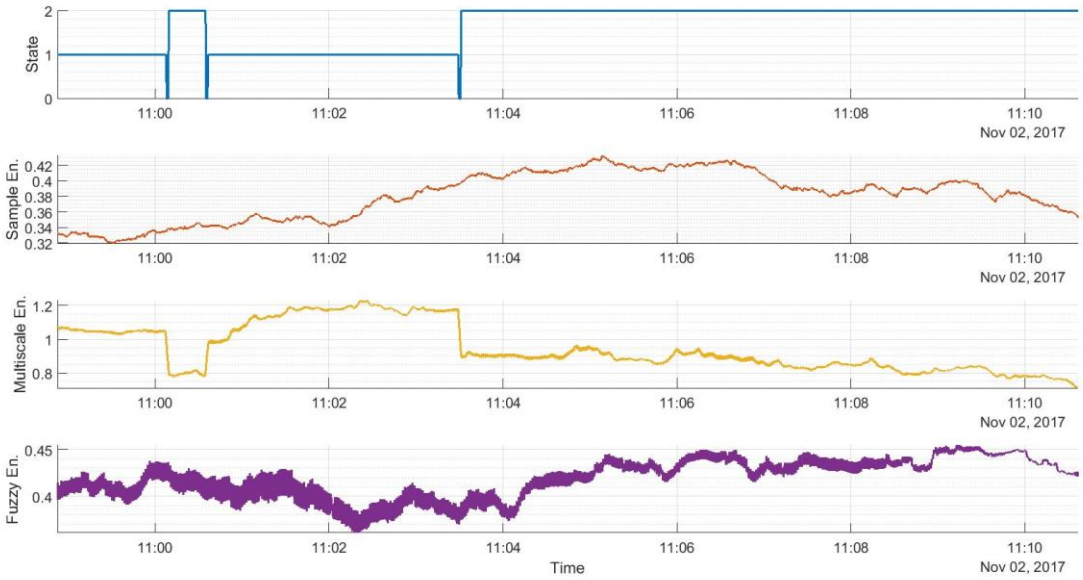

Figure 5.41 – Stage difference, sample, multiscale and fuzzy entropy measures during a non-stressful situation.

6. Discussion

Chapter 6 focusses on the analysis and discussion of the results presented in this dissertation. The logic of this chapter will be the same as the previous one, with the aim of keeping the same organization through it. First, the creation process, results and validation values of the final artefact removal algorithm are discussed. The next section contains a critical overview of the HRV parameters obtained for both groups (healthy and HIE newborns). The last one is regarding all the complexity science methods, applied to the data presented in this dissertation.

6.1. Artefact removal algorithm

Heart rate and its variability are extremely important in critical care medicine. Nevertheless, given the regular assessments and medical interventions in the NICU, distortion of the signal by artefacts is a major problem that restricts the accurate evolution of this important physiological measure. This issue is even bigger when considering newborn ECGs, where the intensity of clinical care and monitoring contributes to the signal to be often noisy and contaminated with artefacts from various sources. To culminate this issue, Silva&Rosenberg algorithm was created to identify and mark all the artefacts in this type of data. The method was based on mathematical aspects of beat to beat time, with a major focus on physiological impossible values.

Regarding the steps of this algorithm, the phases that identified more artefacts were the first and second steps, where it was excluded the RR intervals above 1000 ms and below 300 ms, but also the last step, which eliminated all the RR intervals which had a difference bigger than 200 ms from the previous one. This indicate the type of noise present in the ECGs, normally originated by detached electrodes or missing beats. The last step is also beneficial in terms of removing spikes in the data.

In this algorithm, the most robust step is step 5. Facing the artefacts presented in the data and working in the basis of trial-and-error, it was clear that in long segments of noise, there were still some peaks that were considered by the algorithm as good. As referred, since the algorithm is based on mathematical aspects of the data, even if the R peaks are positioned in a wrong position but its relations with other peaks are within the thresholds defined previously, the algorithm consider those as "good" peaks. The fifth step of the proposed method can prevent these situations to happen, improving the chance of having acquired correct information and, this way, increasing validation parameters.

The remaining steps evolving standard deviation and medians of the signal have less impact than the referred ones above. Still, they are important parts of the process, helping on the identification of subtly artefacts, like demonstrated in **Figure 5.4.**

Observing **Tables 5.1.** and **5.2.**, it is possible to conclude that almost all the validation parameters assume higher values, around 90%. In the case of healthy data, accuracy assume the higher value, whereas in the HIE group it is F1 Score. Recall assumed a large value (95.31 ± 2.63 %), when compared to HIE (91.24 ± 6.03 %). All the parameters have big values of standard deviation, mainly due to different amounts of artefacts in the ECGs, but also because only a small amount of data was used. As expected, HIE subjects have lower values for all the parameters, mainly due to higher presence of artefacts from different sources.

Although the presented algorithm has higher rates of validation, mainly due to a correct identification of medium to long noisy segments, in almost all cases, spikes were not marked as artefacts by the algorithm. To solve the situation presented above, Govindan's algorithm [88] was modified and applied to the same data: in the original method, all the peaks identified as noisy where replaced with the median value of 10 beats starting 15 beats back in time from the current position. In the case of this

dissertation, all the values considered by the algorithm as artefacts were replaced by NaN values, which means that they were eliminated.

In terms of results, as it is possible to analyse in **Figure 5.11**, the algorithm performed well when faced with spikes. In terms of medium to long noisy segments, only few were identified, as we can confirm for the validation results of **Table 5.3.** and **5.4.** Recall for the healthy group had a rate of 57.05% (± 16.30 %) and for HIE a rate of 60.66% (± 6.08 %). The main reason for the difference of these validation results and for the scattered parameters, when comparing to the first algorithm, is mainly because most data analysed had more long artefacts segments than spikes, but also due to the different number of artefacts and spikes present, which vary from subject to subject.

Accuracy is the result when the number of artefact peaks marked as noise and the number of good peaks marked as good peaks by the algorithm, is divided by the total number of peaks in data. It is also a measure of statistical bias. In the methods presented before, for the two groups, this parameter assumed high rates, due to a large value of good peaks marked correctly.

The two algorithms presented above tried to reach the same objectives, although with different approaches. Joining two algorithms, Silva&Rosenberg, that has its higher performance on medium to long noisy segments, and Govindan's method, which is very good on identifying spikes, the creation of one final algorithm is certainly beneficial when working with data with different types of artefacts, which is reflected in the new validation rates (**Table 5.5** and **5.6**).

Observing **Figures 5.13** to **5.15** one can affirm that the final algorithm can correctly identify segments as noise, varying from spikes to long portions. For the final method, Recall assumed higher rates for both groups. Healthy group had a rate of 96.28% (±2.47) whereas the HIE had a rate of 93.97% (±2.17) for this validation parameter. F1 score, which considers both recall and precision, assumes a higher and similar value in both groups. Precision (which is the ratio of the number of artefacts detected correctly by the algorithm, by the number of peaks marked correctly or incorrectly by the same method) continues to assume the lowest rate for both groups (Healthy=92.65 ± 3.28 % and HIE=92.92 ± 0.95 %) because of the wrong marking, by the algorithm, of good peaks as noisy segments. Nevertheless, this rate was considered to be lower enough by the medical staff, when these results were presented. This translate one limitation to consider: lack of a reliable approach to identify an appropriate threshold that would correctly distinguish spikes from physiological components.

Analysing the data after the process that marks the R peaks in the ECG, it was possible to notice that the algorithm does not perform well in all situations, marking peaks in wrong locations. This can contribute to the camouflage of the results and influence the performance of the artefact removal algorithm, since the noise removal process is based on mathematical relations of the beat-to-beat. By this, and to improve the performance of the algorithm and, more importantly, to obtain the true values of heart rate analysis, it is wise to check manually if the R peaks are marked correctly, before starting the signal processing process and consequent HRV analysis. Thus, a suggestion for future work is the creation of an algorithm that could help on this aspect, by verifying if the R peaks were well marked before starting the processing process.

Observing **Figure 5.17** and **5.18**, that represent HRV features before and after the application of the artefact reject algorithm, it is evident the enormous increase on the stability of those parameters. This translates the enormous advantage of applying this algorithm to ECG data, where the probability of having real and reliable information is increased.

6.2.HRV parameters

Resorting to post-processing techniques and the artefact removal algorithm presented in this dissertation, heart rate variability analysis parameters were obtained for two groups: healthy and HIE newborns. This study used electrocardiograms acquired between 3 and 11 hours after birth.

The advantage of the ECG signal is that it is straightforward, well-defined and leads to easy calculation of HRV [46]. A difficulty can arise in the interpretation of the HRV parameters, where, in addition to HIE, heart rate variability is influenced by many factors such as blood pressure, temperature, autonomic nervous system dysfunction, among others.

When comparing healthy and encephalopathic neonates it was found a reduction in all HRV parameters: heart rate, SDNN, rMSSD, pNN50, pNN25, low- and high- frequency and sample entropy. SDNN and low frequency represented the HRV features with lower p-value (<0.01), translating into the HRV parameters that are most important in differentiating both groups. Regarding the other features, all of them assumed as well good values, with an exception for rMSSD, since both results were extremely similar.

Within the subcortical structures of the brain, the brainstem contributes to HRV control, and brainstem injury will result in reduced control and contractility [43], which can justify the differences in all the parameters above described. Regarding HF and LF, in previous literature is assumed that HF feature is mediated by the parasympathetic system, whereas LF represents sympathetic activity [15, 30, 99]. These features demonstrated reduced values when compared to the healthy group, implying a reduction in overall autonomic function in the neonatal encephalopathic group. Since autonomic nervous system plays a significant role in balancing the hemodynamic response to hypoxia and hypercapnia, it is normal that both HF and LF values are lower for the HIE group [122].

Almost all the differences were constant with time, with exceptions to pNN25, pNN50, low- and high- frequency, as can be observed in **Figures 5.23** to **Figure 5.26**, where there was a clear increase for the healthy group. This might be explainable with the maturation of the autonomic nervous system. It is important to refer that since the data analysed was small (4 healthy newborns and 4 HIE newborns), the results were normalise for the graphics present on the mentioned chapter, due to high discrepancies with values. This translates a limitation of the project and a suggestion for future work: the acquisition of more ECGs, whether from healthy or HIE newborns, with the purpose of increasing the data size, and therefore reduce the discrepancies within values of the same parameter.

The results demonstrate that HRV is a useful tool for the prediction of long-term neurodevelopmental outcome, which could be advantageous for NICUs without access to electroencephalography, especially when decisions related to therapeutic and interventions are required. Even when EEG is available, using HRV as a tool could be extremely beneficial as a way of assuring the best options for the patient. Besides, it confirms the idea that a bedside tool could provide a more objective measure of patients “at-risk” of HIE, but also, with more research to improve the accuracy, helping distinguish between grades of hypoxia ischemic encephalopathic [30].

6.3. Entropy Study

The use of entropy methods to define and quantify the complexity of physiological signals in health and disease in human data has become quite popular within the past 20 years [36]. It has been confirmed that HRV analysis is important in early detection and quantitative evaluation of diseases, being different methods of entropy part of that group. In this dissertation, approximate entropy, sample entropy, multiscale entropy and fuzzy entropy were employed to the RR sequences of the HIE and healthy groups.

From **Figure 5.27** to **Figure 5.30**, it is demonstrated the trends of all the entropy methods with r increasing from 0 to 1. Previous literature [36, 38] suggests that r values should be between 0.15 and 0.20. In this analysis, all the methods showed a bigger difference between the two groups, when r was smaller, confirming this way the presented values for this parameter. Fuzzy entropy exhibits a better consistency, when compared to the other methods. The inherent reason for the poor statistical stability in the approximate, sample and multiscale entropy is that these methods are based on the Heaviside function of the classical sets: it is based in a two-state classifier that judges two vectors as either similar or dissimilar, without intermediate states [41]. Fuzzy entropy overcome the poor statistical stability due to the replacement on the method, of the Heaviside function by the Zadeh fuzzy set.

Using a r of 0.20, in **Figure 5.31** and **Figure 5.32** it is possible to observe multiscale entropy and fuzzy entropy plotted according to different scales. For both methods, healthy values were always superior to HIE ones, increasing through the scales. By observing both figures, the strongest separation for multiscale entropy is obtained for time scale 8, being constant for all the further scales. In the case of fuzzy entropy, the solidest separation is around scale 12. Of note, the weakest separation between the two groups occurred for scale one, which is the only scale studied by approximate and sample entropy.

Table 5.10 demonstrates a study between the different scales of the two methods, for the healthy and HIE group, using independent samples *t-test.* For the multiscale entropy analysis, the p-value was lower for the scales 16, 17 and 20 and for the fuzzy entropy the scales were 17, 18 and 19. It is important to refer that higher scales indicate less data in the analysis. This concept is also illustrated by values suggested in previous literature [38] , where it is claimed that the most suitable scales are 2 and 3.

In the next table (**Table 5.11**) it is demonstrated the results of various entropy measures applied to the RR sequences of the healthy and HIE groups. For all the entropy measures, the healthy group assumed higher values, with a smaller standard deviation, when compared to the HIE ones. Considering a confidence interval of 99%, the independent sample *t-test* results demonstrated that ApEn ($p = 0.0679$), SampEn ($p = 0.0416$) and multiscale entropy ($p = 0.0313$) had no statistical value between the two groups; while fuzzy entropy ($p = 0.0078$) had a significant difference. This result showed that FuzzyEn, for this data, has a better performance in distinguishing the hypoxic ischemic encephalopathic newborns from the healthy ones. However, it is important to notice that one of the limitations of Fuzzy Entropy is that it focuses only on the local characteristics of the sequence. However, the global fluctuation in the large scales has been widely found in the sequence. ApEn and SampEn are commonly used in HRV analysis due to the ease of their calculations and the small data requirements [34]. Yet, and as confirmed in this research, these two entropy measures present poor statistical stability.

Observing the boxplots in **Figure 5.33,** it is clear that the distribution ranges of the different methods in the HIE group are larger than those in the healthy group. One reason for this situation could be that the course of HIE is often accompanied by a larger presence of artefacts (that interfere with the acquisition of heart rate), but also arrythmias. Furthermore, the RR sequence of a HIE newborn without arrythmias has a regular change caused by the weakening of the regulatory function of the autonomic nervous system.

Regarding the multidimensional entropy study, it was investigated how different methods of entropy interact with each other and which are the results of that interface, especially to distinguish and identify stressful and normal states.

Associated with a stressful event, there is a high percentage of the signal corrupted by artefacts. However, in some cases it was possible to see a clear distinction between groups of clusters, indicating that in that period, there was a change of state. Not all the time segments from subjects demonstrated differences in stress stages, indicating that there is still room for improvement in the method developed.

One a first analysis, approximate, sample and multiscale entropy were employed during a segment of time of HR data that represent the moment of a stressful event. After that, for the same data, approximate entropy was replaced by fuzzy entropy.

For the stressful event, in both cases (**Figure 5.34** and **Figure 5.36**) it is possible to see a clear distinction of the two major groups and, within each group, another transition. The major two groups undoubtedly represent a transition of stage, between normal to stressful. When considering the four stages present on the graphics, it could translate intermediate stages: relaxed, normal, low-stress and high stress. Considering that stress is normally represented by a decrease in complexity science, it is fair to assume that the clusters that represent the transitions in stress state are the ones located at left. Regarding the replacement of approximate entropy for fuzzy entropy, there was no change between the two figures presented. However, the use of fuzzy entropy is advisable due to a better statistical probability.

In the case of no register of stress written, for the same subject and for the same features, **Figure 5.38** and **Figure 5.40** were obtained. Like expected, it is clear a difference between a stressful and a normal status. In the last case, it is only possible to identify 2 states, even though they are close to each other. With this type of conditions (where supposedly the newborn was not submitted to any kind of stressful event) the variations in entropy measures are not that abrupt and significant. Considering the last four stages mentioned above, in the case of a non-stressful event, for this subject, the results indicate that these conditions might be among normal and low-stress. When considering **Figure 3.40**, where it was applied fuzzy entropy instead of approximate entropy, the results are less stationary, being reflected in the graphic. Nevertheless, it is possible to distinguish two different groups, corresponding to the results described above.

7. Conclusion

Heart rate and its variability offers significant insight in critical care medicine. For newborns with hypoxic ischemic encephalopathy, this feature is even more significant due to its influence on the classification and evaluation of this condition. Nevertheless, the heart rate of the infants monitored in the NICU is susceptible to artefacts, due to the intensity of clinical care and monitoring. These artefacts interfere with the characterization and subsequent evaluation of the heart rate, leading to serious consequences, both in diagnostic and therapeutic decisions.

Although there are many algorithms developed by other groups regarding artefacts in adult ECGs, few perform well in newborns ones, due to all the differences and peculiarities in the signal. Also, they create artificial values as a way of reducing the presence of noise in this type of data, camouflaging and not reflecting the correct and true information.

The algorithm developed in this dissertation focused on the mathematical aspects of beat to beat time and on a well-known method to correctly eliminate spikes. The principal aim of it is to identify artefacts in different types of ECG data, intermixed with artefactual and non-artefactual periods of time. The final algorithm, in addition to fulfilling the objective described above, is also adaptable to different types of artefacts present in the signal, allowing the user, in a very intuitive way, to choose the type of parameters and steps to be applied, being easily usable by professionals from different areas.

The cross validated classification results showed that the proposed algorithm can detect artefacts in newborns electrocardiograms, with an overall Recall rate of 95%, accomplishing the purpose of its creation.

This dissertation contained another algorithm with the purpose of identifying stress situations in newborns. To reach that goal, it was created a multidimensional method employing the different entropy methods used in this research. This algorithm was suitable to see how the different entropy methods interact with each other and what the results of this relationship are, especially in the distinction of normal and stressful states. Unfortunately, associated with a stressful event, there is a high percentage of the signal corrupted by artefacts. However, in some cases it was possible to observe a clear distinction of groups of clusters, indicating that in that period, there was a change of state.

This study has also demonstrated significant differences in heart rate parameters between healthy and HIE neonates. Also, comparing several methods of entropy, fuzzy entropy had a better performance in distinguishing the HIE subjects from the healthy subjects. These results demonstrate the potential of HRV features as physiological markers of HIE in neonates, as well as a useful predictor of long-term neurodevelopmental outcome.

As with any project, more can still be done and improved. Firstly, it is necessary to acquire more electrocardiograms, either from healthy newborns or with hypoxic-ischemic encephalopathy, to increase the sample size and thus decrease the values of the standard deviation in all the calculated parameters. Regarding the stress study, it would be interesting, with a larger sample, the definition of clusters, to have an accurate identification of stressful situations. In addition, the transformation of the software currently written in MATLAB to *GUI* (graphical user interface), with the purpose of making it more accessible by professionals from different areas. Regarding the algorithms proposed, the creation of an algorithm that could verify if the R peaks were well marked before starting the processing process would be extremely beneficial in the artefact detection, improving the ranges presented in **Table 5.6**.

8. References

1. Thoresen, M., et al., *Effective selective head cooling during posthypoxic hypothermia in newborn piglets.* Pediatric research, 2001. **49**(4): p. 594.
2. Tooley, J.R., et al., *Head cooling with mild systemic hypothermia in anesthetized piglets is neuroprotective.* Annals of Neurology: Official Journal of the American Neurological Association and the Child Neurology Society, 2003. **53**(1): p. 65-72.
3. Kamila, N.K., *Handbook of Research on Wireless Sensor Network Trends, Technologies, and Applications*. 2016, India. 589.
4. Bronzino, J.D., *The biomedical engineering handbook*, ed. C.P.I. Llc. Vol. 2. 2006.
5. Bay, A., *Basic electrocardiography: normal and abnormal ECG patterns*. 2008: John Wiley & Sons.
6. Klabunde, R., *Cardiovascular physiology concepts*. 2011: Lippincott Williams & Wilkins.
7. Widmaier, E.P., H. Raff, and K.T. Strang, *Vander's human physiology: the mechanisms of body function*. 2008: McGraw-Hill Higher Education.
8. Altman, D.B. *Introduction to pediatric ECG*. 2017 [cited 2018 08/July].
9. Javorka, K., et al., *Heart Rate Variability in Newborns.* Physiological research, 2017. **66**: p. S203.
10. Fairchild, K.D. and T.M. O'Shea, *Heart rate characteristics: physiomarkers for detection of late-onset neonatal sepsis.* Clinics in perinatology, 2010. **37**(3): p. 581-598.
11. Williams, G., *Chaos theory tamed*. 2014: CRC Press.
12. Vaillancourt, D.E. and K.M. Newell, *Changing complexity in human behavior and physiology through aging and disease.* Neurobiol Aging, 2002. **23**(1): p. 1-11.
13. McCraty, R. and F. Shaffer, *Heart Rate Variability: New Perspectives on Physiological Mechanisms, Assessment of Self-regulatory Capacity, and Health Risk.* Global Advances in Health and Medicine, 2015. **4**(1): p. 46-61.
14. Vergales, B.D., et al., *Depressed heart rate variability is associated with abnormal EEG, MRI, and death in neonates with hypoxic ischemic encephalopathy.* American journal of perinatology, 2014. **31**(10): p. 855-862.
15. von Rosenberg, W., et al., *Resolving ambiguities in the LF/HF ratio: LF-HF scatter plots for the categorization of mental and physical stress from HRV.* Frontiers in physiology, 2017. **8**: p. 360.
16. Chanwimalueang, T., et al. *Modelling stress in public speaking: evolution of stress levels during conference presentations*. in *Acoustics, Speech and Signal Processing (ICASSP), 2016 IEEE International Conference on*. 2016. IEEE.
17. Malik, M., et al., *Heart rate variability: Standards of measurement, physiological interpretation, and clinical use.* European heart journal, 1996. **17**(3): p. 354-381.
18. Baek, H.J., et al., *Reliability of ultra-short-term analysis as a surrogate of standard 5-min analysis of heart rate variability.* Telemedicine and e-Health, 2015. **21**(5): p. 404-414.
19. Shaffer, F. and J.P. Ginsberg, *An Overview of Heart Rate Variability Metrics and Norms.* Front Public Health, 2017. **5**: p. 258.
20. Salahuddin, L., et al. *Ultra short term analysis of heart rate variability for monitoring mental stress in mobile settings*. in *Engineering in Medicine and Biology Society, 2007. EMBS 2007. 29th Annual International Conference of the IEEE*. 2007. IEEE.
21. Kleiger, R.E., et al., *Decreased heart rate variability and its association with increased mortality after acute myocardial infarction.* The American journal of cardiology, 1987. **59**(4): p. 256-262.

22. Mehta, S.K., et al., *Heart rate variability in healthy newborn infants.* The American journal of cardiology, 2002. **89**(1): p. 50-53.
23. Umetani, K., et al., *Twenty-four hour time domain heart rate variability and heart rate: relations to age and gender over nine decades.* Journal of the American College of Cardiology, 1998. **31**(3): p. 593-601.
24. Diffen. *Parasympathetic vs. Sympathetic Nervous System*. 2018 [cited 2018 04/July].
25. Chanwimalueang, T., et al., *Stage call: Cardiovascular reactivity to audition stress in musicians.* PloS one, 2017. **12**(4): p. e0176023.
26. Goldberger, J.J., *Sympathovagal balance: how should we measure it?* American Journal of Physiology-Heart and Circulatory Physiology, 1999. **276**(4): p. H1273-H1280.
27. Pagani, M., et al., *Power spectral analysis of heart rate and arterial pressure variabilities as a marker of sympatho-vagal interaction in man and conscious dog.* Circulation research, 1986. **59**(2): p. 178-193.
28. Billman, G.E., *The LF/HF ratio does not accurately measure cardiac sympatho-vagal balance.* Frontiers in physiology, 2013. **4**: p. 26.
29. Sacha, J. and W. Pluta, *Different methods of heart rate variability analysis reveal different correlations of heart rate variability spectrum with average heart rate.* Journal of electrocardiology, 2005. **38**(1): p. 47-53.
30. Goulding, R.M., et al., *Heart rate variability in hypoxic ischaemic encephalopathy: correlation with EEG grade and two-year neurodevelopmental outcome.* Pediatric research, 2015. **77**(5).
31. He, T., G. Clifford, and L. Tarassenko, *Application of independent component analysis in removing artefacts from the electrocardiogram.* Neural Computing & Applications, 2006. **15**(2): p. 105-116.
32. Logier, R., J. De Jonckheere, and A. Dassonneville. *An efficient algorithm for RR intervals series filtering*. in *Engineering in Medicine and Biology Society, 2004. IEMBS'04. 26th Annual International Conference of the IEEE*. 2004. IEEE.
33. Pincus, S.M., *Approximate entropy as a measure of system complexity.* Proceedings of the National Academy of Sciences, 1991. **88**(6): p. 2297-2301.
34. Richman, J.S. and J.R. Moorman, *Physiological time-series analysis using approximate entropy and sample entropy.* American Journal of Physiology-Heart and Circulatory Physiology, 2000. **278**(6): p. H2039-H2049.
35. Costa, M., A.L. Goldberger, and C.-K. Peng, *Multiscale entropy analysis of complex physiologic time series.* Physical review letters, 2002. **89**(6): p. 068102.
36. Yentes, J.M., et al., *The appropriate use of approximate entropy and sample entropy with short data sets.* Annals of biomedical engineering, 2013. **41**(2): p. 349-365.
37. Pincus, S.M. and W.-M. Huang, *Approximate entropy: statistical properties and applications.* Communications in Statistics-Theory and Methods, 1992. **21**(11): p. 3061-3077.
38. Lake, D.E., et al., *Sample entropy analysis of neonatal heart rate variability.* American Journal of Physiology-Regulatory, Integrative and Comparative Physiology, 2002. **283**(3): p. R789-R797.
39. Chen, X., I.C. Solomon, and K.H. Chon. *Comparison of the use of approximate entropy and sample entropy: applications to neural respiratory signal*. in *Engineering in Medicine and Biology Society, 2005. IEEE-EMBS 2005. 27th Annual International Conference of the*. 2006. IEEE.
40. Chen, W., et al., *Characterization of surface EMG signal based on fuzzy entropy.* IEEE Transactions on neural systems and rehabilitation engineering, 2007. **15**(2): p. 266-272.
41. Liu, C., et al., *Analysis of heart rate variability using fuzzy measure entropy.* Computers in biology and Medicine, 2013. **43**(2): p. 100-108.

42. Jacobs, S.E., et al., *Whole-body hypothermia for term and near-term newborns with hypoxic-ischemic encephalopathy: a randomized controlled trial.* Archives of pediatrics & adolescent medicine, 2011. **165**(8): p. 692-700.
43. Volpe, J.J., *Neurology of the Newborn E-Book*. 2008: Elsevier Health Sciences.
44. Temko, A., et al., *Multimodal predictor of neurodevelopmental outcome in newborns with hypoxic-ischaemic encephalopathy.* Computers in biology and medicine, 2015. **63**: p. 169-177.
45. Itoo, B.A., Z.M. Al-Hawsawi, and A.H. Khan, *Hypoxic ischemic encephalopathy. Incidence and risk factors in North Western Saudi Arabia.* Saudi medical journal, 2003. **24**(2): p. 147-153.
46. Matić, V., et al., *Heart rate variability in newborns with hypoxic brain injury*, in *Oxygen Transport to Tissue XXXV*. 2013, Springer. p. 43-48.
47. Badawi, N., et al., *Antepartum risk factors for newborn encephalopathy: the Western Australian case-control study.* Bmj, 1998. **317**(7172): p. 1549-1553.
48. Sarnat, H.B. and M.S. Sarnat, *Neonatal encephalopathy following fetal distress: a clinical and electroencephalographic study.* Archives of neurology, 1976. **33**(10): p. 696-705.
49. Gressens, P. and D. Luton, *Fetal MRI: obstetrical and neurological perspectives.* Pediatric radiology, 2004. **34**(9): p. 682-684.
50. Shankaran, S., *Neonatal encephalopathy: treatment with hypothermia.* Journal of neurotrauma, 2009. **26**(3): p. 437-443.
51. Zanelli, S., et al., *Implementation of a 'Hypothermia for HIE' program: 2-year experience in a single NICU.* Journal of Perinatology, 2008. **28**(3).
52. Busto, R., et al., *The importance of brain temperature in cerebral ischemic injury.* Stroke, 1989. **20**(8): p. 1113-1114.
53. Chen, H., et al., *The effect of hypothermia on transient middle cerebral artery occlusion in the rat.* Journal of Cerebral Blood Flow & Metabolism, 1992. **12**(4): p. 621-628.
54. Chopp, M., et al., *Mild hypothermic intervention after graded ischemic stress in rats.* Stroke, 1991. **22**(1): p. 37-43.
55. Gluckman, P.D., et al., *Selective head cooling with mild systemic hypothermia after neonatal encephalopathy: multicentre randomised trial.* The Lancet, 2005. **365**(9460): p. 663-670.
56. Javorka, K., et al., *Heart rate variability in newborns.* Physiological research, 2017. **66**.
57. Van Ravenswaaij-Arts, C., et al., *Spectral analysis of heart rate variability in spontaneously breathing very preterm infants.* Acta Paediatrica, 1994. **83**(5): p. 473-480.
58. Kantor, L., V. Curtisova, and L. Dubrava, *Development of heart rate variability during the first three days of life.* Acta Med Mart, 2003. **3**: p. 22-29.
59. Makarov, L., et al., *QT dynamicity, microvolt T-wave alternans, and heart rate variability during 24-hour ambulatory electrocardiogram monitoring in the healthy newborn of first to fourth day of life.* Journal of electrocardiology, 2010. **43**(1): p. 8-14.
60. Gonzales, G. and A. Salirrosas, *Pulse oxygen saturation and neurologic assessment in human neonates after vaginal and cesarean delivery.* International Journal of Gynecology & Obstetrics, 1998. **63**(1): p. 63-66.
61. Toth, B., A. Becker, and B. Seelbach-Göbel, *Oxygen saturation in healthy newborn infants immediately after birth measured by pulse oximetry.* Archives of gynecology and obstetrics, 2002. **266**(2): p. 105-107.
62. Kozár, M., et al., *Changes of cardiovascular regulation during rewarming in newborns undergoing whole-body hypothermia.* Neuroendocrinol Letters, 2015. **36**(5): p. 101-105.
63. Metzler, M., et al., *Pattern of brain injury and depressed heart rate variability in newborns with hypoxic ischemic encephalopathy.* Pediatric research, 2017. **82**(3): p. 438.

64. Ulusar, U.D., et al. *Adaptive rule based fetal QRS complex detection using Hilbert transform*. in *Engineering in Medicine and Biology Society, 2009. EMBC 2009. Annual International Conference of the IEEE*. 2009. IEEE.
65. Massaro, A.N., et al., *Heart rate variability in encephalopathic newborns during and after therapeutic hypothermia.* Journal of Perinatology, 2014. **34**(11): p. 836.
66. Benitez, D., et al., *The use of the Hilbert transform in ECG signal analysis.* Computers in biology and medicine, 2001. **31**(5): p. 399-406.
67. Pan, J. and W.J. Tompkins, *A real-time QRS detection algorithm.* IEEE Trans. Biomed. Eng, 1985. **32**(3): p. 230-236.
68. Dahmen, W., et al., *Biorthogonal multiwavelets on the interval: cubic Hermite splines.* Constructive approximation, 2000. **16**(2): p. 221-259.
69. Lasky, R.E., et al., *Changes in the PQRST intervals and heart rate variability associated with rewarming in two newborns undergoing hypothermia therapy.* Neonatology, 2009. **96**(2): p. 93-95.
70. Doyle, O., et al., *Heart rate variability during sleep in healthy term newborns in the early postnatal period.* Physiological measurement, 2009. **30**(8): p. 847.
71. Kovatchev, B.P., et al., *Sample asymmetry analysis of heart rate characteristics with application to neonatal sepsis and systemic inflammatory response syndrome.* Pediatric research, 2003. **54**(6): p. 892.
72. Holzinger, A., et al. *On applying approximate entropy to ECG signals for knowledge discovery on the example of big sensor data*. in *International conference on active media technology*. 2012. Springer.
73. Berntson, G.G. and J.R. Stowell, *ECG artifacts and heart period variability: don't miss a beat!* Psychophysiology, 1998. **35**(1): p. 127-132.
74. Ros, H., A. Koeleman, and T. Akker, *The technique of signal averaging and its practical application in the separation of atrial and His-Purkinje activity.* Signal averaging technique in Clinical Cardiology, 1981.
75. Evanich, M., O. Newberry, and L. Patridge, *Some limitations of periodic noise removal by averaging techniques.* J. Appl. Physiol, 1972. **33**: p. 536-541.
76. Flowers, N.C., et al., *Surface recording of His-Purkinje activity on an every-beat basis without digital averaging.* Circulation, 1981. **63**(4): p. 948-952.
77. Talmon, J., J. Kors, and J. Van Bemmel, *Adaptive Gaussian filtering in routine ECG/VCG analysis.* IEEE transactions on acoustics, speech, and signal processing, 1986. **34**(3): p. 527-534.
78. Thakor, N.V. and Y.-S. Zhu, *Applications of adaptive filtering to ECG analysis: noise cancellation and arrhythmia detection.* IEEE transactions on biomedical engineering, 1991. **38**(8): p. 785-794.
79. Barros, A.K. and N. Ohnishi, *MSE behaviour of biomedical event-related filters [impedance cardiography application]*. IEEE Transactions on Biomedical Engineering, 1997. **44**(9): p. 848-855.
80. Vaz, C., X. Kong, and N. Thakor, *An adaptive estimation of periodic signals using a Fourier linear combiner*. IEEE Transactions on Signal Processing, 1994. **42**(1): p. 1-10.
81. Kanjilal, P.P. and S. Palit, *On multiple pattern extraction using singular value decomposition.* IEEE transactions on signal processing, 1995. **43**(6): p. 1536-1540.
82. Wisbeck, J.O. and R.G. Ojeda. *Application of neural networks to separate interferences and ECG signals*. in *Devices, Circuits and Systems, 1998. Proceedings of the 1998 Second IEEE International Caracas Conference on*. 1998. IEEE.

83. Speirs, C.A., et al. *Ventricular late potential detection from bispectral analysis of ST− segments*. in *Proceedings of EUSIPCO*. 1994.
84. Cardoso, J.-F. *Multidimensional independent component analysis*. in *ICASSP*. 1998. Citeseer.
85. Lippman, N., K.M. Stein, and B.B. Lerman, *Comparison of methods for removal of ectopy in measurement of heart rate variability.* American Journal of Physiology-Heart and Circulatory Physiology, 1994. **267**(1): p. H411-H418.
86. dos Santos, L., et al., *Application of an automatic adaptive filter for heart rate variability analysis.* Medical engineering & physics, 2013. **35**(12): p. 1778-1785.
87. Wessel, N., et al., *Nonlinear analysis of complex phenomena in cardiological data.* Herzschrittmachertherapie und Elektrophysiologie, 2000. **11**(3): p. 159-173.
88. Govindan, R., et al., *A spike correction approach for variability analysis of heart rate sick infants.* Physica A: Statistical Mechanics and its Applications, 2016. **444**: p. 35-42.
89. Clifford, G., P. McSharry, and L. Tarassenko. *Characterizing artefact in the normal human 24-hour RR time series to aid identification and artificial replication of circadian variations in human beat to beat heart rate using a simple threshold*. in *Computers in Cardiology, 2002*. 2002. IEEE.
90. Kaufmann, T., et al., *ARTiiFACT: a tool for heart rate artefact processing and heart rate variability analysis.* Behavior research methods, 2011. **43**(4): p. 1161-1170.
91. Nagaraj, S.B., et al. *Heart rate variability as a biomarker for sedation depth estimation in ICU patients*. in *Engineering in Medicine and Biology Society (EMBC), 2016 IEEE 38th Annual International Conference of the*. 2016. IEEE.
92. Kim, D., et al. *Detection of subjects with higher self-reporting stress scores using heart rate variability patterns during the day*. in *Engineering in Medicine and Biology Society, 2008. EMBS 2008. 30th Annual International Conference of the IEEE*. 2008. IEEE.
93. Sato, N. and S. Miyake, *Cardiovascular reactivity to mental stress: relationship with menstrual cycle and gender.* Journal of Physiological Anthropology and Applied Human Science, 2004. **23**(6): p. 215-223.
94. Yashima, K., et al. *Application of wavelet analysis to the plethysmogram for the evaluation of mental stress*. in *Conf Proc IEEE Eng Med Biol Soc*. 2005.
95. Shinba, T., et al., *Decrease in heart rate variability response to task is related to anxiety and depressiveness in normal subjects.* Psychiatry and clinical neurosciences, 2008. **62**(5): p. 603-609.
96. Schubert, C., et al., *Effects of stress on heart rate complexity—a comparison between short-term and chronic stress.* Biological psychology, 2009. **80**(3): p. 325-332.
97. Nakamura, Y., Y. Yamamoto, and I. Muraoka, *Autonomic control of heart rate during physical exercise and fractal dimension of heart rate variability.* Journal of Applied Physiology, 1993. **74**(2): p. 875-881.
98. Butler, G.C., Y. Yamamoto, and R.L. Hughson, *Fractal nature of short-term systolic BP and HR variability during lower body negative pressure.* American Journal of Physiology-Regulatory, Integrative and Comparative Physiology, 1994. **267**(1): p. R26-R33.
99. Hagerman, I., et al., *Chaos-related deterministic regulation of heart rate variability in time-and frequency domains: effects of autonomic blockade and exercise.* Cardiovascular research, 1996. **31**(3): p. 410-418.
100. Blásquez, J.C.C., G.R. Font, and L.C. Ortís, *Heart-rate variability and precompetitive anxiety in swimmers.* Psicothema, 2009. **21**(4): p. 531-536.
101. Filaire, E., et al., *Effect of lecturing to 200 students on heart rate variability and alpha-amylase activity.* European journal of applied physiology, 2010. **108**(5): p. 1035-1043.

102. Berntson, G.G., et al., *Heart rate variability: origins, methods, and interpretive caveats.* Psychophysiology, 1997. **34**(6): p. 623-648.
103. Eckberg, D.L., *Sympathovagal balance: a critical appraisal.* Circulation, 1997. **96**(9): p. 3224-3232.
104. Billman, G.E., *Heart rate variability–a historical perspective.* Frontiers in physiology, 2011. **2**: p. 86.
105. Malliani, A., et al., *Cardiovascular variability is/is not an index of autonomic control of circulation.* Journal of Applied Physiology, 2006. **101**(2): p. 684-688.
106. Pincus, S.M. and R.R. Viscarello, *Approximate entropy: a regularity measure for fetal heart rate analysis.* Obstet Gynecol, 1992. **79**(2): p. 249-255.
107. Caldirola, D., et al., *Approximate entropy of respiratory patterns in panic disorder.* American Journal of Psychiatry, 2004. **161**(1): p. 79-87.
108. Williamon, A., et al., *Complexity of physiological responses decreases in high-stress musical performance.* Journal of The Royal Society Interface, 2013. **10**(89): p. 20130719.
109. Vuksanović, V. and V. Gal, *Heart rate variability in mental stress aloud.* Medical engineering & physics, 2007. **29**(3): p. 344-349.
110. Lucchini, M., et al. *Multi-parametric heart rate analysis in premature babies exposed to sudden infant death syndrome*. in *Engineering in Medicine and Biology Society (EMBC), 2014 36th Annual International Conference of the IEEE*. 2014. IEEE.
111. Taylor, A., N.M. Fisk, and V. Glover, *Mode of delivery and subsequent stress response.* The Lancet, 2000. **355**(9198): p. 120.
112. Saugstad, O.D., *Oxidative stress in the newborn–a 30-year perspective.* Neonatology, 2005. **88**(3): p. 228-236.
113. Dawson, J.A., et al., *Defining the reference range for oxygen saturation for infants after birth.* Pediatrics, 2010: p. peds. 2009-1510.
114. Chanwimalueang, T., W. von Rosenberg, and D.P. Mandic. *Enabling R-peak detection in wearable ECG: Combining matched filtering and Hilbert transform*. in *Digital Signal Processing (DSP), 2015 IEEE International Conference on*. 2015. IEEE.
115. Wathen, J.E., et al., *Accuracy of ECG interpretation in the pediatric emergency department.* Annals of emergency medicine, 2005. **46**(6): p. 507-511.
116. Powers, D.M., *Evaluation: from precision, recall and F-measure to ROC, informedness, markedness and correlation.* 2011.
117. MathWorks. *knnsearch.* [cited 2018 25 August].
118. Groenen, P.J. and K. Jajuga, *Fuzzy clustering with squared Minkowski distances.* Fuzzy Sets and Systems, 2001. **120**(2): p. 227-237.
119. Aggarwal, C.C., et al. *Fast algorithms for projected clustering*. in *ACM SIGMoD Record*. 1999. ACM.
120. Krivulin, N., *An algebraic approach to multidimensional minimax location problems with Chebyshev distance.* arXiv preprint arXiv:1211.2425, 2012.
121. Ester, M., et al. *A density-based algorithm for discovering clusters in large spatial databases with noise*. Kdd. 1996.
122. Campen, M.J., et al., *Heart rate variability responses to hypoxic and hypercapnic exposures in different mouse strains.* Journal of Applied Physiology, 2005. **99**(3): p. 807-813.

9. Appendices

This section contains the appendices referring to the project developed in this dissertation. The original MATLAB codes written through this project are also include in this chapter, with the objective of demonstrate the computational logic of each algorithm.

Appendix I – Diagram describing the algorithm used to extract R peaks from ECGs;

Appendix II – Silva&Rosenberg Algorithm;

Apendix III – Altered Govindan's Algorithm;

Appendix IV – Main HRV analysis Algorithm;

Appendix V – Entropy Measures Algorithm;

Appendix VI – Multidimensional Entropy Study Algorithm;

Appendix I

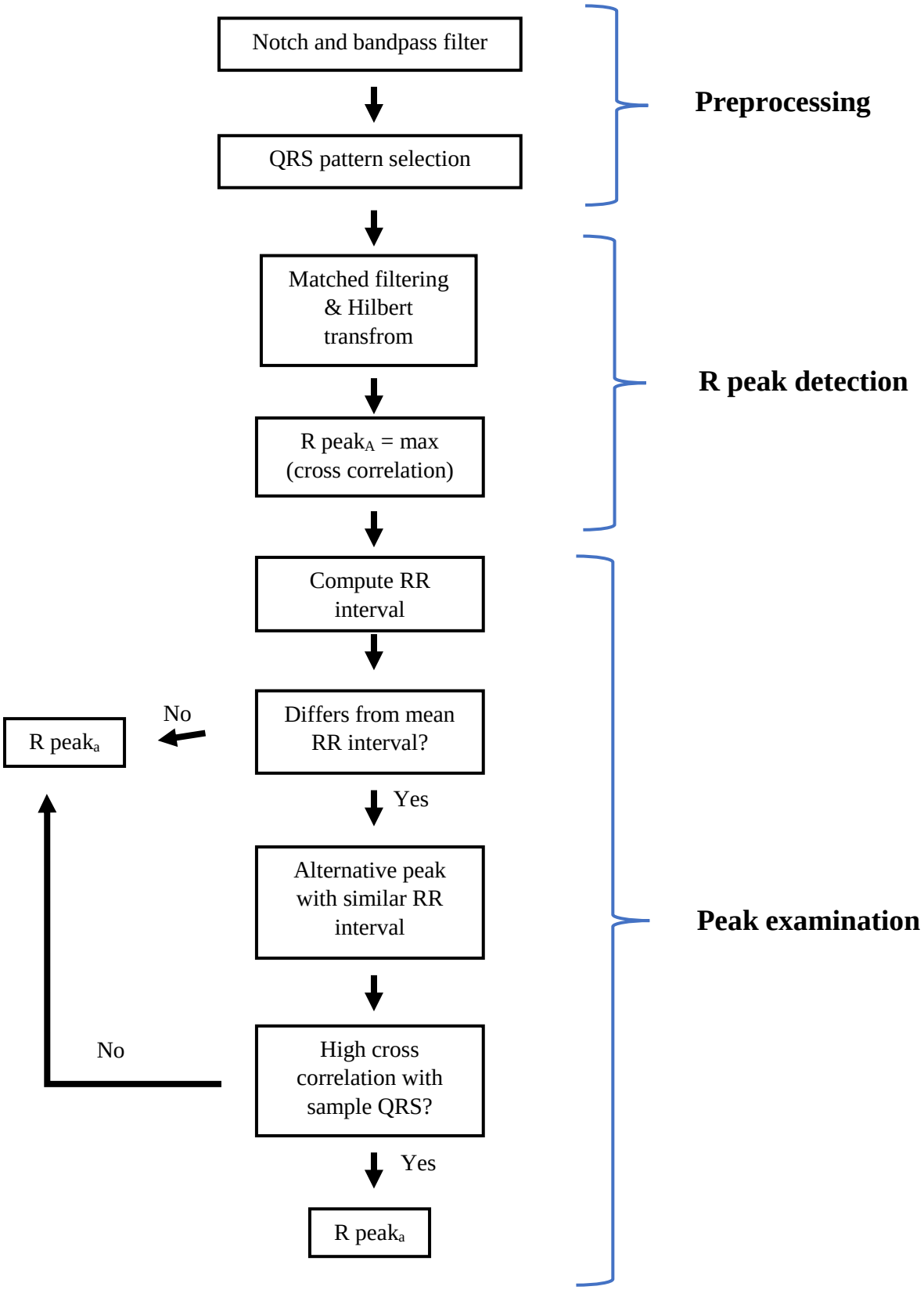
Notch and bandpass filter
QRS pattern selection
Preprocessing
Matched filtering & Hilbert transfrom
R peak$_A$ = max (cross correlation)
R peak detection
Compute RR interval
Differs from mean RR interval?
No
R peak$_a$
Yes
Alternative peak with similar RR interval
High cross correlation with sample QRS?
No
Yes
R peak$_a$
Peak examination

Appendix II

```
%% Artefact reject algorithm ( Silva&Rosenberg)
% Mariana Santos Silva

function out = HRV_rejectnoise2(varargin)

parameter_fields = {'Directory',
'out','selection','Corrections','saving','plotting'};
default_values   = {'',1 ,'all','Raw','no', 1};
[Directory, out, selection, Corrections, saving, plotting] =
gen_getInputParams(parameter_fields, default_values, varargin);

if and(~isstruct(out), strcmp(Directory,''))
    error('The directory or ''out'' need to be specified') ;
end

% Find all files of interest and load them:

if ~isstruct(out) % if out and Directory are specified, out wins
    names_RR = gen_findFiles(Directory,'*', '_RR', '.mat');
    [filePaths, fileNames, out] = gen_loadFiles(names_RR); clear names_RR
else
    filePaths = out.filePaths;
    fileNames = out.fileNames;
end

if strcmp(selection,'all')
    selection = (1:length(fileNames));
end % If not, it must be a vector containing indices

corrects = strsplit(Corrections, '--');

for k = selection
    subject = out.(gen_getLetterIndex(k));
    for correction = corrects
        node    = gen_sup_loadNode(subject, correction{1});
        if ~isstruct(node)
            disp(['Skipping HRV_rejectnoise for (', num2str(find(k ==
selection)),'/',num2str(length(selection)),'): ', [fileNames{k}], ' ...']);
        else
            disp(['Checking for noisy segments in (', num2str(find(k ==
selection)),'/',num2str(length(selection)),'): ', [fileNames{k}], ' ...']);

            rr_time_raw     = node.rr_time; %non-interpolated time points of RRI
            rr_val_raw      = node.rr_val; %non-interpolated values of RRI

            %% Steps
            % Enables the user to switch the filters to be used in the
            % analysis. 1 is on and 0 is off.
            F1=1;
            F2=1;
            F3=1;
            F4=1;
            F5=1;
            F6=1;
            F7=1;
            F8=1;

            for i=1:4

                if i == 1
                    rr_val_tmp = rr_val_raw;
                    rr_time_tmp = rr_time_raw;
```

```
                else
                    A= exist ('rr_val_new','var');

                    if A == 0
                        % This case shouldn't happen:
                        %                         error('No new variable was
created')
                        rr_val_tmp = rr_val_raw;
                    else
                        rr_val_tmp = rr_val_new;
                        rr_time_tmp = rr_time_new;
                    end
                end
                total_raw = length(rr_val_tmp);
                rr_val_excl_extremes = rr_val_tmp;

                if F1==1
                    %%      F1     %%
                    %Exclude the values above 1000 ms (60 bpm)
                    idx_max = find( abs(rr_val_tmp) > 1000);
                    rr_val_raw_excl_max= rr_val_tmp;
                    rr_val_raw_excl_max(idx_max) = nan;
                    rr_val_excl_extremes(idx_max) = nan;

                    %Calculates the % of data excluded of F1
                    F1_size=length(idx_max);
                    F1=(F1_size)/(total_raw);
                end

                if F2==1
                    %%      F2     %%
                    %Exclude the values below 300 ms (200 bpm)
                    idx_min = find(abs(rr_val_tmp) < 300);
                    rr_val_raw_excl_min = rr_val_tmp;
                    rr_val_raw_excl_min(idx_min) = nan;
                    rr_val_excl_extremes(idx_min)= nan;

                    %Calculates the % of data excluded of F2
                    F2_size=length(idx_min);
                    F2=(F2_size)/(total_raw);
                end

                if F3==1
                    %%      F3     %%
                    % Go through the rr_val_excl_extremes in intervals of 10
intervals, calculating the mean and
                    %standard deviation in each one
                    %Intervals that are outside of a range of +/- 50% of the mean
                    %of the last 15 intervals are discarded

                    rr_val_F3 = rr_val_excl_extremes;

                    new_mean = movmean(rr_val_F3,10,'omitnan');
                    new_std = movstd(rr_val_F3,10,'omitnan');

                    idx_interval=find(and((abs(rr_val_F3) >
(new_mean+(0.5*rr_val_F3))),(abs(rr_val_F3)< (new_mean-(0.5*new_mean)))));
                    rr_val_excl_extremes(idx_interval+1)=nan;

                    %Calculates the % of data excluded of F3
                    F3_size=length(idx_interval);
                    F3=(F3_size)/(total_raw);
                end

                if F4==1
                    %%      F4     %%
```

```
                    %Discard the intervals whose difference from the previous
                    %interval is not within 5 standard deviations of the mean of
                    %the previous 512 differences (64-second moving window-512
                    %samples)

                    rr_val_F4=rr_val_excl_extremes;
                    difference_F4 = diff(rr_val_F4);
                    mean_4 = movmean(difference_F4,512,'omitnan');

                    idx_4=find( and( (abs(difference_F4) >
(5*(std(mean_4)))),(abs(difference_F4) < (5*(std(mean_4)))) ) );
                    rr_val_excl_extremes(idx_4+1)=nan;

                    %Calculates the % of data excluded of F4
                    F4_size=length(idx_4);
                    F4=(F4_size)/(total_raw);
                end

                if F5==1
                    %%      F5     %%
                    %After the processing with the filters above, there are some
                    %noisy parts that are not eliminated, having excluded values
(NaN) with RR values.
                    %Considering that the NaN represent eliminated parts, it does
                    %not make sense having RR intervals between this values.


                    for j=1:5

                        new_rr_val_extremes=rr_val_excl_extremes;

                        new_rr_val_extremes(~isnan(new_rr_val_extremes))=0; %Change
numbers to 0
                        new_rr_val_extremes(isnan(new_rr_val_extremes))=1; %Change
Nan to 1

                        sum_rri_5=movsum(new_rr_val_extremes,5); %Calculates the
sum of intervals of 5
                        sum_rri_6=movsum(new_rr_val_extremes,6); %Calculates the
sum of intervals of 6
                        sum_rri_8=movsum(new_rr_val_extremes,8); %Calculates the
sum of intervals of 8
                        sum_rri_10=movsum(new_rr_val_extremes,10); %Calculates the
sum of intervals of 8

                        %For one value between NaNs

rr_val_excl_extremes(and((new_rr_val_extremes==0),(sum_rri_5==4)))=nan;

rr_val_excl_extremes(and((new_rr_val_extremes==0),(sum_rri_5==3)))=nan;

rr_val_excl_extremes(and((new_rr_val_extremes==0),(sum_rri_5==2)))=nan;

                        %For two value between NaNs

rr_val_excl_extremes(and((new_rr_val_extremes==0),(sum_rri_6==4)))=nan;

rr_val_excl_extremes(and((new_rr_val_extremes==0),(sum_rri_8==6)))=nan;

                        %Delete the isolated values between NaNs

rr_val_excl_extremes(and((new_rr_val_extremes==0),(sum_rri_10==5)))=nan;

                    end
```

```
                    %Calculates the % of data excluded of F5
                    F5_size=length(new_rr_val_extremes)-
length((rr_val_excl_extremes));
                    F5=(F5_size)/(total_raw);
                end

                if F6==1
                    %%      F6     %%
                    %Threshold with a 20's moving window, with 99% Confidence
Interval
                    %(changed to 5sd, to be according to the previous filters)

                    rr_val_std  = rr_val_excl_extremes;

                    M = movmean(rr_val_std,20,'omitnan');
                    S= movstd(rr_val_std, 20,'omitnan');

                    idx_F6= find(rr_val_std < abs(M-5*S));
                    idx_F61= find(rr_val_std > abs(M+5*S));

                    rr_val_std(idx_F6+1)=nan;
                    rr_val_std(idx_F61+1)=nan;
                    rr_val_excl_extremes(idx_F6+1)=nan;
                    rr_val_excl_extremes(idx_F61+1)=nan;

                    %% After conditions %%

                    %% C1: RRi<M-2S and RR(i-1)>M+2S

                    for i=1:length(rr_val_std)
                        if i==1
                            idx_C1=find(abs(rr_val_std)>2000);
                        else
                            idx_C1=find(abs(rr_val_std(i))<(M(i)-2*S(i)) &
abs(rr_val_std(i-1))>(M(i-1)*2*S(i-1)));
                        end
                    end

                    %% C2: RRi<0.75R(i+1) or RR(i+1)<0.75RR(i-1)
                    for i=1:length(rr_val_std)

                        if i==length(rr_val_std) || i==1

                            idx_C2=find(abs(rr_val_std)>2000);

                        else
                            idx_C2=find(abs(rr_val_std(i)) < 0.75*rr_val_std(i+1))
| abs(rr_val_std(i+1)) < 0.75*rr_val_std(i-1);
                        end

                    end

                    %% C3: RRi>  2RR(i-1)
                    for i=1:length(rr_val_std)
                        if i==1
                            idx_C3=find(abs(rr_val_std)>2000);
                        else
                            idx_C3=find(abs(rr_val_std(i)) > 2*abs(rr_val_std(i-
1)));

                        end
                    end

                    %             rr_val_excl_extremes(idx_C1+1)=nan;
                    rr_val_excl_extremes(idx_C2+1)=nan;
```

```
                    rr_val_excl_extremes(idx_C3+1)=nan;


                    %Calculates the % of data excluded of F6
                    F61_size = length(idx_F6);
                    F62_size = length(idx_F61);
                    %             F63_size = length(idx_C1);
                    F64_size = length(idx_C2);
                    F65_size = length(idx_C3);

                    %             F6_size = F61_size + F62_size + F63_size +
F64_size + F65_size;
                    F6_size = F61_size + F62_size +  F64_size + F65_size;
                    F6=(F6_size)/(total_raw);
                end

                if F7==1
                    %%      F7     %%
                    %Excludes the intervals which difference is five times the
total standard
                    %desviation

                    rr_val_7  = rr_val_excl_extremes;

                    std_total = std(rr_val_7, 'omitnan'); %std of the data
                    difference = diff(rr_val_7);

                    idx_F7 = find(abs(difference) > 5*std_total);

                    rr_val_excl_extremes(idx_F7+1)=nan;

                    F7_size=length(idx_F7);
                    F7=(F7_size)/(total_raw);
                end

                if F8==1
                    %%      F8     %%
                    %Exclude the RR interval differences bigger than 200
                    %(physiological impossible)

                    rr_F8 = rr_val_excl_extremes;
                    diff_F8 = diff(rr_F8);

                    idx_F8 = find( abs(diff_F8) > 200);

                    rr_val_excl_extremes(idx_F8+1)=nan;

                    F8_size=length(idx_F8);
                    F8=(F8_size)/(total_raw);


                    rr_time_new = rr_time_tmp(~isnan(rr_val_excl_extremes));
                    rr_val_new  =
rr_val_excl_extremes(~isnan(rr_val_excl_extremes));
                end
            end

            A= exist ('rr_val_new','var');

            if A == 0
                %                 error('No new variables were created')
                rr_val_new = rr_val_raw;
                rr_time_new = rr_time_raw;
            end
```

```
            %%
            % Plots only the new RRI
            if plotting
                figure; clf; hold all; title(['New RRI, after ' num2str(i)
'iterations, correction: ' correction{1}])
                plot(rr_time_raw, rr_val_raw,'+');
                plot(rr_time_new, rr_val_new);
                legend('previous RRIs', 'new RRI time series')
            end

            min_rr=min(rr_val_raw);
            max_rr=max(rr_val_raw);
            F=[F1, F2, F3, F4, F5, F6, F7, F8];


            fprintf('The maximum of RR intervals(raw) is %d. \n ',max_rr);
            fprintf('The minimum of RR intervals(raw) is %d. \n',min_rr);

            %% Calculate the ratio of removed RRI:
            rr_time_raw     = subject.Raw.rr_time; %Non-interpolated time points of
RRI
            rr_time_corr    = rr_time_new; %Time points of RRI after corrections

            length_raw = length(rr_time_raw);
            length_corr = length(rr_time_corr);

            usefulDuration_fraction =(length_corr)/(length_raw);
            %%

            RR_TIME = rr_time_new(1):1/node.RR_fs:rr_time_new(end);
            RR_VAL =
interp1(rr_time_new(1:end),rr_val_new(1:end)/1000,RR_TIME,'pchip');

            node_new = [];
            node_new.rr_val         = rr_val_new;
            node_new.rr_time        = rr_time_new;
            node_new.RR_fs          = node.RR_fs;
            node_new.rr_val_interp  = RR_VAL';
            node_new.rr_time_interp = RR_TIME';
            node_new.usefulDuration_fraction = usefulDuration_fraction;
            node_new.updated        = clock;
            node_new.Filters        =F;
            node_new.Validation        = rr_val_excl_extremes;

            subject     = gen_sup_addNode(subject, node_new, [correction{1}
'++noise']);
            clear node_new;

            if strcmp(saving,'save')
                disp(['Saving (', num2str(find(k ==
selection)),'/',num2str(length(filePaths)),'): ', fileNames{k}, ' ...']);
                corrs = strsplit(correction{1}, '++');
                % eval([corrs{1} ' = subject.(corrs{1});']); % corrs{1} will
usually be 'Raw'
                % save([filePaths{k}(1:end-4), '.mat'], corrs{1}, '-append');
                gen_sup_saveVariable([filePaths{k}(1:end-4), '.mat'], corrs{1},
subject.(corrs{1}))
            end

        end

    end
    out.(gen_getLetterIndex(k)) = subject;
end
end
```

Appendix III

```
%% Trial to replicate Govindan work (2016) on noise reduction
%Mariana Santos Silva 09/04/2017

clear
tic
E = 1.05:0.05:2.05;

figure(5); clf; % To have a handle to refer to

% Load data - only once since that can be slow
L = load('data.mat');
rr_time_loaded = L.Raw.rr_time;
rr_val_loaded  = L.Raw.rr_val;

RMS_correction = nan(1,length(E));
iter = RMS_correction;
for k = 1:length(E)
    e = E(k);

    rr_val = rr_val_loaded*0.001; % Change RRI to seconds

    % Step 1
    yy_adjusted = rr_val;
    yy_start = nan(size(yy_adjusted));

    iteration_counter = 0;
    while ~isequal(yy_start, yy_adjusted)
        iteration_counter = iteration_counter + 1;
        if iteration_counter > 300
            break;
        end
        yy_start = 60./yy_adjusted; % Starting with heart rate (from next iteration
it's step 1.d)

        % Outsource the next part, since it is used four times in this script:
        yy_adjusted = replace_maxima(yy_start, e);
    end
    iter(k) = iteration_counter;

    % Check, if last step was in HR or RRI; transform to HR
    if mean(yy_adjusted)<10
        HR = 60./yy_adjusted;
    else
        HR = yy_adjusted;
    end

    %%Calculation of the RMS of the difference between uncorrected HR and corrected
HR
    RMS_correction(:,k) = rms(HR-60./rr_val);

    % Step 2: iteration for different e
end; clear k e;
toc
disp(iter);

%% Step 2
%Identification of the optimal E: E*=min{RMSj-RMSj+1}, j=1 to n-1
difference_RMS  = -diff(RMS_correction);
[~, idx_e_opt]  = min(difference_RMS);
opt_e = E(idx_e_opt);
%RMS plotted as a function of E
figure(6); clf;
plot(E,RMS_correction);
title('RMS plotted as a function of E');
xlabel('E')
ylabel('RMS')
```

```
hold on

%% Step 3 %%
%Calculation of all the parameters with the optimal e and plots of
%different phases
rr_time = rr_time_loaded./60;
% Step 1
yy_adjusted = rr_val_loaded*0.001; % Change RRI to seconds
yy_start = nan(size(yy_adjusted));

figure(5); clf;
subplot(6,1,1)
plot(rr_time_loaded./60, 60./yy_adjusted)% Change time axis to minutes
title('Uncorrected HR');
xlabel('Time (minutes)')
ylabel('HR (min)')

iteration_counter = 0;
while ~isequal(yy_start, yy_adjusted)
    iteration_counter = iteration_counter + 1;
    yy_start = 60./yy_adjusted; % Starting with heart rate (from next iteration
it's step 1.d)

    yy_adjusted = replace_maxima(yy_start, opt_e);

    if iteration_counter >300
        break; % Emergency exit
    end
    if or(iteration_counter == 1, iteration_counter == 3)
        figure(5)
        subplot(6,1,iteration_counter+1)
        plot(rr_time, yy_adjusted);
        title(['Iteration ' num2str((iteration_counter+1)/2) ', \epsilon = '
num2str(opt_e)]);
        xlabel('Time (minutes)')
        ylabel('HR (min)')
    elseif or(iteration_counter == 2, iteration_counter == 4)
        figure(5)
        subplot(6,1,iteration_counter+1)
        plot(rr_time, yy_adjusted);
        title(['Iteration ' num2str(iteration_counter/2) ', \epsilon = '
num2str(opt_e)]);
        xlabel('Time (minutes)')
        ylabel('RRI (s)')
    end
end

% Check, if last step was in HR or RRI; transform to HR
if mean(yy_adjusted)<10
    HR = 60./yy_adjusted;
else
    HR = yy_adjusted;
end

HR_corrections_removed = HR;
HR_corrections_removed(HR~=60./(rr_val_loaded*0.001))=nan;

figure(5)
subplot(6,1,6); hold all;
plot(rr_time, HR);
plot(rr_time, HR_corrections_removed);
title('Final output');
xlabel('Time (minutes)')
ylabel('HR (bpm)')
hold on
```

Appendix IV

```
% Main HRV processed and analysis algorithm
% Apply after _RR has been created
close all; clear; clc;
tic

% Independent of TW:
AddPatientData          = 0;
AddEventData            = 0;
RemoveIrregularities    = 1;
DetrendRRI              = 1;
% Dependent on TW:
StressComplexity        = 1;
StressFrequency         = 1;
StressTime              = 1;
% Post-processing:

% Plotting:
CreateLinePlots         = 1;
CreateBandPlots         = 1;
CreateBandPlotsAll      = 1;

%
ExportToExcel           = 0;

% Classification
Categorising            = 0;

Directory   = [gen_getOwnCloudDirectory() '\Results_Thesis\'];
Interval    = 60;
TWs         = [300];
saving      = 'save';
select      = 'all';

corrects     = 'Raw--Raw++Govindan--Raw++DUD++SP++noise--Raw++Govindan++DetrendH--
Raw++DUD++SP++noise++DetrendH--Raw++DUD++SP++noise++Govindan';
plotCorrects = 'Raw--Raw++DUD++SP++noise++Govindan';
% For Calculations:
TimeParams  = 'avgHR--SDNN--rMSSD--pNN50--pNN25';
% For Plotting and Analysis:
LineParams  = 'HR--RRI--LFiA--LFp--HFiA--HFp--LFSE--SDNN--HFSE--pNN25';
BandParams  = 'HFp--LFp--HFiA--LFiA--HFSE--LFSE--avgHR--SDNN--rMSSD--pNN50--pNN25';
ClasParams  = 'HFp--LFp--HFiA--LFiA--SEAll--TFSE--HFSE--LFSE--avgHR--SDNN--pNN25--
rMSSD--pNN50';
E_beg       = '';%'Useful start';
E_end       = '';%'Useful stop';
E_nam       = 'Test';%'Useful';

% Make compatible with all operating systems:
Directory = strrep(Directory, '\',  gen_getFolderDelimiter);
Directory = strrep(Directory, '/', gen_getFolderDelimiter);

%%%%%
names_RR = gen_findFiles(Directory, '*', '_RR', '.mat'); % For only one file
replace '*'
[filePaths, fileNames, out] = gen_loadFiles(names_RR); clear names_RR
%%%%%
%%% To clean all calculated data apart from raw RRI and meta-data:
% ECG_clearRRFiles(Directory, 'prefix','*')
%%%%%

%%

if AddPatientData

HRV_addPatientData_HIE('pathFolder',Directory,'pathFile','C:\Users\Utilizador\ownCl
oud\HIE\UpdateMarianaMay\Data-Wilhelm-2\birthdates.csv');
```

```
end

if AddEventData
    HRV_addEventData_HIE('pathFolder',Directory);
end

if RemoveIrregularities
    out = HRV_rejectPeaks('PeakType','DownUpDown', 'Corrections','Raw',
'fact_std',4, ...
       'out',out, 'saving',saving, 'selection',select, 'plotting',0);
    out = HRV_rejectPeaks('PeakType','SinglePeaks', 'Corrections','Raw++DUD',
'fact_std',10, ...
       'out',out, 'saving',saving, 'selection',select, 'plotting',0);
    out = HRV_rejectnoise2('Corrections','Raw--Raw++DUD++SP','out',out,
'saving',saving, 'selection',select, 'plotting',0);
    out = HRV_rejectGovindan('Corrections','Raw--Raw++DUD++SP++noise','out',out,
'saving',saving, 'selection',select, 'plotting',0, 'median2nan','yes');
   out = HRV_markRejections('Corrections','Raw--Raw++Govindan--Raw++DUD++SP++noise-
-Raw++DUD++SP++noise++Govindan', 'W',20, 'fraction',0.3, ...
       'out',out, 'saving',saving, 'selection',select, 'plotting',0);% A bit more
than specified 5s since that was excluding one RRI between normal peaks
end

if DetrendRRI
     out = HRV_detrend('Corrections','Raw--Raw++Govindan--Raw++DUD++SP++noise',
'method','highpass', ...
         'out',out, 'saving',saving, 'selection',select);
     % One detrending algorithm should be enough
%      out = HRV_detrend('Corrections','Raw--Raw++Govindan--Raw++DUD++SP++noise',
'method','movAvg',    ...
%          'out',out, 'saving',saving, 'selection',select);
end

%% Calculate stress indices
for TW = TWs
    if StressTime       % Stress indices in the time domain
        out = HRV_calcStressIndexOneD('Types',TimeParams, 'TW',TW,
'Interval',Interval, ...
            'Corrections',corrects, 'saving',saving, 'selection',select,
'out',out);
    end

    if StressComplexity % Stress indices in the frequency domain
        out = HRV_calcStressIndexOneD('Types','SEAll', 'TW',TW,
'Interval',Interval, ...
            'saving',saving, 'selection',select, 'out',out,
'Corrections',corrects);
        out = HRV_calcStressIndexTwoD('Types','SE',    'TW',TW,
'Interval',Interval, ...
            'saving',saving, 'selection',select, 'out',out,
'Corrections',corrects);
    end
    if StressFrequency  % Stress indices in the frequency domain
        out = HRV_calcStressIndexTwoD('Types','power--instAmp', 'Age','Newborn',
'TW',TW, 'Interval',Interval, ...
            'saving',saving, 'selection',select, 'out',out,
'Corrections',corrects);
    end
end

%% Plot line plots
for TW = TWs
    if CreateLinePlots % Plot stress parameters over time
        A_S = ''; A_E = 'start--stop';
        HRV_plotLines('Types',LineParams, 'TW',TW, 'Interval',Interval, ...
            'AnnoStart',A_S, 'AnnoEnd',A_E,  'showComments','no', ...
            'saving',saving, 'selection',select, 'out',out,
'Corrections',plotCorrects);
```

```
    end

    if CreateBandPlots
        EBuffer     = ones(length(strfind(E_beg,'--'))+1,2)*round(TW/2);
        [Data, D_info] = HRV_extractStressIndices('Types',BandParams, 'TW',TW,
'Interval',Interval, ...
            'EventBegins',E_beg, 'EventEnds',E_end, 'EventNames',E_nam,
'EventBuffer',EBuffer, ...
            'out',out, 'selection',select, 'Corrections',corrects);
        HRV_plotAreasTime(Data, D_info, 'BySubjects');
    end
end


%% Temporary Solution to extract the full files
if ExportToExcel
    TW = TWs(1);
    for i = 1:length(fileNames)
        out.(char(64+i)).info.Events{1,1} = 'Tmp_Start';
        out.(char(64+i)).info.Events{1,2} = 0;
        out.(char(64+i)).info.Events{2,1} = 'Tmp_Stop';
        out.(char(64+i)).info.Events{2,2} = 1e12;
    end
    E_beg = 'Tmp_Start';
    E_end = 'Tmp_Stop';
    E_nam = 'all';
    EBuffer         = ones(length(strfind(E_beg,'--'))+1,2)*round(TW/2);
    [Data, D_info]  = HRV_extractStressIndices('Types',BandParams, 'TW',TW,
'Interval',Interval, ...
        'EventBegins',E_beg, 'EventEnds',E_end, 'EventBuffer',EBuffer,
'EventNames',E_nam, ...
        'out',out, 'selection',select, 'Corrections',corrects);
    % Data: cell-Array containing the HRV tables for all subjects and
    % corrections; there is one row per subject and one column per correction;
    % the order of rows and columns corresponds to the fileNames and corrects,
    % respectively (it's also the order of the entries in D_info). Every cell
    % contains one table for all times and parameters as specified in
    % BandParams. Normally you would choose certain events, but in this case
    % it's the whole files.
    for k = 1:length(D_info.FileNames)
        for c = 1:length(D_info.Corrections)
            file = D_info.FileNames{k};
            correction = D_info.Corrections{c};
            TableToExport = Data{k,c};
            % I'm not sure about the following line:
            writetable(TableToExport,[correction '.xls'],'Sheet',file);
        end
    end
end

for TW = TWs
    if CreateBandPlotsAll
        EBuffer         = ones(length(strfind(E_beg,'--'))+1,2)*round(TW/2);
        [Data, D_info]  = HRV_extractStressIndices('Types',BandParams, 'TW',TW,
'Interval',Interval, ...
            'EventBegins',E_beg, 'EventEnds',E_end, 'EventBuffer',EBuffer,
'EventNames',E_nam, ...
            'out',out, 'selection',select, 'Corrections',corrects);
        % HRV_plotAreasTime(Data, D_info, 'MixSubjectsAll');
        %%%%%%%%%%%%%%%%%%%%%%%%%%%%%%%%%%%%%%%%%%%%%%%%%%%%%%%%%%%%%%%%%%%%%%%
        for i = 1:length(fileNames)
            if strcmp(fileNames{i}(1:2),'H0')
                D_info.Labels{i} = 'Healthy';
            else
                D_info.Labels{i} = 'HIE';
            end
        end
        D_info.Directory = Directory;
```

```
        %%%%%%%%%%%%%%%%%%%%%%%%%%%%%%%%%%%%%%%%%%%%%%%%%%%%%%%%%%%%%%%%%%%%%%%
        %%%
        %%% Assign colours to people according to sickness:
        %%%
        Idx_HIE                = find(not(cellfun('isempty', strfind(D_info.Labels,
'HIE'))));
        Idx_Healthy            = find(not(cellfun('isempty', strfind(D_info.Labels,
'Healthy'))));
        Idx_Unsure             = find(not(cellfun('isempty', strfind(D_info.Labels,
'Unsure'))));
        colours_HIE            = autumn(numel(Idx_HIE)+1);     % +1 to avoid yellow
        colours_Healthy        = summer(numel(Idx_Healthy)+1); % +1 to avoid yellow
        colours_Unsure         = gray(numel(Idx_Unsure)+1);    % +1 to avoid white
        colours                = nan(length(fileNames),3);
        colours(Idx_HIE,:)     = colours_HIE(1:end-1,:);
        colours(Idx_Healthy,:) = colours_Healthy(1:end-1,:);
        colours(Idx_Unsure,:)  = colours_Unsure(1:end-1,:);

        HRV_plotAreasTime(Data, D_info, 'SubjectsPerEventAll', 'colours',colours)
    end

    %%
    if Categorising

        EBuffer     = ones(length(strfind(E_beg,'--'))+1,2)*round(TW/2);

        corrects = 'Raw++DUD++SP++DetrendH--Raw';
        out.A.info.Label = {'Healthy'};
        out.D.info.Label = {'Healthy'};
        out.E.info.Label = {'Healthy'};
        [Data, D_info] = HRV_extractStressIndices('Types',ClasParams, 'TW',TW,
'Interval',Interval, ...
            'EventBegins',E_beg, 'EventEnds',E_end, 'EventBuffer',EBuffer,
'EventNames',E_nam, ...
            'out',out, 'selection',select, 'Corrections',corrects);

        if 0 % All correction and parameter combinations:
            [trainedClassifier, DataTable_Values, validationAccuracy] =
HRV_classifyScenarios(Data, D_info, ...
                'sameCorrection', 'Label', 'Group','all', ...
                'KernelFunction','polynomial', 'saveResults','no',
'includeTime','no', ...
                'combinations2Dplots',{'Raw__HFiA','Raw__LFiA';
'Raw__HFp','Raw__LFp'});
        else % Specify mix of correction and parameter
            corrections = strsplit(corrects, '--');
            CorrectionParam = {corrections{2},'HFiA'; corrections{2},'LFiA'; ...
                corrections{2},'HFp'; corrections{2},'LFp'; ...
                corrections{2},'HFSE'; corrections{2},'LFSE'; ...
                corrections{2},'TFSE'; corrections{2},'rMSSD'; ...
                corrections{2},'pNN25'; corrections{1},'SDNN';
corrections{1},'SEAll'};

            [trainedClassifier, DataTable_Values, validationAccuracy] =
HRV_classifyScenarios(Data, D_info, ...
                'individualCorrection', 'Label', 'Group','all',
'CorrectionParam',CorrectionParam, ...
                'KernelFunction','polynomial', 'saveResults','no',
'includeTime','no', ...
                'combinations2Dplots',{'Raw__HFiA','Raw__LFiA';
'Raw__HFp','Raw__LFp'}, 'Margin',1/3);
        end
    end
end

toc
```

Appendix V

```
%% Entropy measures algorithm
% Mariana Santos Silva

%% Clear and load data
clear all;
load('babyData.mat');

N = 1000;
P = 3;

%% Plot filtered RRI data
L = length(babyData);
figure; hold on;
for i = 1:L
    time = babyData{i}.rr_time;
    RRI = medfilt1( babyData{i}.rr_val, 5 );

    plot(time, RRI);
end
grid on; grid minor;
set(gca, 'fontsize', 16);

%% Compute entropy measures for RRI data

dataPath = ['C:\Users\ms8517\ownCloud\Multidimensional_Analysis\'];

for i = 9:9
    time = babyData{i}.rr_time;
    realTime = datetime(babyInfo{i,1}.DateStartDevice) + seconds(time);
    RRI = medfilt1( babyData{i}.rr_val, 5 );

    idx = [1:length(RRI)-N+1; N:length(RRI)];

    M = size(idx,2);
    M = 5000;

    %ApEn = zeros(M, 1);
    %SampleEn = zeros(M,1);
    MSE = zeros(M, P);
    %FuzzEnt = zeros(M, P);

    for j = 1:M
        tmp = RRI(idx(1,j):idx(2,j));
        r = 0.2 * std(tmp);
        ApEn(j) = ApEntr(3, r, tmp);
        SampleEn(j) = sampleEntropy(tmp, 3, r, 1);
        MSE(j, :) = ECG_TC_mmse(tmp, 3, 1, P)';
        FuzzEnt(j, :) = mmfe(tmp,3,1,0.15,2,P)';
        [i, 100*j/M]
    end

save([dataPath, 'results_MSE\MSE_baby_' num2str(1) '.mat'], 'MSE');
end

%%


for ii = 1:1

    time = babyData{ii}.rr_time;
    realTime = datetime(babyInfo{ii,1}.DateStartDevice) + seconds(time);
    RRI = medfilt1( babyData{ii}.rr_val, 5 );
    idx = [1:length(RRI)-N+1; N:length(RRI)];
    ApEn = load([dataPath 'results_Ap\ApEn_baby_' num2str(ii) '.mat']);
    ApEn = struct2array(ApEn);
```

```
    SampleEn = load([dataPath 'results_SE\SampleEn_baby_' num2str(ii) '.mat']);
    SampleEn = struct2array(SampleEn);

    figure;
    ax1 = subplot(2,1,1); hold on;
    plot(realTime(idx(2,:)), ApEn, 'linewidth', 2);
    plot(realTime(idx(2,:)), SampleEn, 'linewidth', 2);
    legend('Approx. Entropy', 'Sample Entropy')
    set(gca, 'fontsize', 18)

    ax2 = subplot(2,1,2); hold on;
    plot(realTime(idx(2,:)), RRI(idx(2,:)), 'linewidth', 2);
    set(gca, 'fontsize', 18);
    legend('RRI')


    linkaxes([ax1, ax2], 'x')

end
```

Appendix VI

```
%% Multidimensional Entropy Study algorithm
% Mariana Santos Silva

%% Clear and load data
clear all;
load('babyData.mat');

dataPath = ['C:\Users\Utilizador\ownCloud\Multidimensional_Analysis\'];

%%
% choose baby
ii = 1;

% choose samples to analyse
a = 3500;
b = 5000;

% choose scale of multiscale entropy to use
scale = 3;

% window size for entropy measures
N = 1000;

time = babyData{ii}.rr_time;
realTime = datetime(babyInfo{ii,1}.DateStartDevice) + seconds(time);
idx = [1:length(time)-N+1; N:length(time)];
realTime = realTime(idx(2,:));

ApEn = load([dataPath 'results_Ap\ApEn_baby_' num2str(ii) '.mat']);
ApEn = struct2array(ApEn);
SampleEn = load([dataPath 'results_SE\SampleEn_baby_' num2str(ii) '.mat']);
SampleEn = struct2array(SampleEn);
MultiScEn = load([dataPath 'results_MSE\MSE_baby_' num2str(ii) '.mat']);
MultiScEn = struct2array(MultiScEn);
Fuzzy = load([dataPath 'results_Fuzzy\FE_baby_' num2str(ii) '.mat']);
Fuzzy = struct2array(Fuzzy);

All_filts = [ApEn(a:b,:), SampleEn(a:b,:), smooth(MultiScEn(a:b, scale), 5)];

All_filts = [SampleEn(a:b,:), smooth(MultiScEn(a:b, scale), 5), Fuzzy(a:b,scale)];

[Idx,D] = knnsearch(All_filts, All_filts, 'K', 2);
epsilon = 0.03;
idx = DBSCAN(All_filts, epsilon, 5);

c = [0.2143    0.8935    0.1305;
    0.5938    0.9052    0.0916;
    0.2208    0.5387    0.1187;
    0.5984    1.2011    0.1300;
    0.5998    0.9085    0.1321];

% [idx, centroids] = kmeans(All_filts, 5, 'Start', c);

figure; hold on;
colormap(jet);
scatter3(All_filts(:,1), All_filts(:,2), All_filts(:,3), 15, idx);

grid on; grid minor;
set(gca, 'fontsize', 16);

view(3);

xlabel('Sample Entropy');
ylabel('Multiscale Entropy (scale = 3)')
zlabel('Fuzzy Entropy (scale = 3)');
```

```
%%
colors = [0    0.4470    0.7410;
    0.8500    0.3250    0.0980;
    0.9290    0.6940    0.1250;
    0.4940    0.1840    0.5560;
    0.4660    0.6740    0.1880;
    0.3010    0.7450    0.9330;
    0.6350    0.0780    0.1840;
    0 0 0;
    0    0.4470    0.7410;
    0.8500    0.3250    0.0980;
    0.9290    0.6940    0.1250];

tit_str = {'State', 'Approx. En.', 'Sample En.', 'Multiscale En.'};

figure;
ax(1) = subplot(4,1,1); hold on;
plot(realTime(a:b), idx, 'linewidth', 2);
grid on; grid minor; axis tight;
ylabel(tit_str{1})
set(gca, 'fontsize', 16);

for ii = 1:3
    ax(ii+1) = subplot(4,1,ii+1); hold on;
    plot(realTime(a:b), All_filts(:, ii), 'linewidth', 2, 'color', colors(ii+1,:));
    grid on; grid minor; axis tight;
    ylabel(tit_str{ii+1})
    if(ii==3)
        xlabel('Time');
    end
    set(gca, 'fontsize', 16);
end

linkaxes(ax, 'x')
```